INTERNAL STRUCTURE AND MAGNETISM IN PLANETS

Daniele Viganò

8 July 2024, ICE-CSIC

7th ICE Summer School

Multiwavelength approach to exoplanets

European Research Council
Established by the European Commission
Institute of Space Sciences
CSIC IEEC
CONSEJO SUPERIOR DE INVESTIGACIONES CIENTÍFICAS
IAC3 Institute of Applied Computing & Community Code.
vigano@ice.csic.es

Outline

- *Magnetic fields basis*
- *Solar planets magnetism*
- *Hot Jupiters and their inflated radii*
- *Radio emission mechanisms and relation with magnetic fields*
- *The quest for exoplanetary radio emission*
- *Brief mention to Star-Planet interaction*

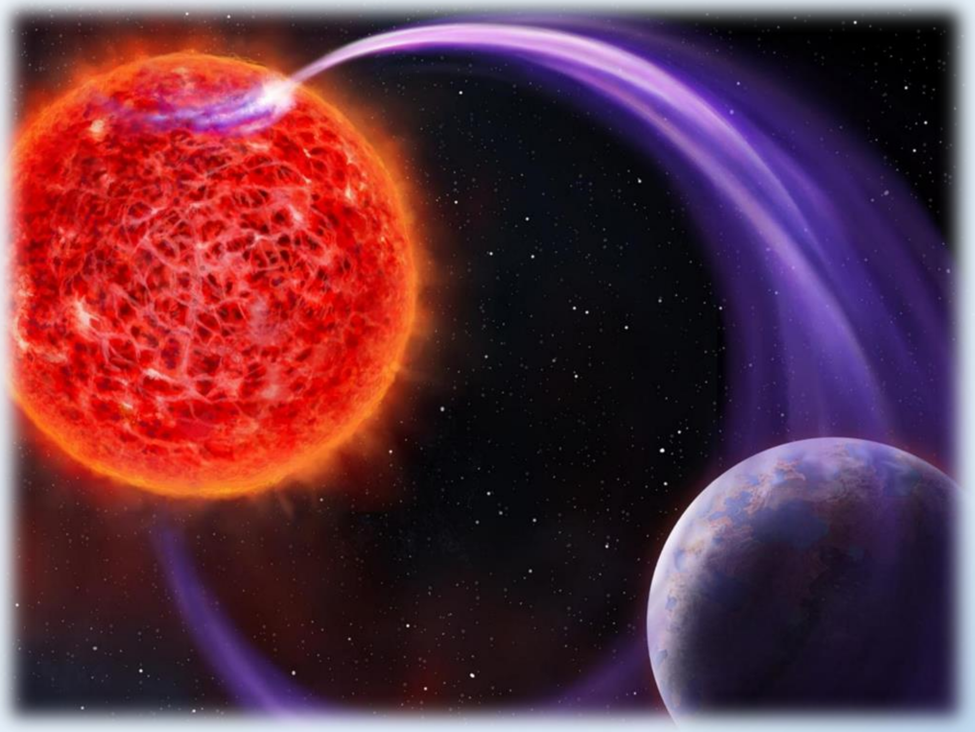

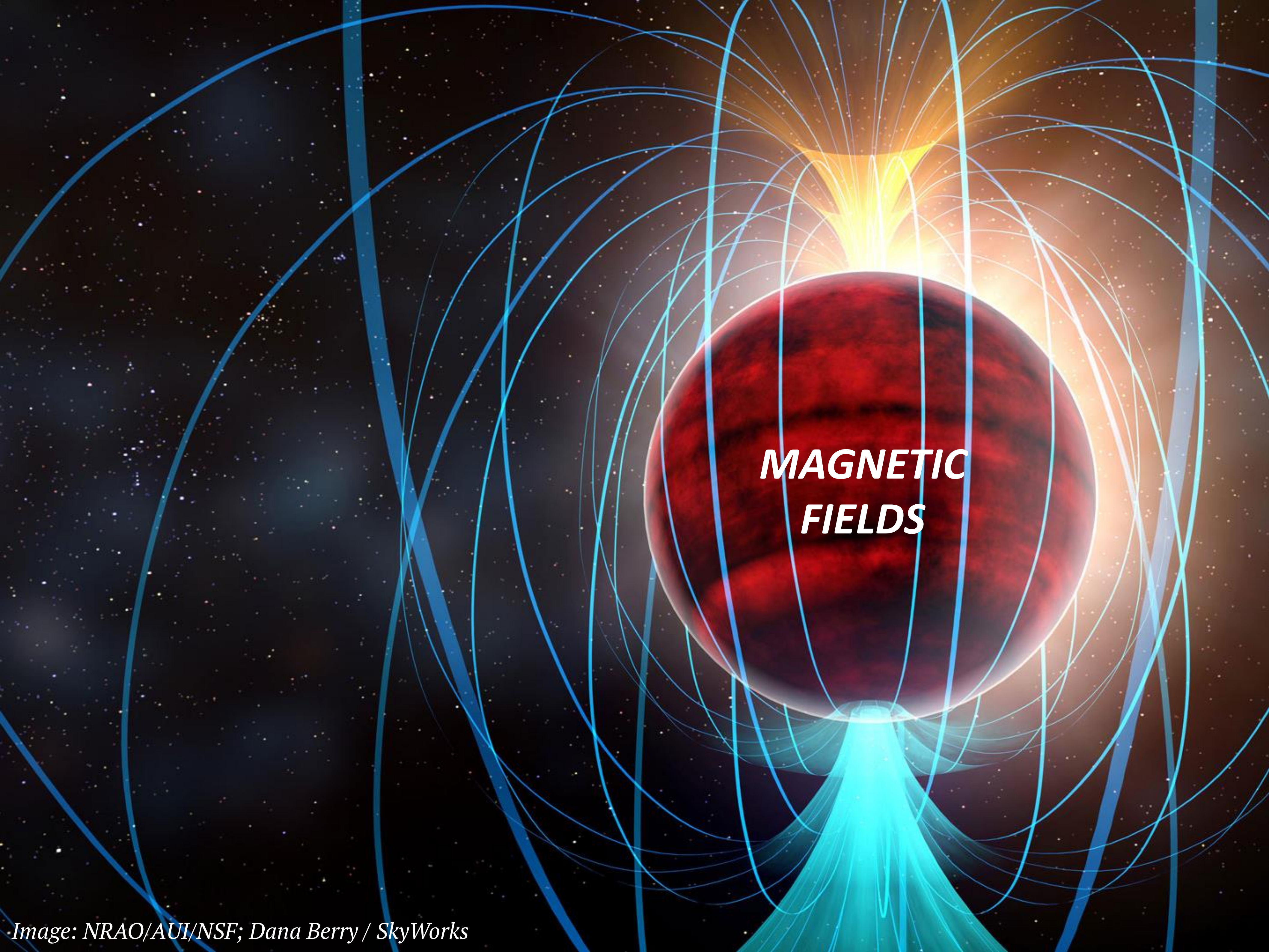
MAGNETIC
FIELDS
Image: NRAO/AUI/NSF; Dana Berry / SkyWorks

Dipoles (large-scale fields)

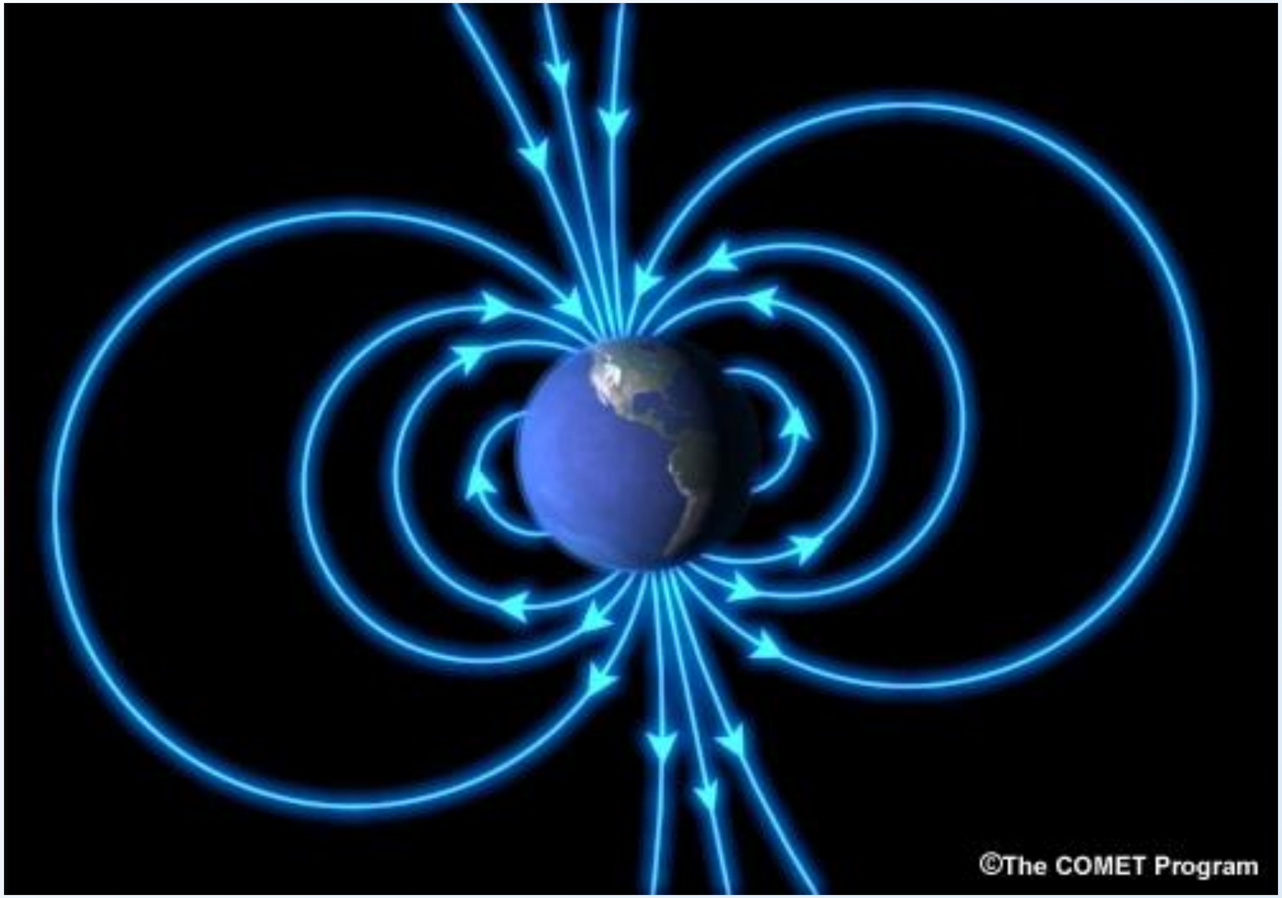

It's the simplest possible configuration, since div(B)=0.
However, such simple, pure "magnets" don't exist in nature

Some magnetic terminology: multipoles

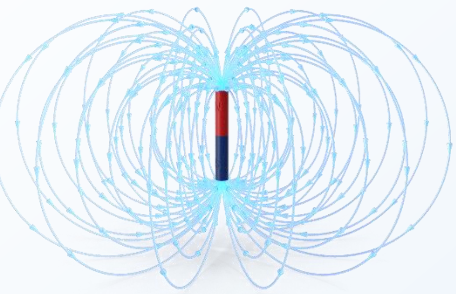

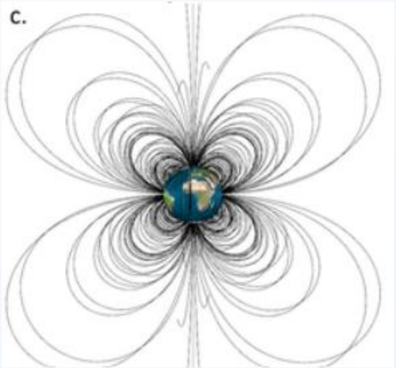

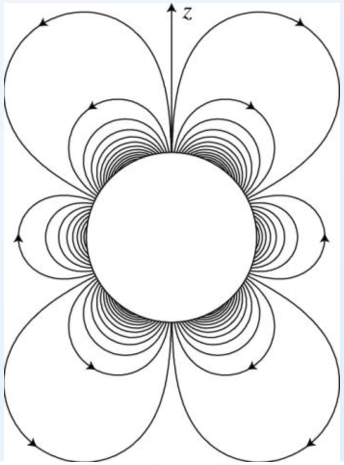

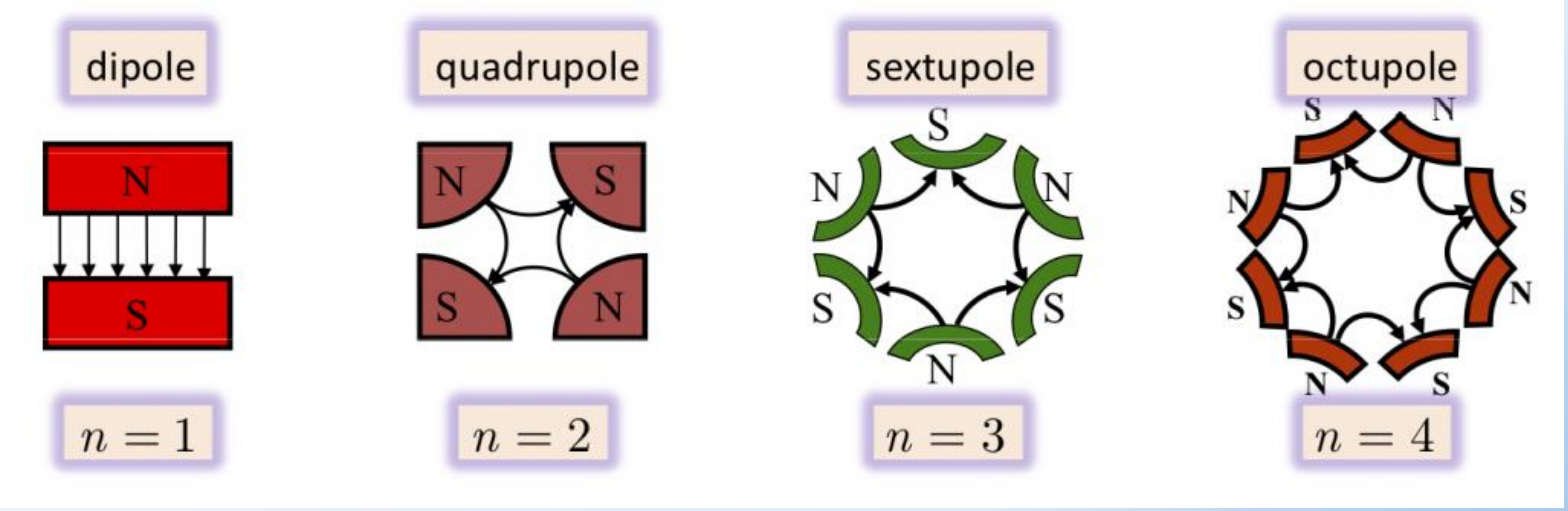

Some magnetic terminology: Poloidal – Toroidal

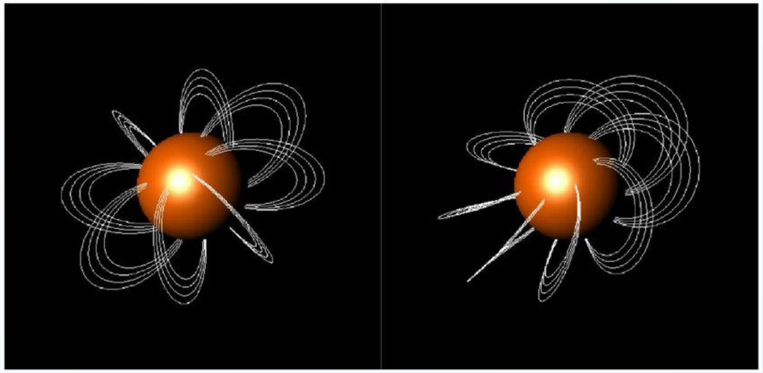

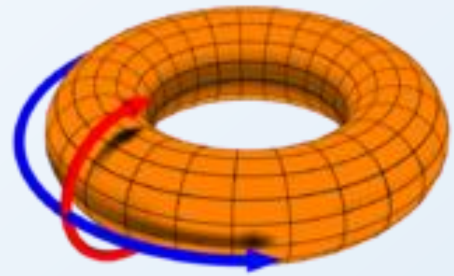

$\vec{B}$ can also be expressed by two scalar functions $\Phi(\vec{x})$, $\Psi(\vec{x})$, that define its *poloidal* and *toroidal* components as follows:

$$\vec{B}_{pol} = \vec{\nabla} \times (\vec{\nabla}\Phi \times \vec{r}) \ ,$$
$$\vec{B}_{tor} = \vec{\nabla}\Psi \times \vec{r} \ .$$

In axial symmetry:
Poloidal = meridional components of the field (r, θ)
Toroidal = azimuthal component (φ)

In 3D poloidal has all (r, θ, φ), toroidal has the tangential ones (θ, φ).

In the absence of currents (curl(B)=0), you can only have a poloidal field.

Magnetism in astrophysical bodies

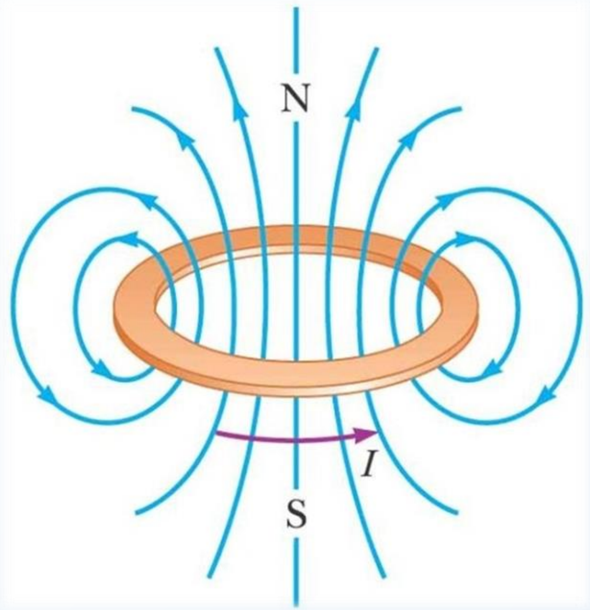

- planets: up to 10 G (Solar system)
- brown dwarfs, main-sequence: up to 10^4 G
- white dwarfs: $10^3 - 10^8$ G
- neutron stars: $10^8 - 10^{15}$ G

Ingredients for sustaining a magnetic field:

1. *Electrically conducting fluid*
2. *Circulation of charge carriers: differential rotation, convection, turbulence, buoyancy…*
3. *Timescales and intensity depend on the energy input and the decay timescale of the magnetic field*

Conducting fluids in astrophysical objects:

- Molten Iron/Nickel in the outer core (Earth, Mercury)
- Metallic hydrogen (Jupiter, Saturn)
- Salty oceans (Uranus, Neptune)
- Ionized atmosphere/plasma (hot Jupiters, Sun)
- Compositional buoyancy (core freezing in rocky planets, white dwarfs)
- Free electrons (neutron stars' crust)

Advection and resistivity in magneto-hydrodynamics (MHD)

Induction equation

$$\partial \vec{B} / \partial t = -\nabla \times \vec{E}$$

$$\vec{E} + \vec{V} \times \vec{B} = \eta \vec{J}$$

$$\nabla \times \vec{B} = \mu_0 \vec{J}$$

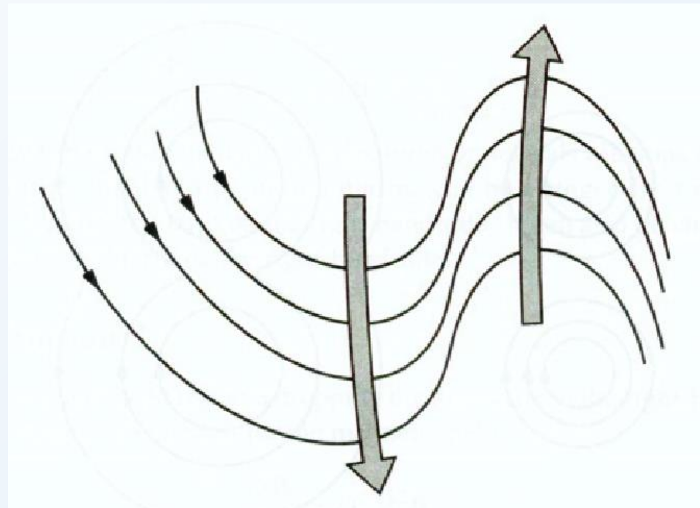

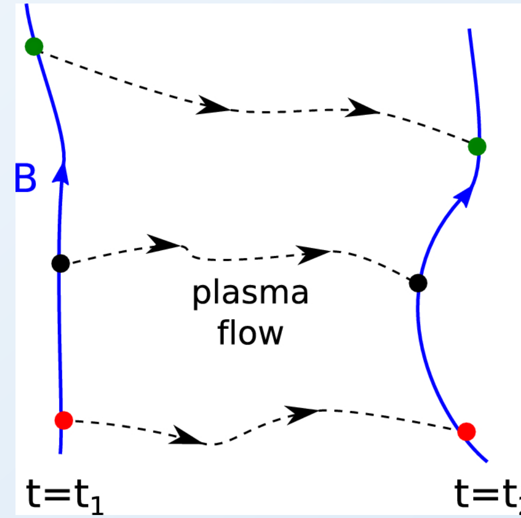

The first term of the electric field (-**v** x **B**) is the MHD "ideal term": magnetic field lines are advected by the fluid motions. This is responsible for magnetic flux conservation. See Alfvén's theorem, or the frozen-in flux theorem.
η is the magnetic diffusivity, inversely proportional to the electrical conductivity, σ, and tries to simplify the field configuration, by dissipating currents Ohmically.

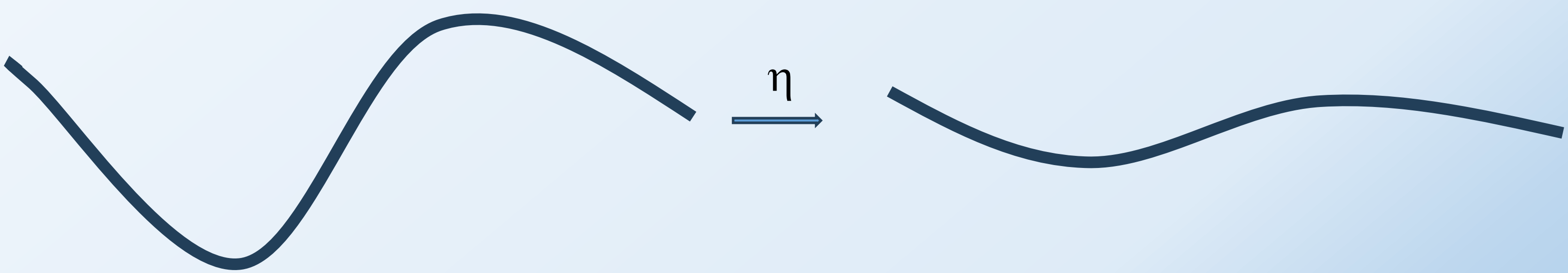

General sketch of MHD energy interchange

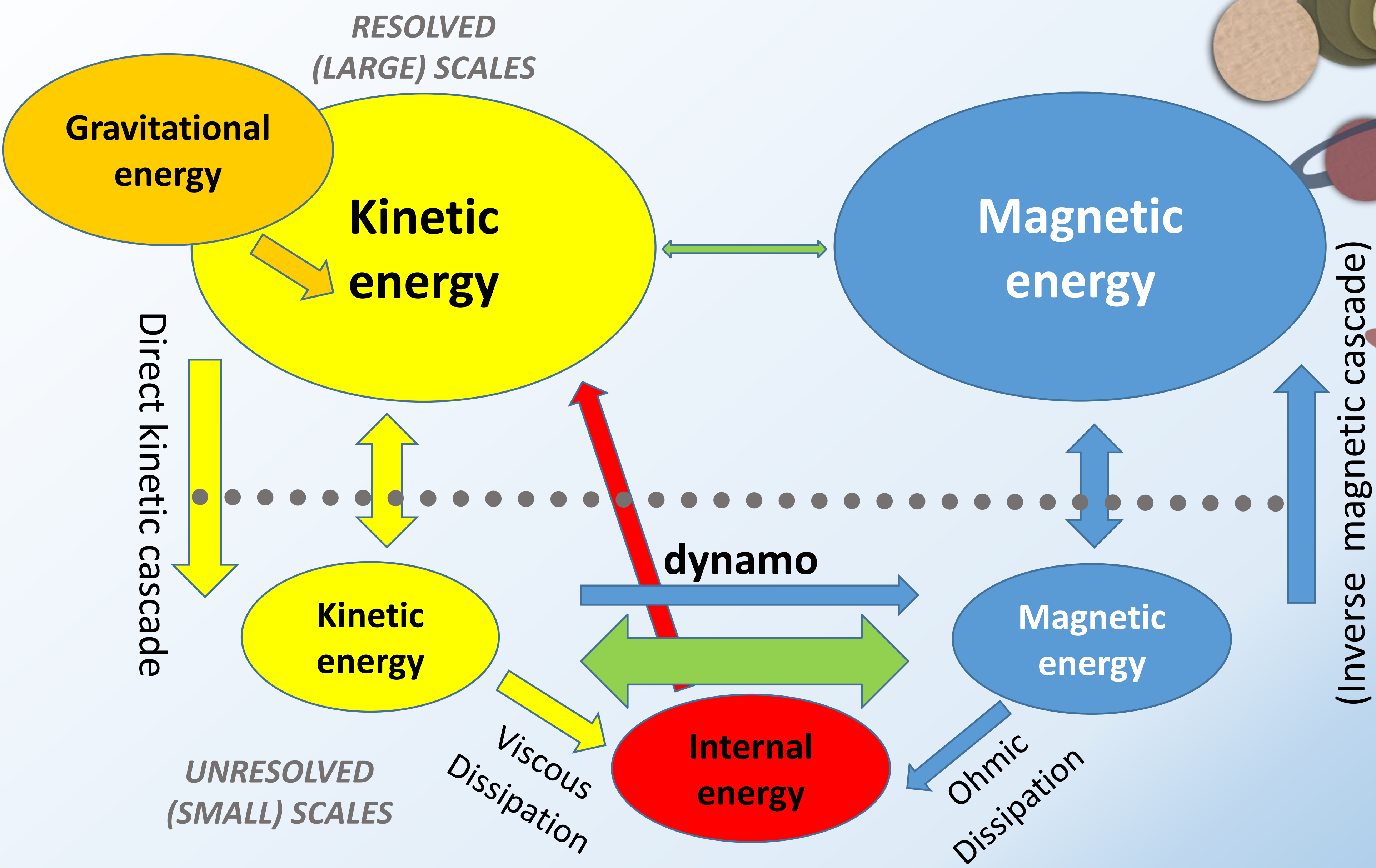

Sustained dynamo in a nutshell

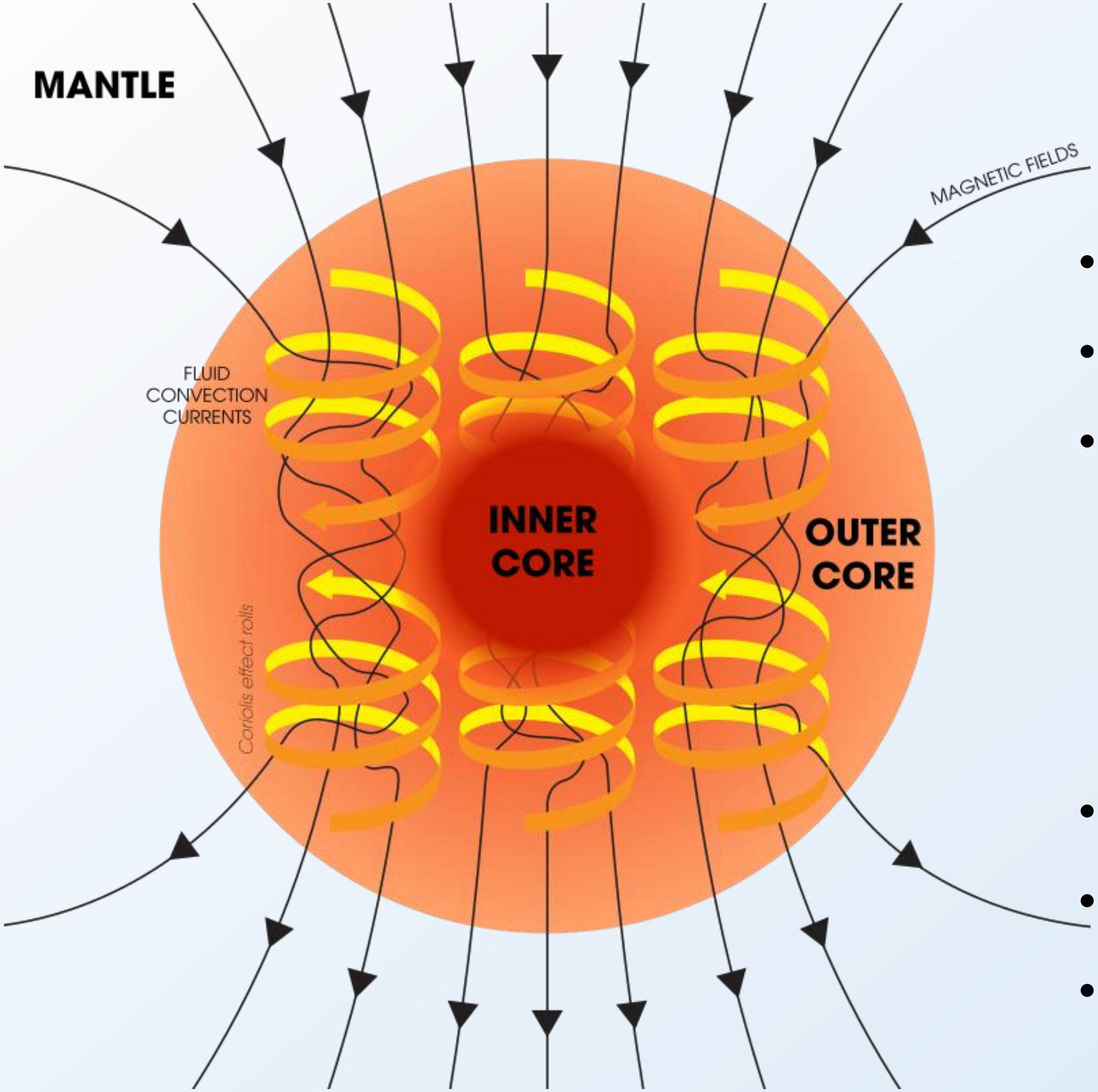

Dynamo is the transfer between kinetic and magnetic energy.

The macroscopic ingredients are mainly:

- Convection
- Rotation
- Differential rotation / Shear / Winding

Need an engine to sustain the thermal-driven convection.

Microscopic ingredients play an important role:

- Viscosity
- Resistivity
- Thermal diffusivity

See Fabio's lecture

Sustained dynamo in a nutshell

In presence of a sustained fluid movement, magnetic field lines are advected by the fluid.

Differential rotation (or other shears, i.e. non-uniform velocities), convection and Coriolis forces lead to the stretching and twisting of magnetic field lines, which mean a transfer from kinetic to magnetic energy.

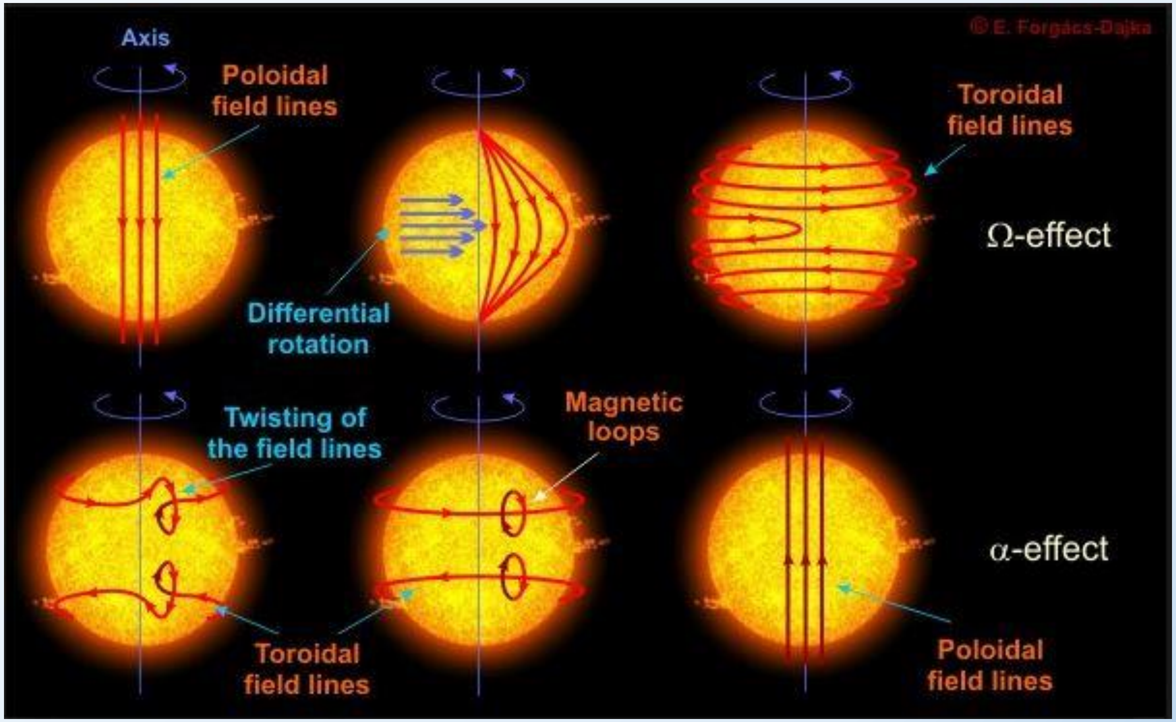

Turbulent fields

In turbulence, the kinetic and magnetic energy is distributed across all scales. Therefore, there are no clear coherent, large-scale structures. This is typical or regions where the magnetic field is produced, but these small structures, due to their size, are "invisible" outside the region where the magnetic field is created (e.g. at the surface).

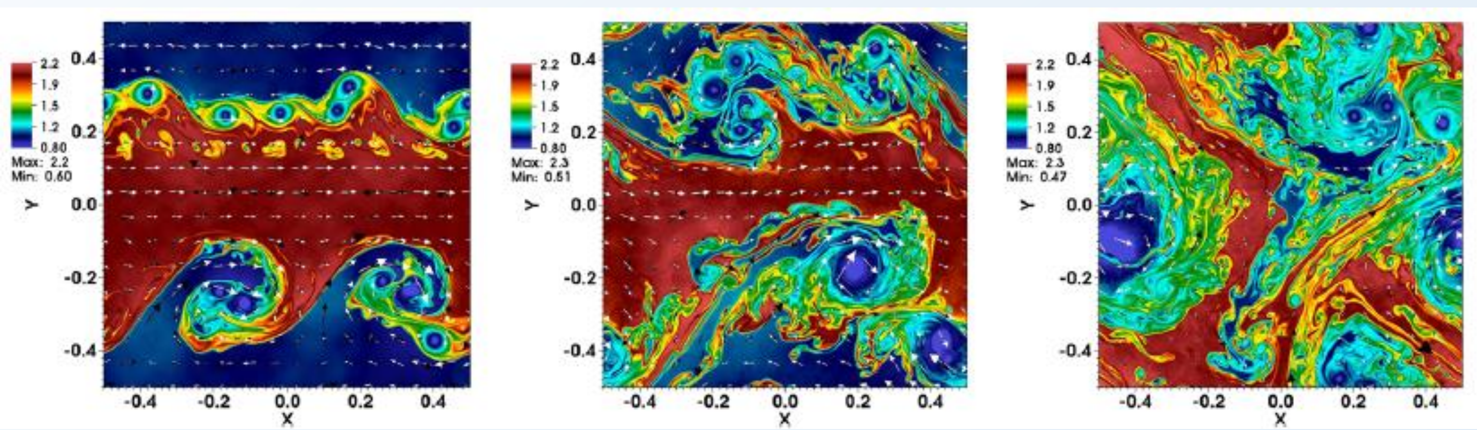

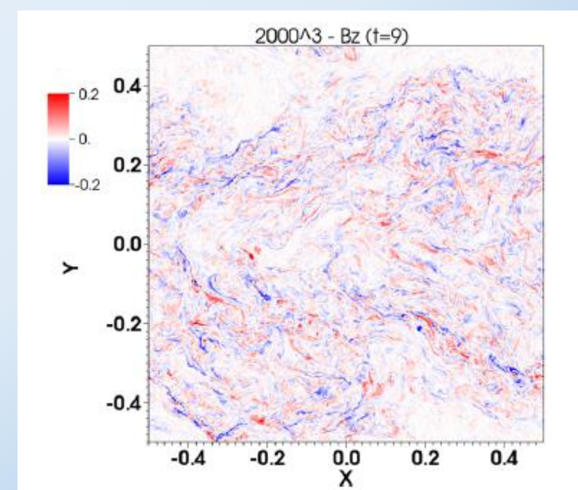

Outside the dynamo region: magnetosphere

Outside the dynamo region, if no more currents are present, the field is potential ($\nabla\times B=0$).
However, in presence of interaction with other bodies/environment, wind or any other currents, the solution is not potential anymore.

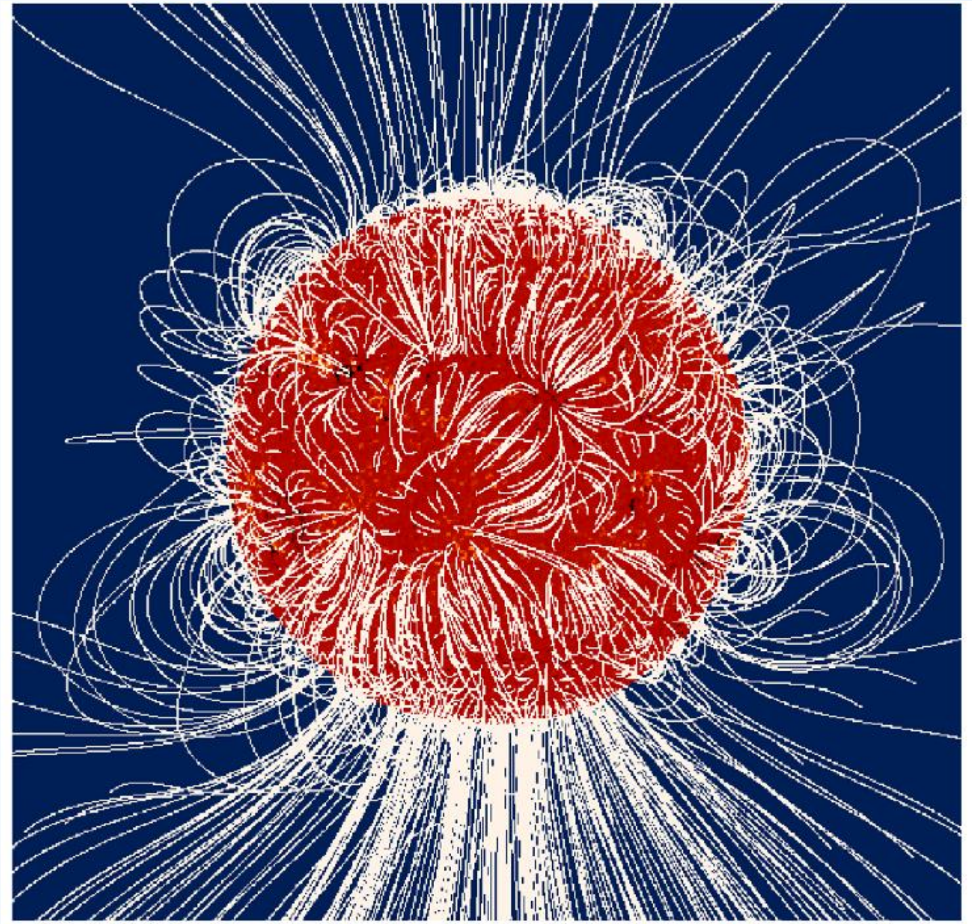

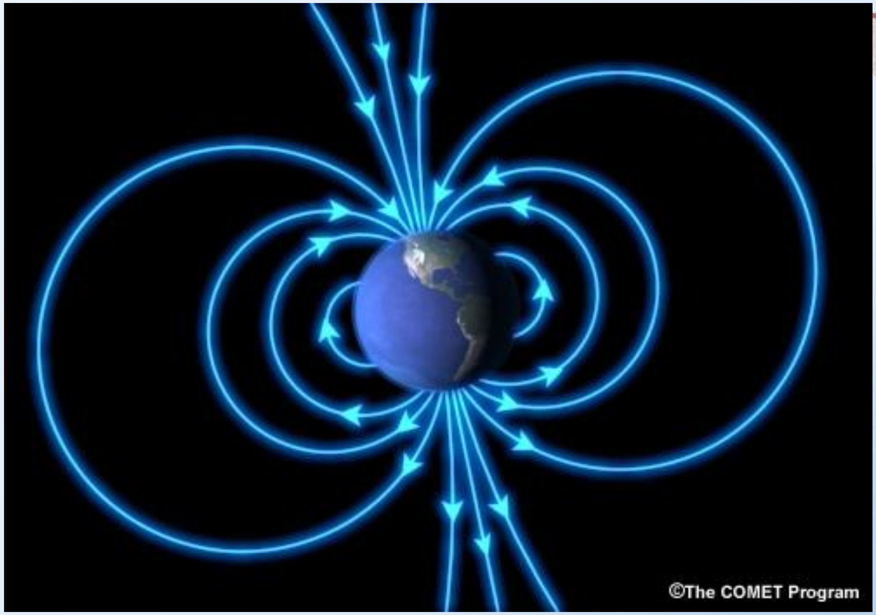

[Staub et al. 2020]

Outside the dynamo region: magnetosphere

The interaction with the stellar wind is important and distorts the magnetosphere. Reconnections can also occur (related to aurorae).

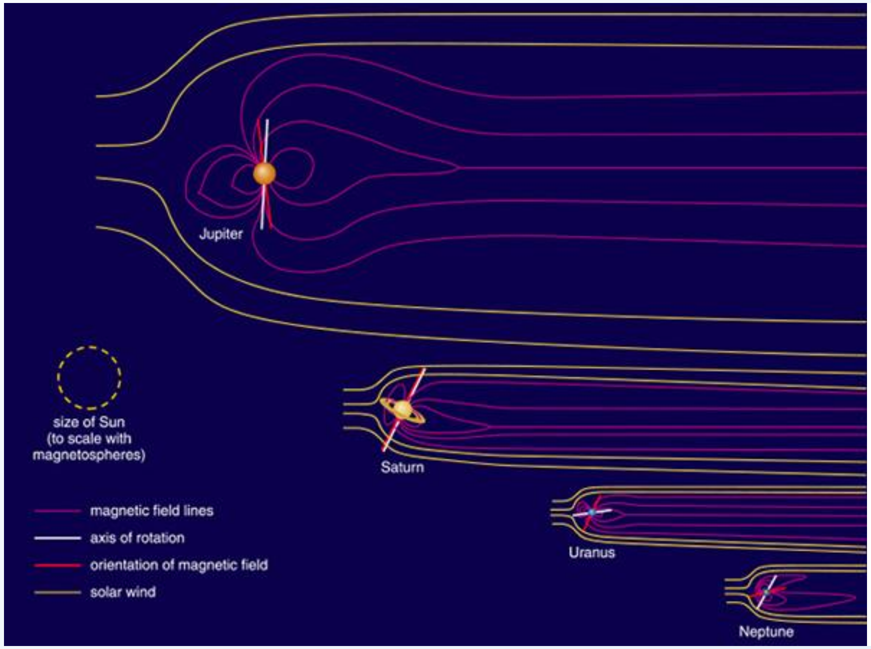

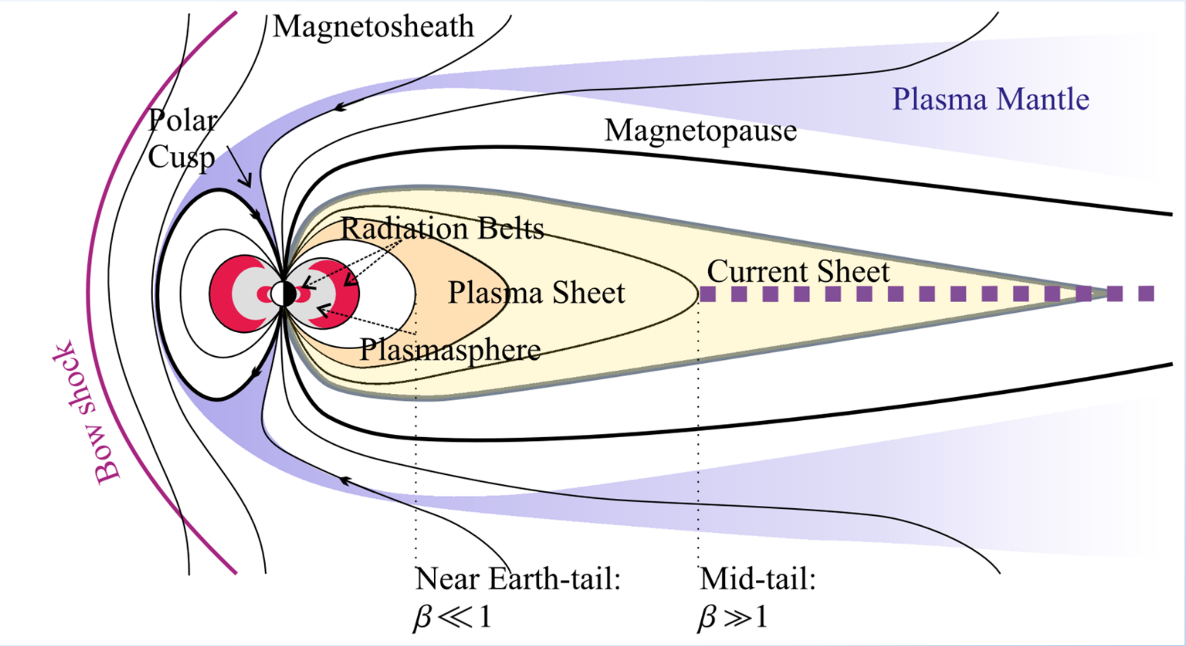

Earth: extends from 60-000 km sunward to 300.000 km in the magnetotail
Jupiter: 3-6 Million km sunward, magnetotail more than 10 times further.

Magnetospheric reconstruction: example of the Sun

1. *Measurements in a sample of points (photosphere or through an orbit).*
2. *Make assumptions about the global flow of electrical currents in the region where you want to extract the magnetic fields*
3. *Use some numerical techniques to reconstruct the magnetic field all over in the space.*

The full reconstructed 3D field in the whole magnetosphere are very assumption-dependent!

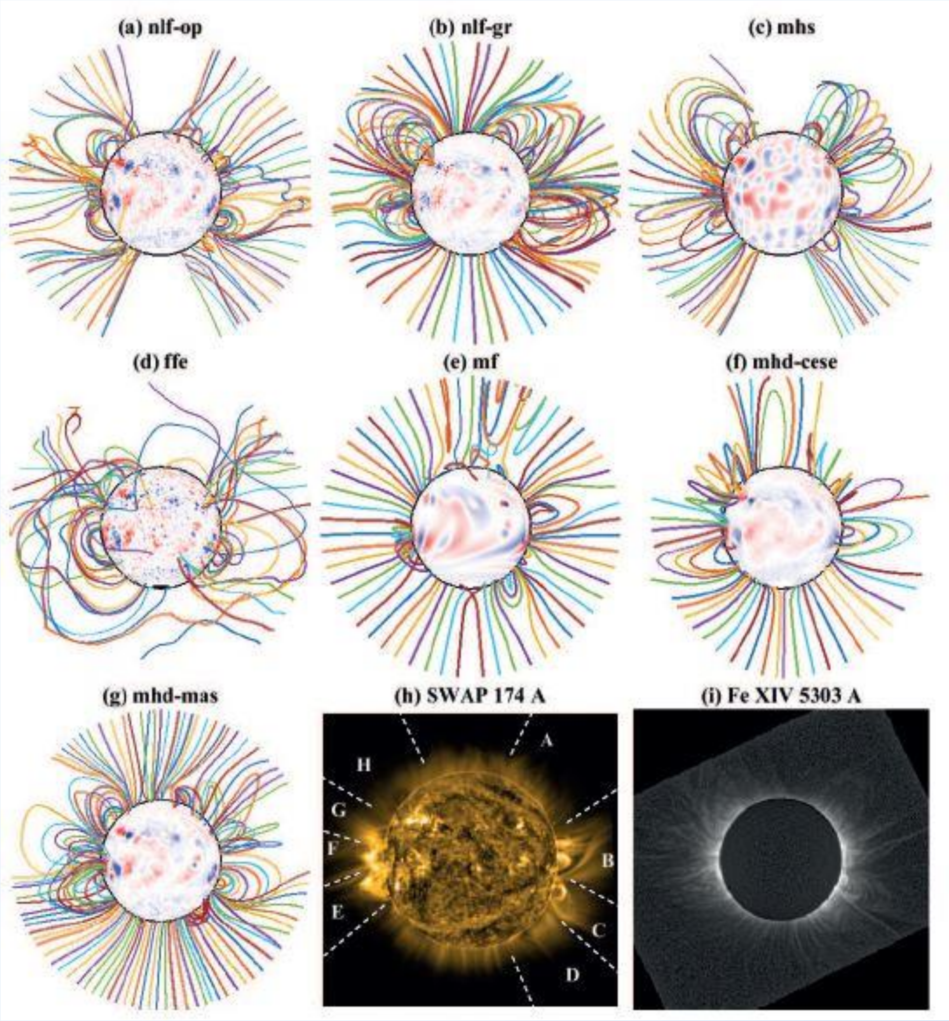

[Yeates 2015]

Spherical harmonics decomposition

In general, planetary fields reconstructed from measurements are expressed as a combination of a potential solution, and a minor correction due to external currents.

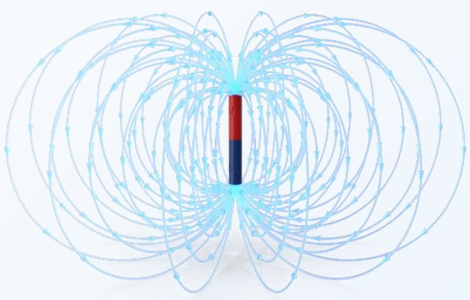

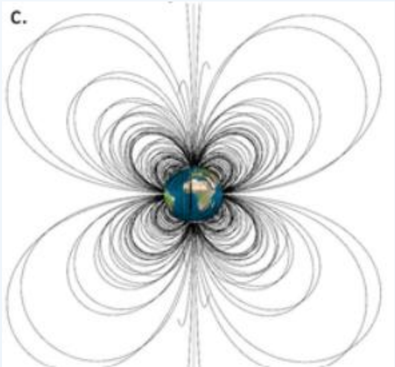

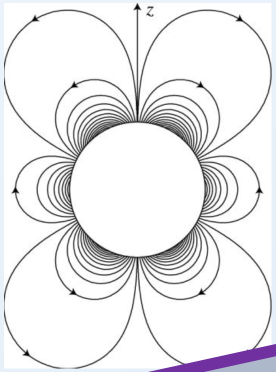

See Albert's hands-on session

$$\mathbf{B} = -\nabla V_p + \mathbf{b}$$

The potential V is a series expansion of spherical harmonic functions that are solutions to Laplace's equation in spherical coordinates (e.g., Chapman & Bartels, 1940):

$$V_p = a \sum_{n=1}^{n_{\max}} \left(\frac{a}{r}\right)^{n+1} \sum_{m=0}^{n} \left\{ P_n^m(\cos\theta) \left[g_n^m \cos(m\phi) + h_n^m \sin(m\phi) \right] \right\}$$

where a is Jupiter's equatorial radius (71,492 km), r is the radial distance to the planet's center, and the angles θ and ϕ are colatitude and longitude, respectively. The P_n^m (cos θ) are Schmidt quasi-normalized associated Legendre functions of degree n and order m, and the g_n^m and h_n^m are the Schmidt coefficients that parameterize the internal magnetic field model. These are presented in units of Gauss or nanoteslas

Magnetism in the Earth

The core is made of molten (outer) and solid (inner) Iron, Nickel, Sulphur; the inner core slowly grows due to long-term cooling.

Sources of heat: residual (from birth), radioactive decay, precipitation of ionized elements.

Sources of electrical currents: convection in the outer core, precipitation/buoyancy of elements.

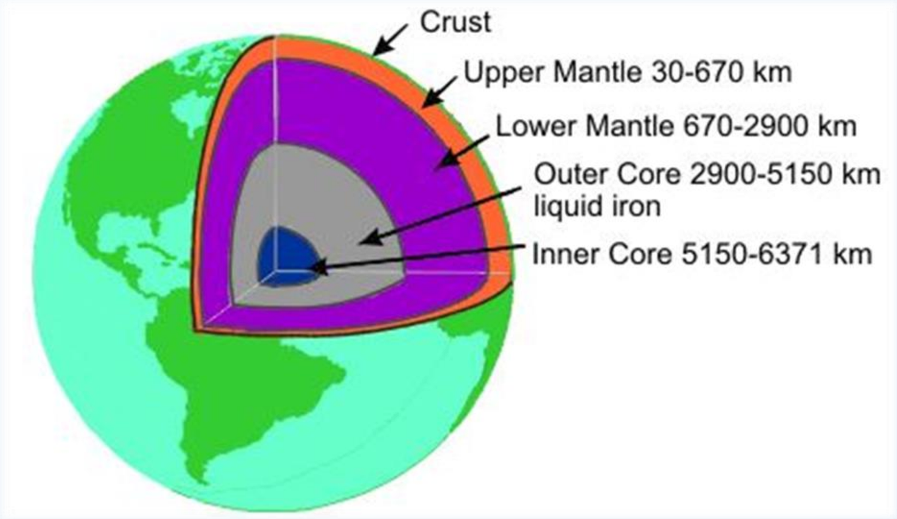

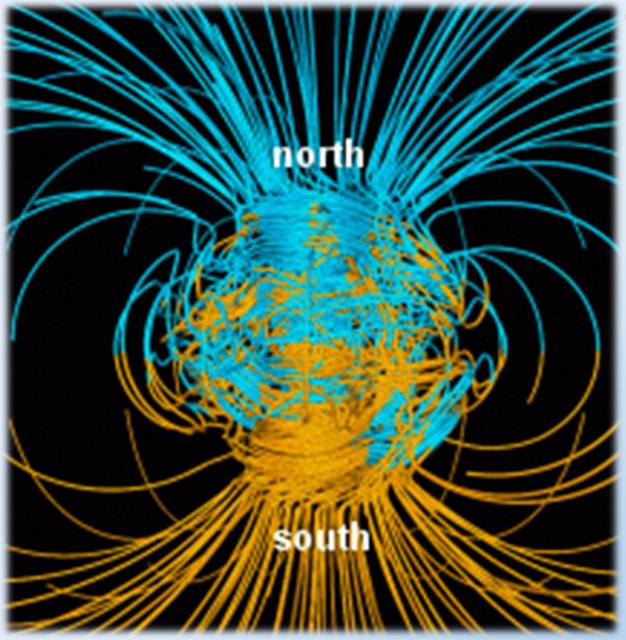

Glitzmayer & Roberts' geo-dynamo model

Magnetism in the Earth: historical perspective

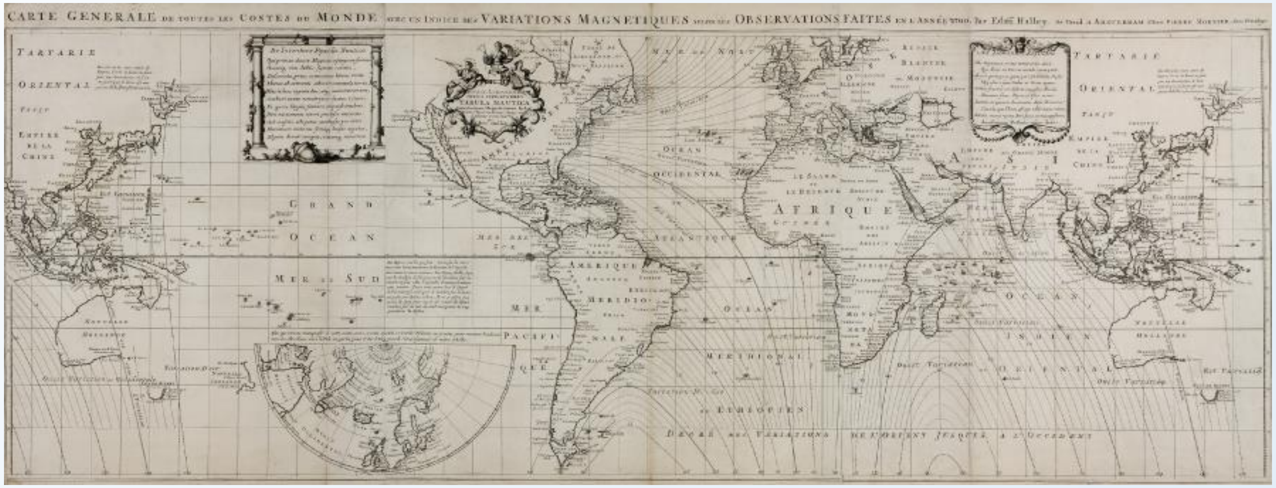

Magnetism began with the study or natural magnets (600 BC in Greece and 300 BC in China)

Geomantism required the realization that there is an ambient magnetic field of the Earth (1st century in China)

Compasses were used since the 10th century in China and 12th century in Europe.

They noticed that the magnetic north did not always point to the north star (geographic north): the Earth seems a slightly tilted magnet.

Then in the 16th century they realized that things were not so simple…

Magnetism in the Earth: current observatories

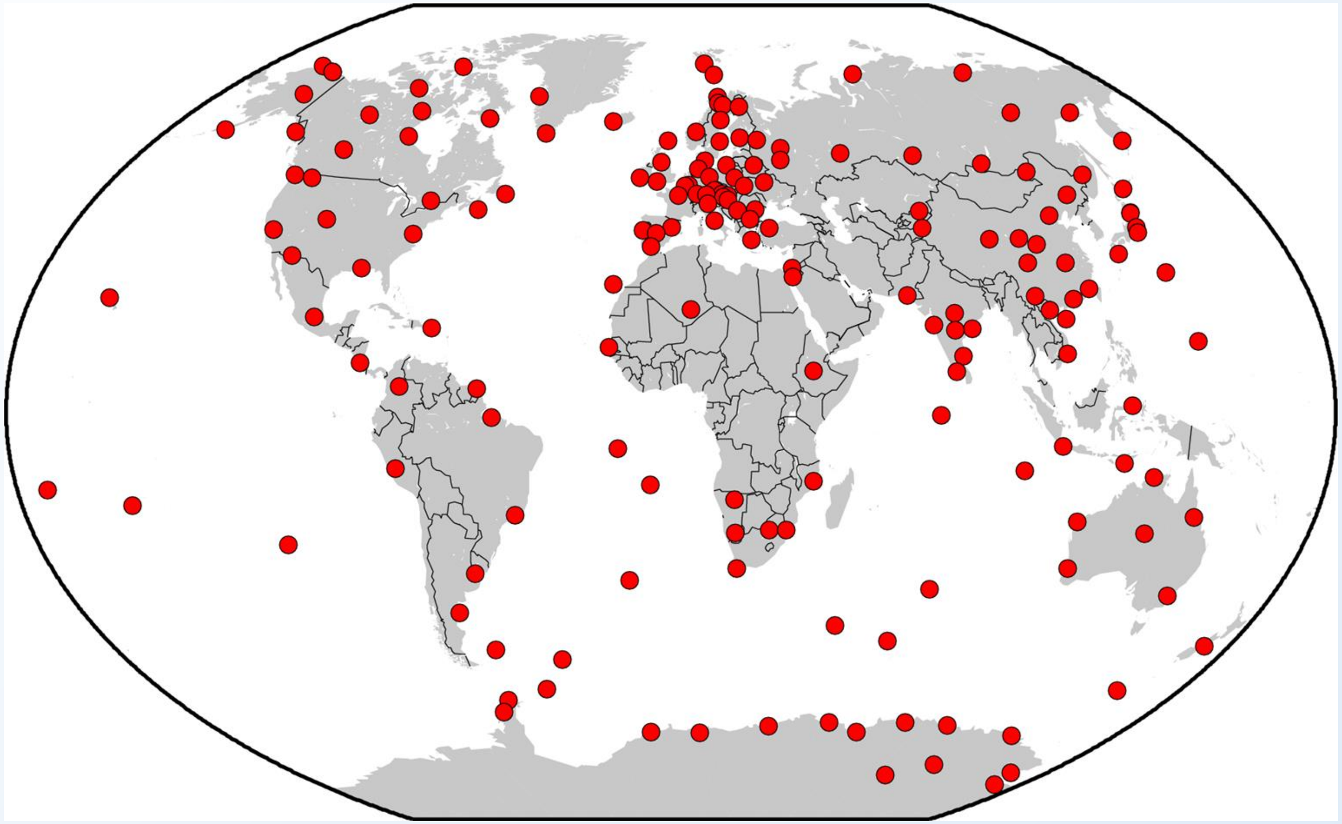

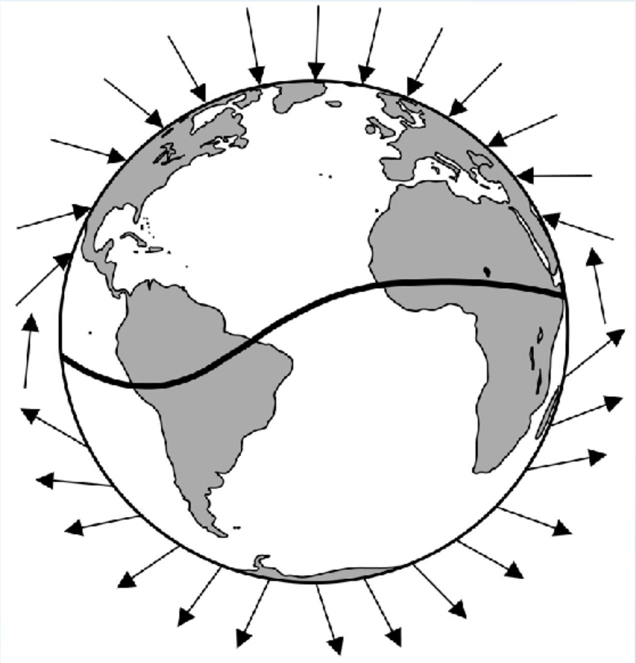

Current Earth observatories: magnetometers that capture the direction and intensity of B.

Does the magnetic field look like a dipole?

Magnetism in the Earth: topology

The magnitude is about 0.5 G, is higher at the poles and lower in the equator.

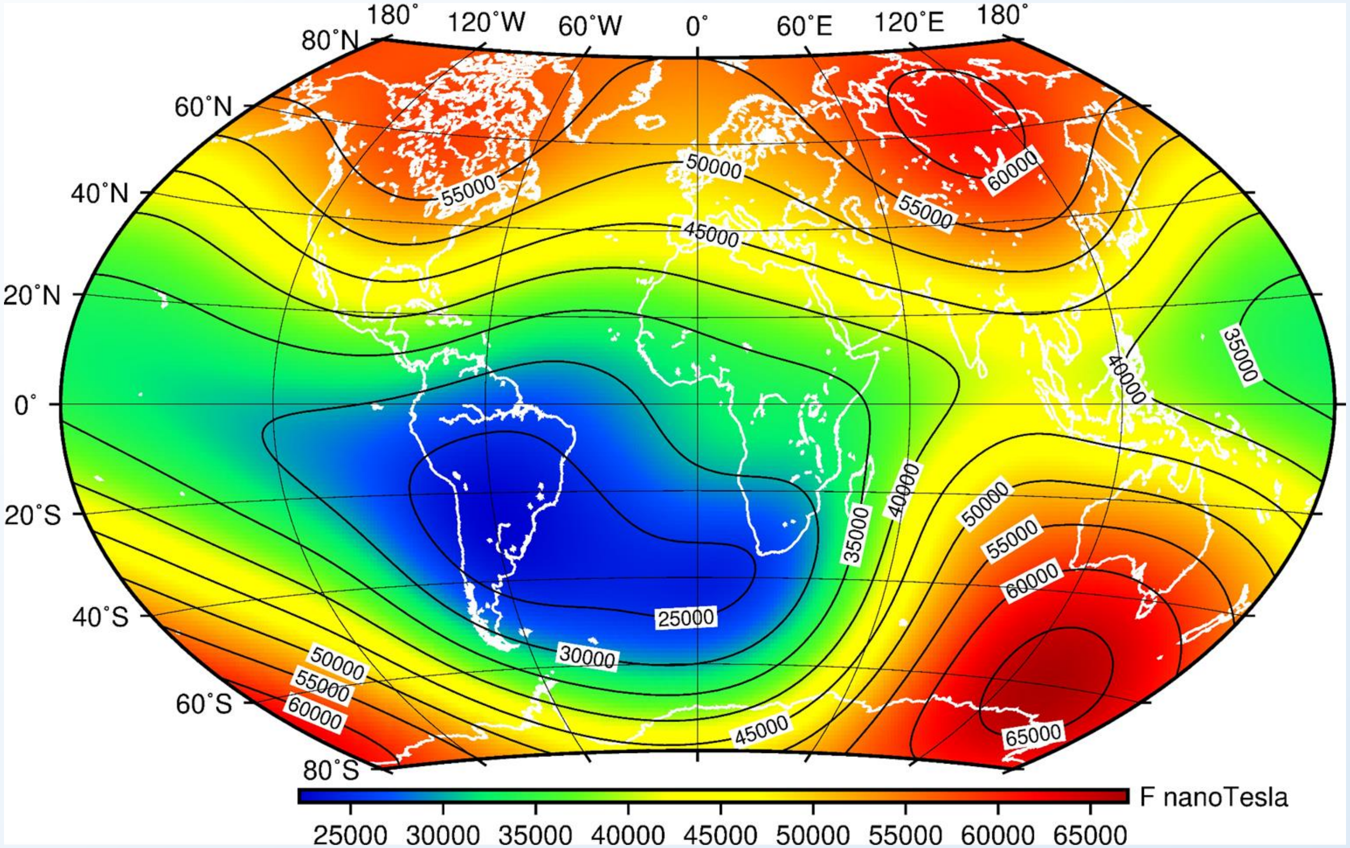

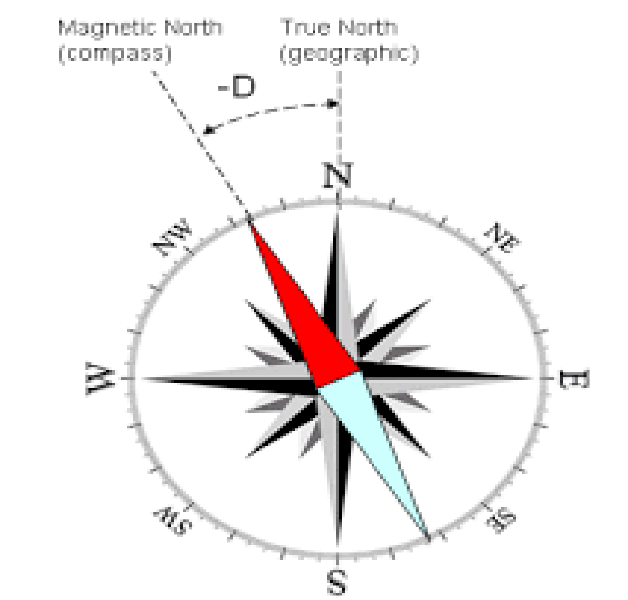

South Atlantic Anomaly (B<0.32 G). Increased flux of energy particles, and exposes orbiting satellites. Van Allen radiation belt change reach deeper in the atmosphere.

Magnetism in the Earth: time variations

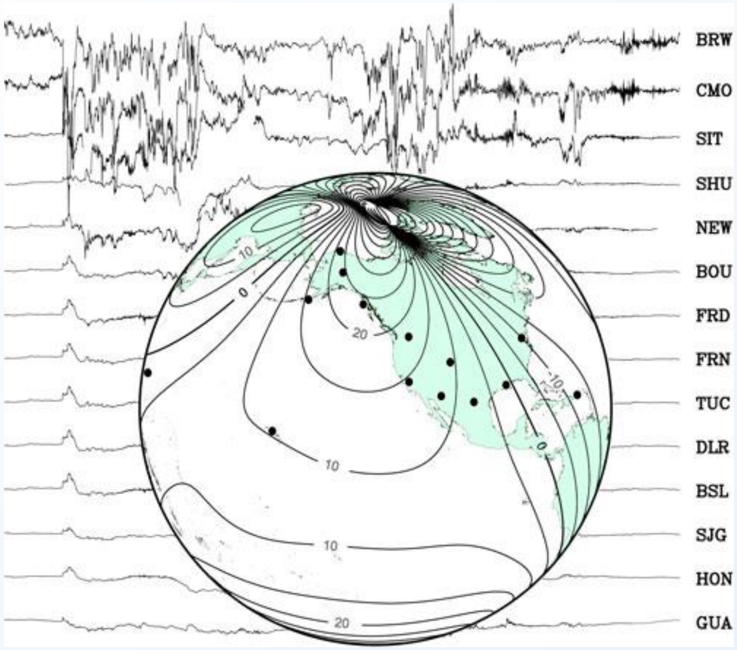

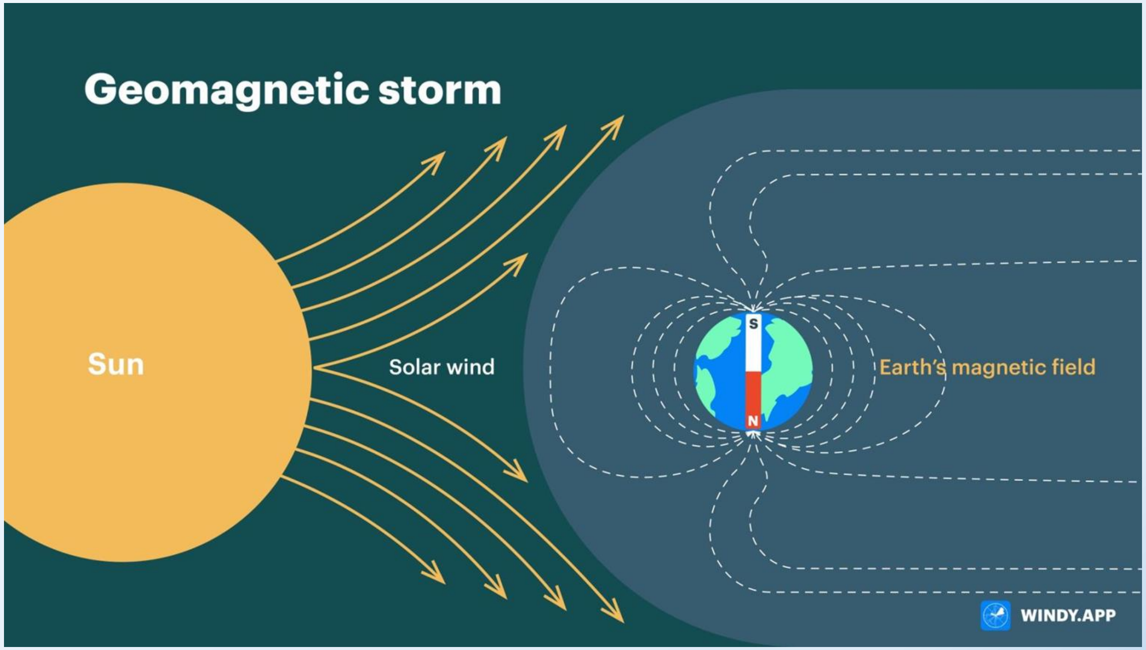

Interactions with solar wind leads to geomagnetic storms (auroras are a symptom of such storms), this is also known as space weather.

See Julián's and Ekaterina's lectures

Magnetism in the Earth: time variations

Surface magnetic field changes notably across years.

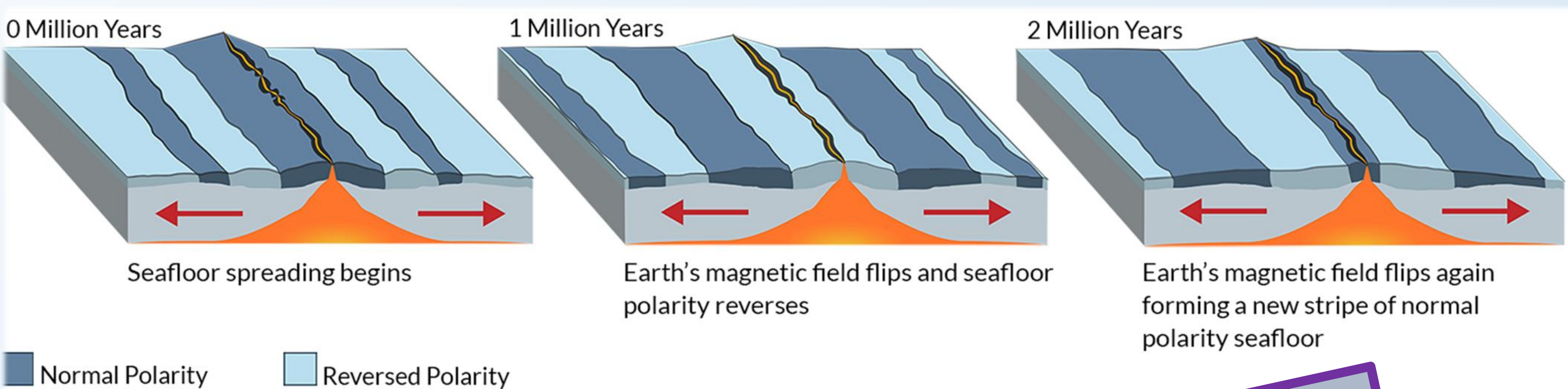

Earth's magnetic field has been there during the last 3.5 billion years at least. Fundamental for habitability

See Sudeshna's lecture

Magnetism on Earth: dynamo & reversal polarity modeling

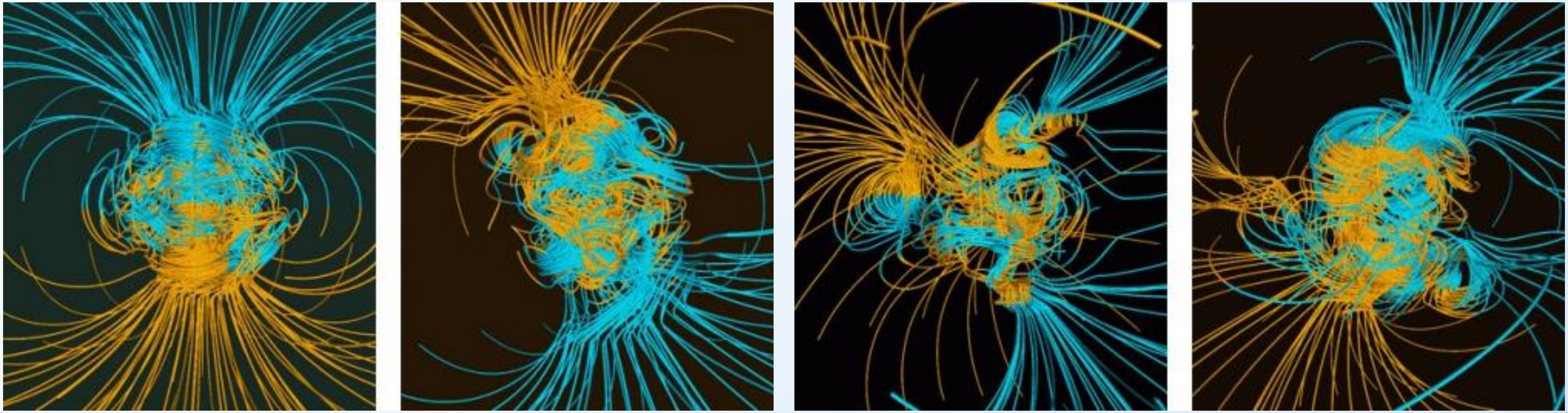

Spontaneous, period reversal of the magnetic field (typical timescales: thousands of years) in the Glatzmeier and Roberts dynamo model. During the reversal, the magnetic field is weaker for some millennia.

Magnetism in Jupiter

Jupiter is well studied, magnetic field of about 10 G:

- Juno collected data in-situ at a low orbit (> 1.2 Rj).
- Strong deviations from a dipole, very asymmetric.
- Allows a reconstruction of the magnetic field outside.
- Indicates a quite shallow dynamo inside, but no details.

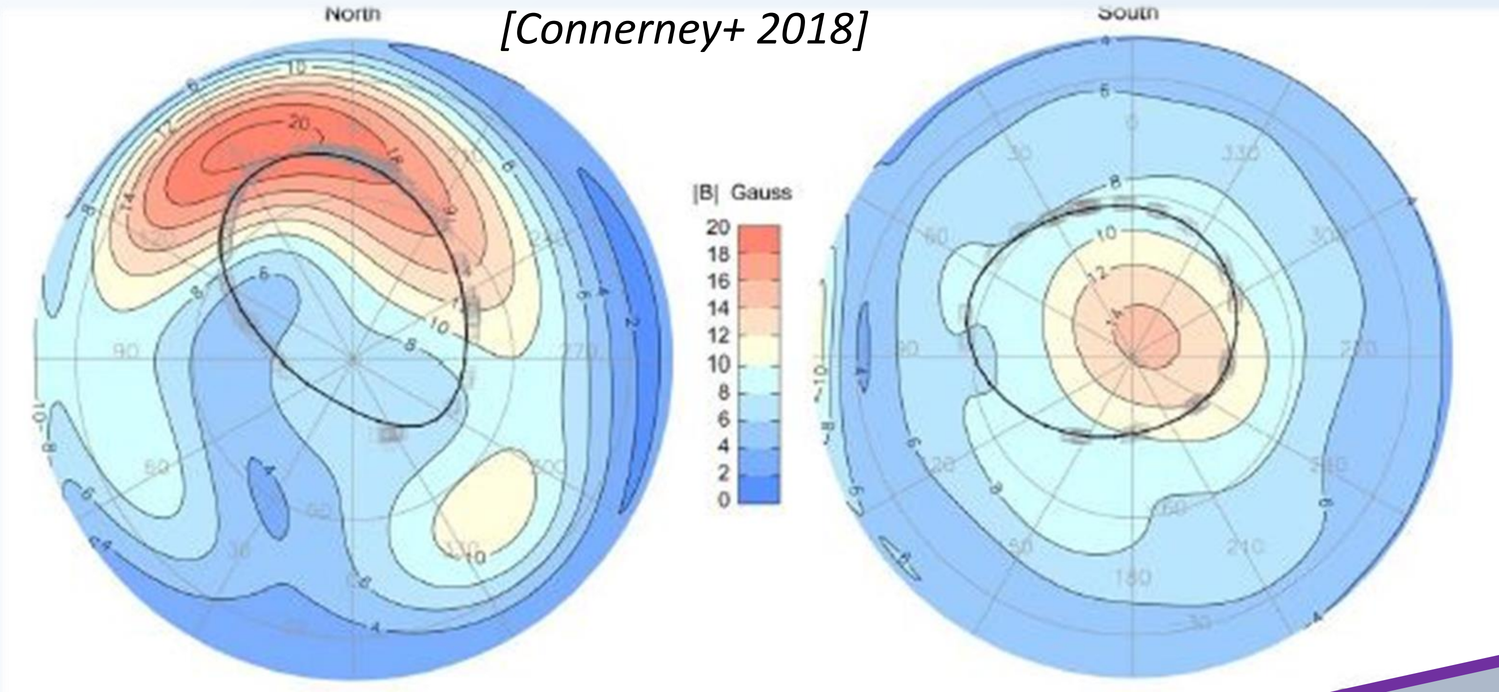

[Connerney+ 2018]

See Albert's hands-on session

The magnetic variety in the Solar system

See Albert's hands-on session

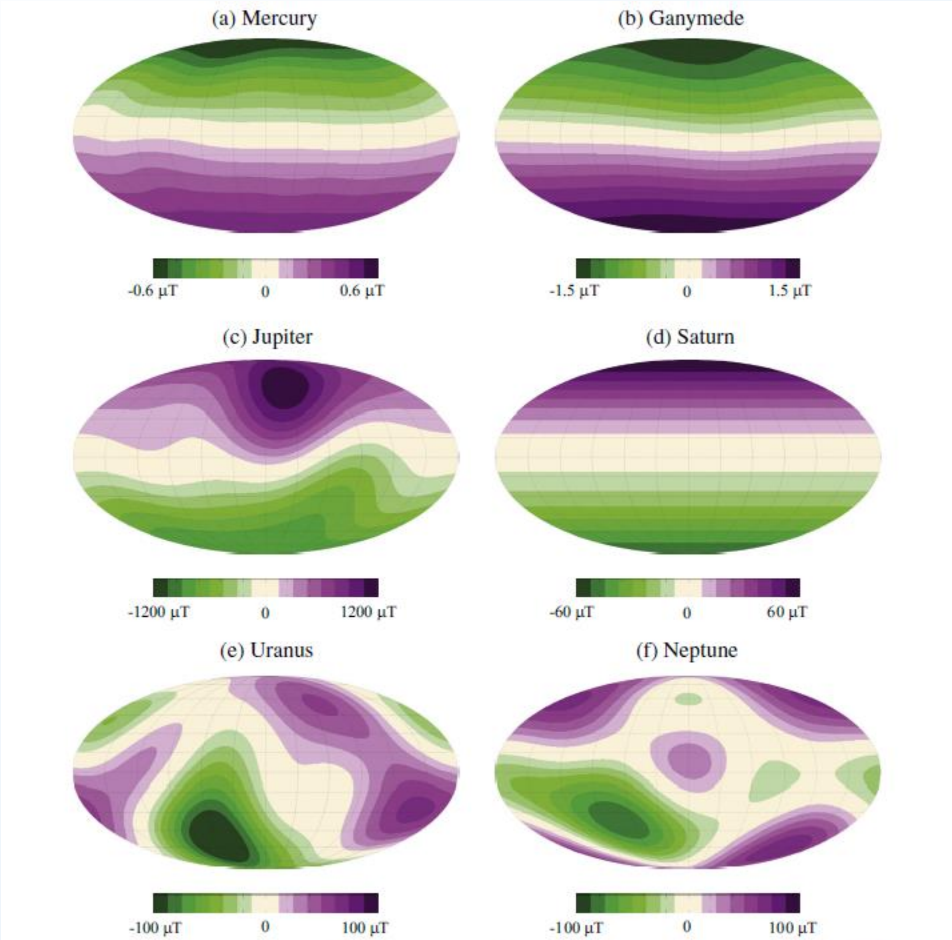

Fig. 2. Radial magnetic field at the surfaces of (a) Mercury, (b) Ganymede, (c) Jupiter, (d) Saturn, (e) Uranus, and (f) Neptune. Data taken from Uno et al. (2009) for Mercury (with spectral resolution $l, m \leqslant 3$), Kivelson et al. (2002) for Ganymede ($l, m \leqslant 2$), Yu et al. (2010) for Jupiter ($l, m \leqslant 3$), Burton et al. (2009) for Saturn ($l, m \leqslant 3$), and Holme and Bloxham (1996) for the ice giants ($l, m \leqslant 3$).

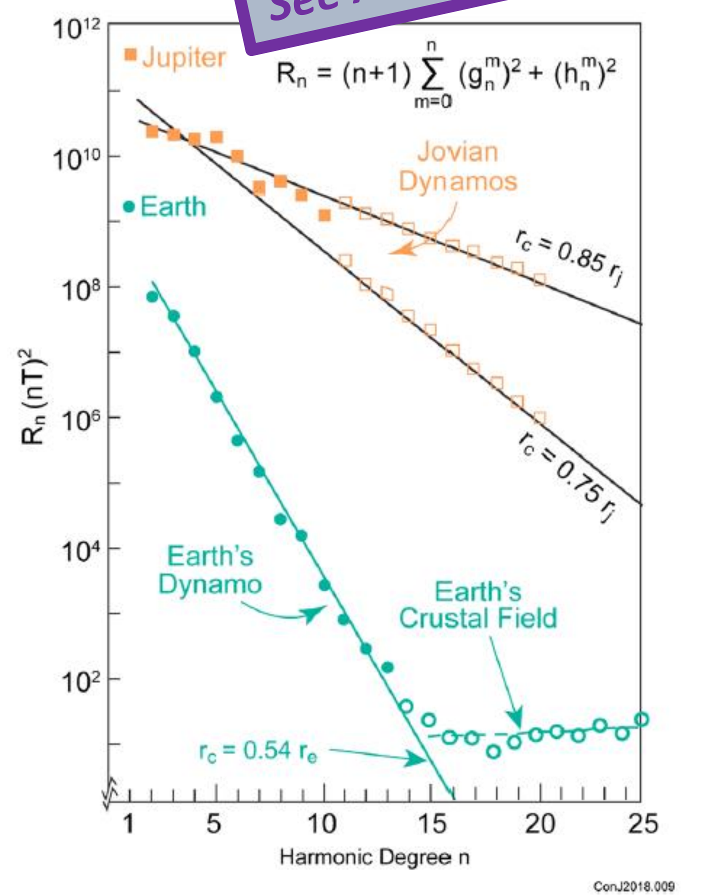

Figure 5. A comparison of the Lowes' spectrum for Earth and Jupiter using the JRM09 model magnetic field through degree/order 10.

[Schubert & Suderlund 2011]

[Connerney et al. 2021]

The magnetic variety in the Solar system

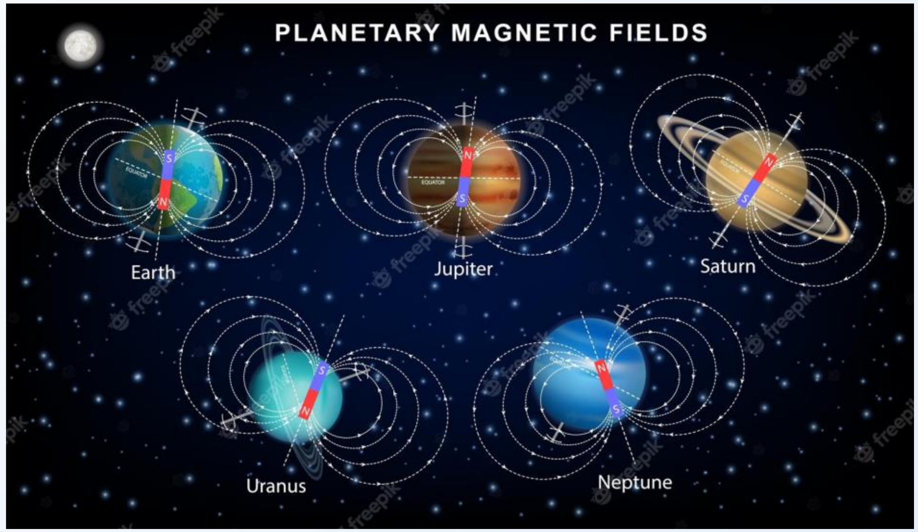

Planet	Mass[1] (10^{24} kg)	Radius[1] (km)	$\overline{\text{Density}}$[1] (kg/m^3)	MOI[2–4]	Surface $\overline{\lvert B_r \rvert}$ (μT)	Dipolarity	Dipole tilt (°)
Mercury	0.33	2440	5.4	0.33	0.30	0.71	3
Venus	4.87	6052	5.2	0.33	–	–	–
Earth	5.97	6371	5.5	0.33	38	0.61	10
Moon	0.07	1738	3.3	0.39	$\lesssim$100	–	–
Mars	0.64	3390	3.9	0.37	$\lesssim$0.1	–	–
Jupiter	1900	69,911	1.3	0.25	550	0.61	9
Io	0.09	1821	3.5	0.38	–	–	–
Europa	0.05	1565	3.0	0.35	–	–	–
Ganymede	0.15	2634	1.9	0.31	0.91	0.95	4
Callisto	0.11	2403	1.9	0.35	–	–	–
Saturn	570	58,232	0.7	0.21	28	0.85	<0.5
Titan	0.13	2575	1.9	0.34	–	–	–
Uranus	87	25,362	1.3	0.23	32	0.42	59
Neptune	100	24,624	1.6	0.23	27	0.31	45

[Schubert & Suderlund 2011]

Low-mass stars

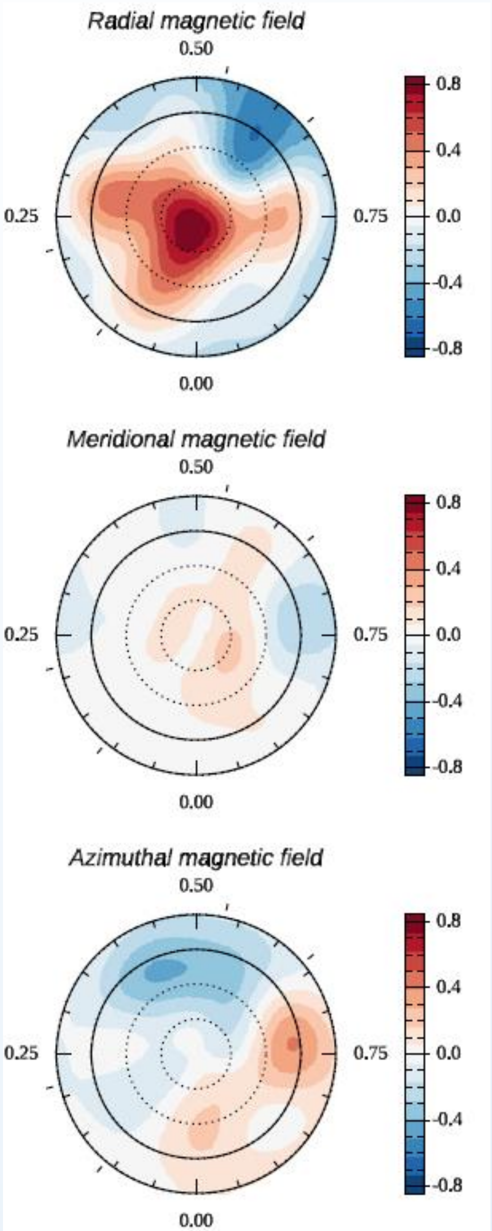

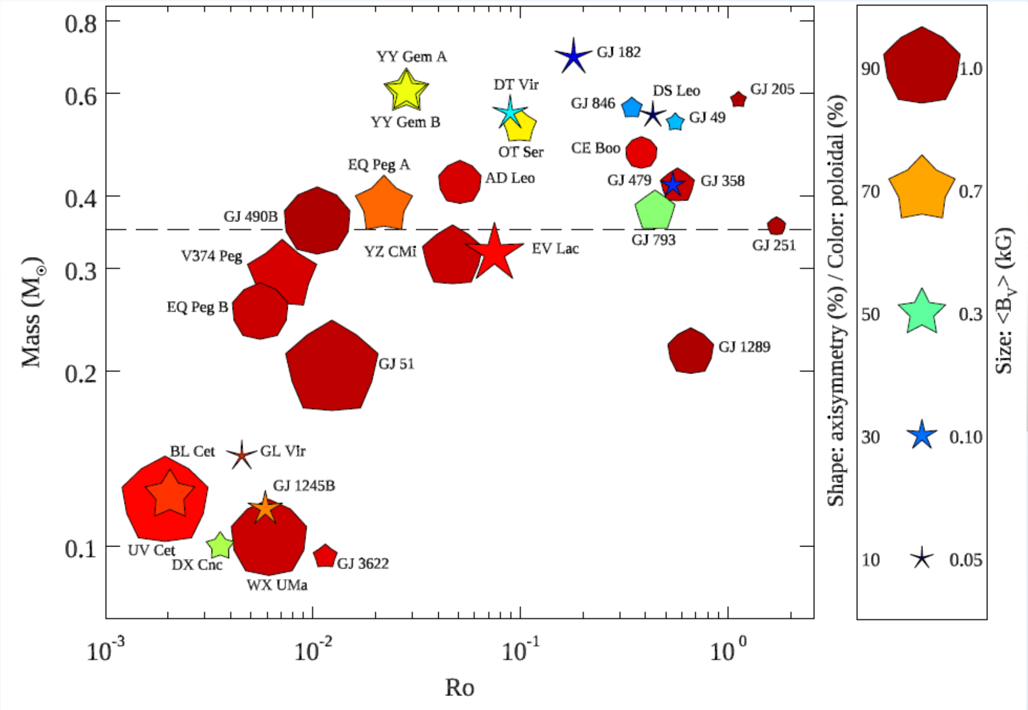

Fig. 14 Properties of the global magnetic field topologies of M dwarfs obtained with the ZDI modelling

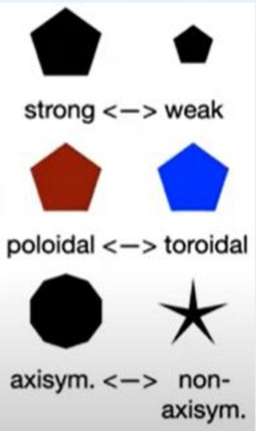

[Kochakhov 2021]

Zeeman-Doppler imaging can reconstruct the surface topology

- Many of them show activity and cycles
- Intensity up to kG
- High variability
- Complex topology
- Rotation-activity relation (saturating at short periods)

See Rim’s and Julián’s lectures

Low-mass stars

- Clear correlation with period (inverse of Rossby number)
- **Correlation with activity indicators: Lx, Hα, Ca lines**

See Rim's lecture

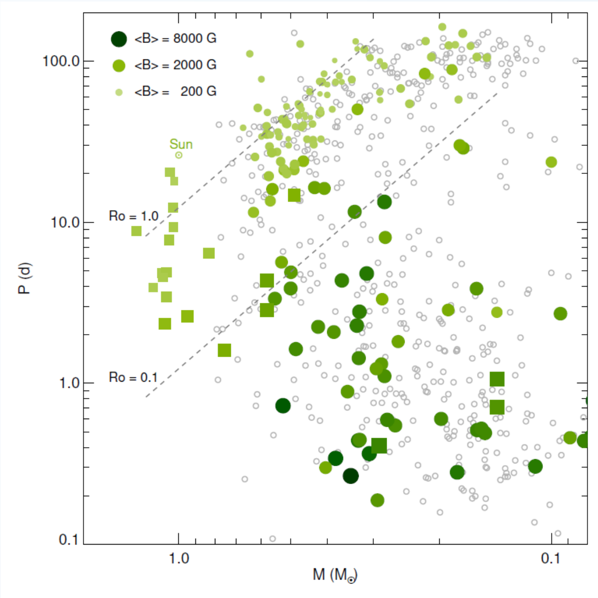

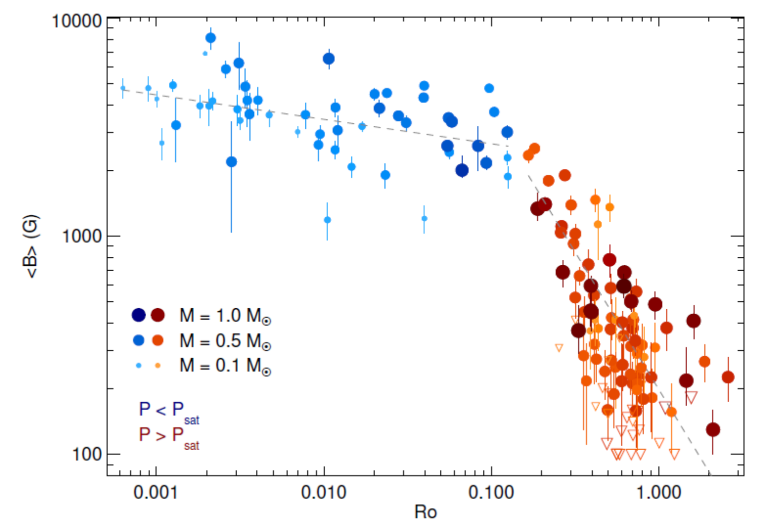

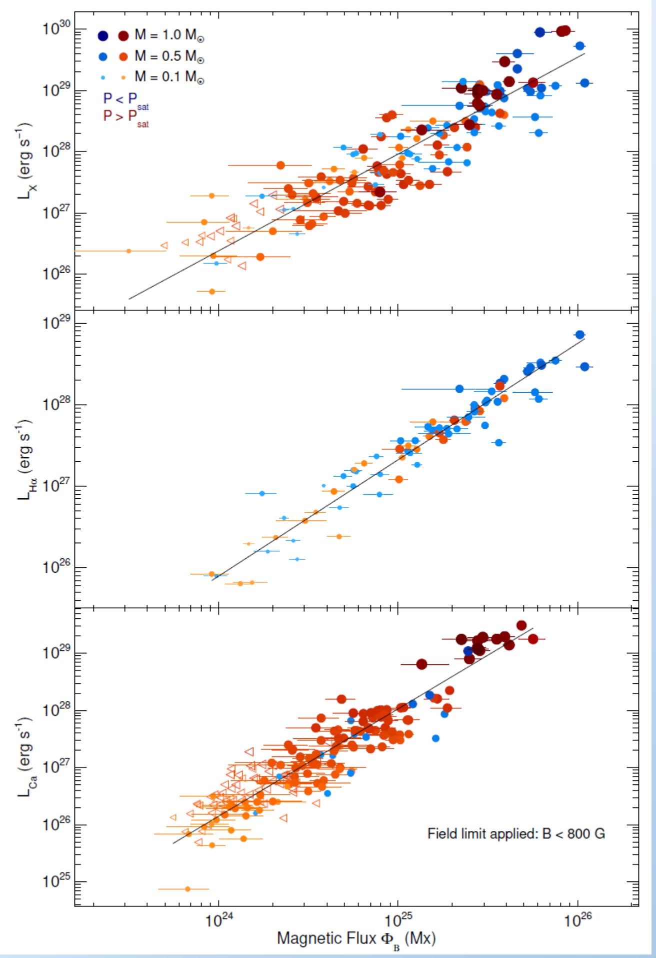

[Reiners+ 2022]

Intermediate and high-mass stars

- Mostly non-magnetic
- Magnetic fields seen almost only in Ap/Bp stars (chemically peculiar) and in some massive OB stars (up to tens kG)
- Large-scale, no variability (exception in figure)
- The magnetic ones are slower rotators than non-magnetic
- Compatible with fossil fields origin
- Relevant for initial magnetic fields in compact objects (white dwarfs and neutron stars)

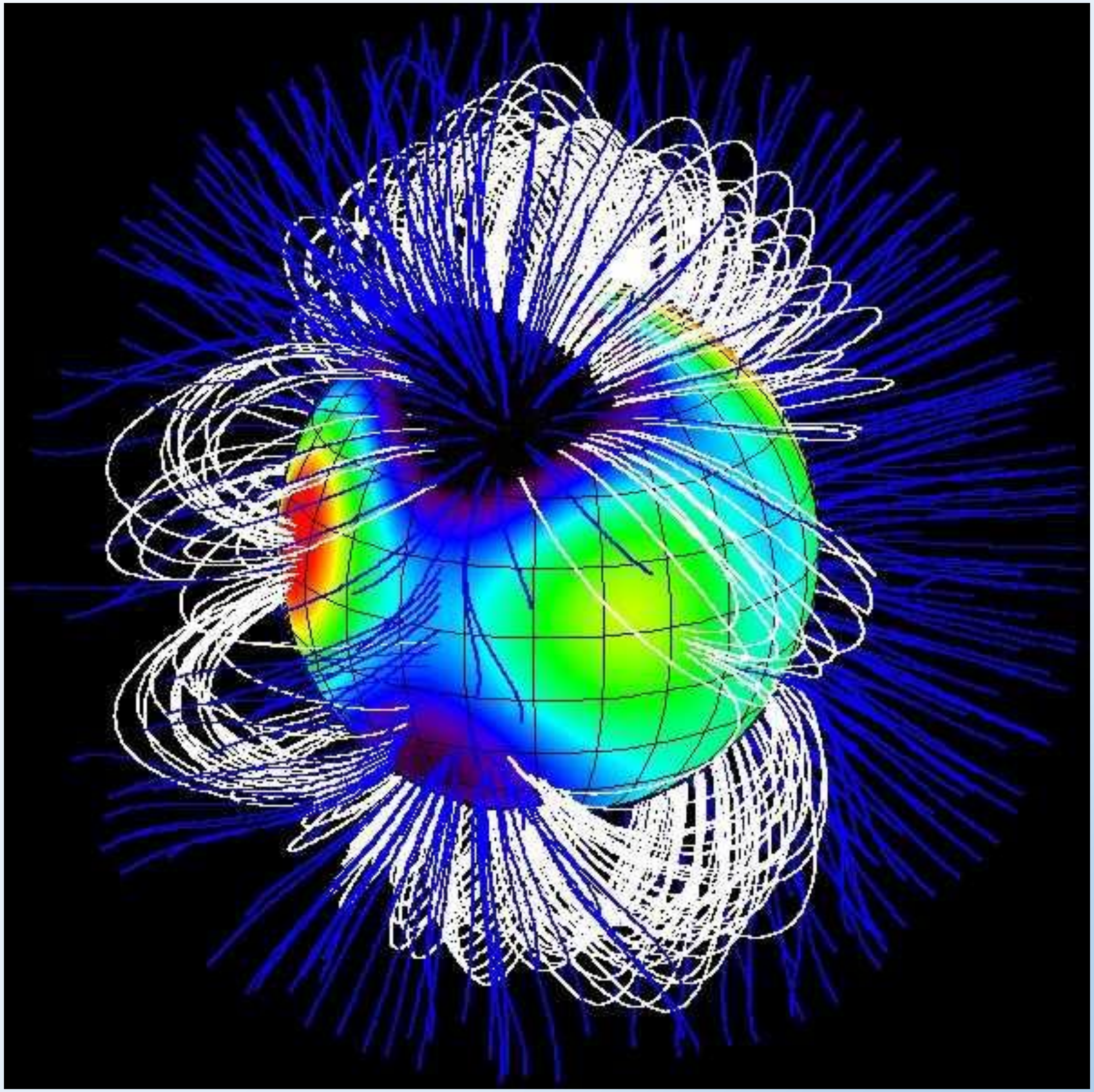

[B star Tau Scorpii, 15 solar masses, X-ray bright Image credit: M. M. Jardine/J. F. Donati]

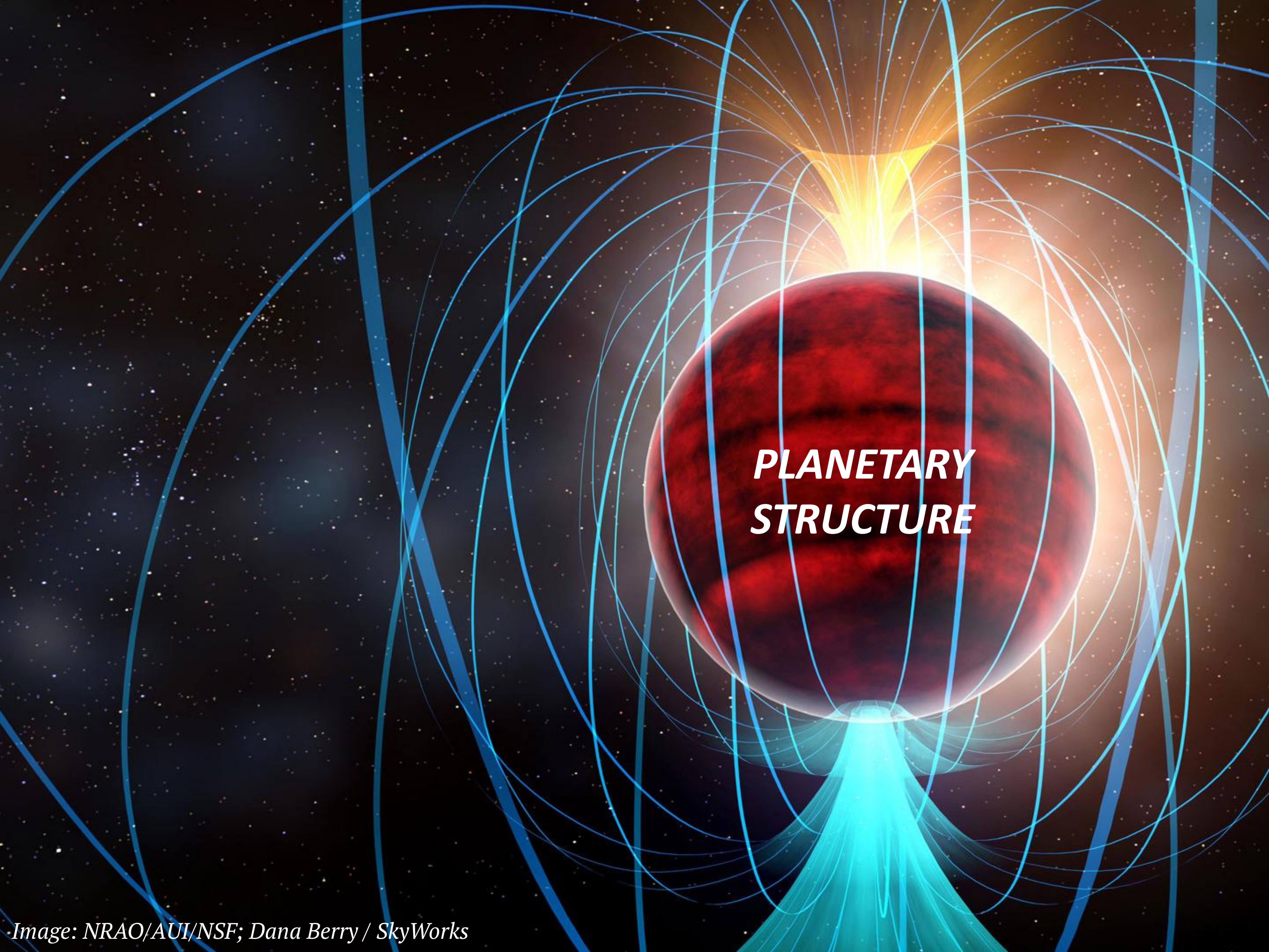

Image: NRAO/AUI/NSF; Dana Berry / SkyWorks

Planetary internal structure & cooling

Planets are born very hot and slowly cool down from the surface, shrinking if they are gaseous.
The evolution is solved as a series as hydrostatic, spherically symmetric (= 1D) solution of the following equations (mass, momentum and energy), complemented by an equation of state, who relates P with T, density and depends on the composition

$$\frac{\partial r}{\partial m} = \frac{1}{4\pi r^2 \rho},$$

$$\frac{\partial P}{\partial m} = \frac{-Gm}{4\pi r^4},$$

$$\frac{\partial L}{\partial m} = -T\frac{\partial S}{\partial t}.$$

Here r is the radius of a mass shell, m is the mass of a given shell, ρ is the local mass density, P is the pressure, G is the gravitational constant, L is the planet's intrinsic luminosity, T is the temperature, S is the specific entropy, and t is the time.

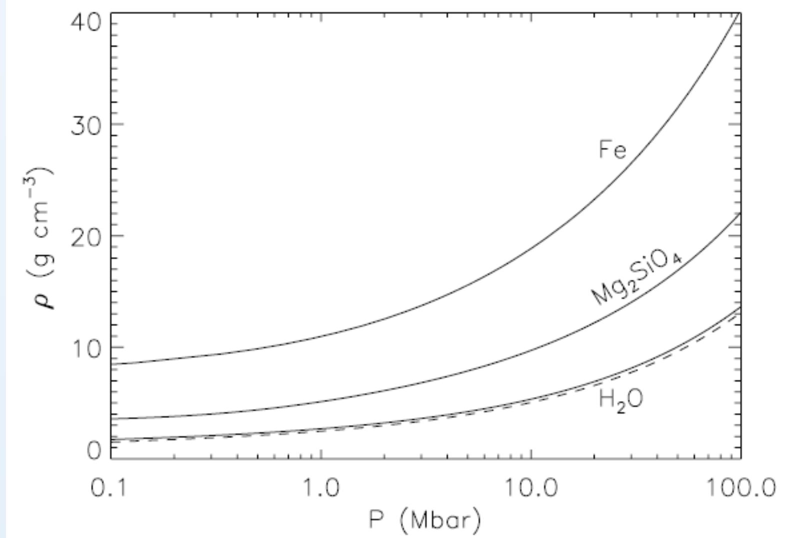

FIG. 1.—Zero-temperature pressure-density relations for iron (Fe), rock (Mg_2SiO_4), and water ice (H_20). For ice, the dashed curve shows our EOS with the thermal correction described in § 4.1.

[Fortney et al. 2007]

Magnetic fields are strongly related to convective motion. Convection requires a steep temperature gradient (Schwarschild criterion):

$$\left|\frac{dT}{dr}\right| < \frac{T}{P}\left|\frac{dP}{dr}\right|\left(1 - \frac{1}{\gamma_{ad}}\right)$$

Rocky planets

Plate tectonics (Earth), in which the crust is brittle enough respond to mantle convective motion, is thought to play an important role in enhancing the cooling.
Conversely, stagnant lid in Venus could be associated to its absent magnetic fields.

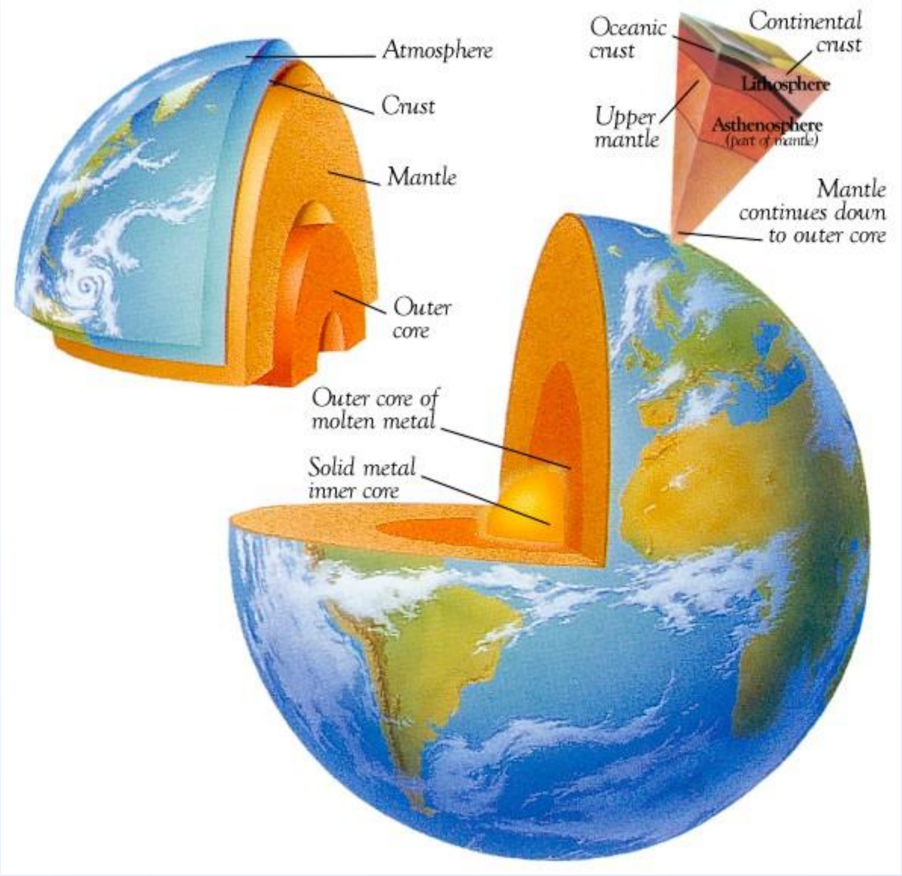

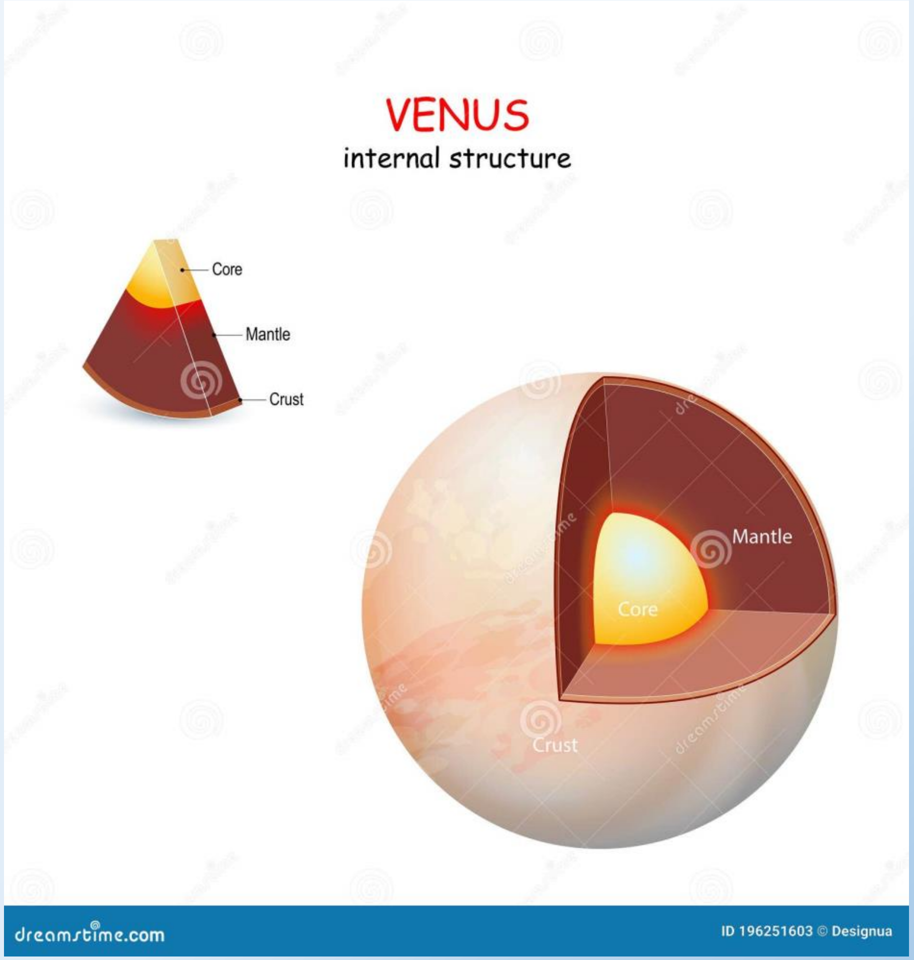

Gas giants: internal structure

At high pressures (50-100 GPa, i.e. 0.5-1 Mbar), the pressure is so high that hydrogen becomes metallic.

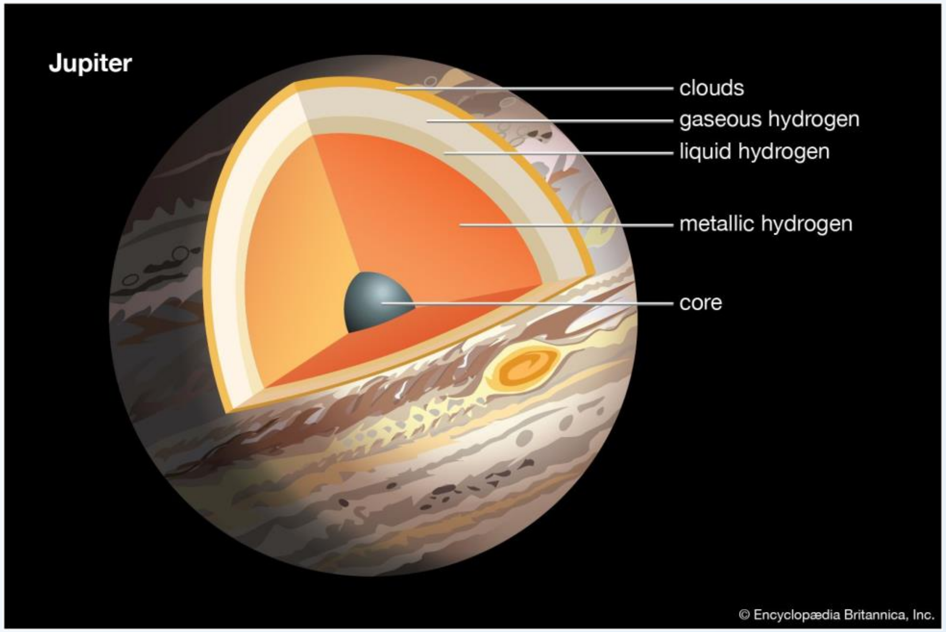

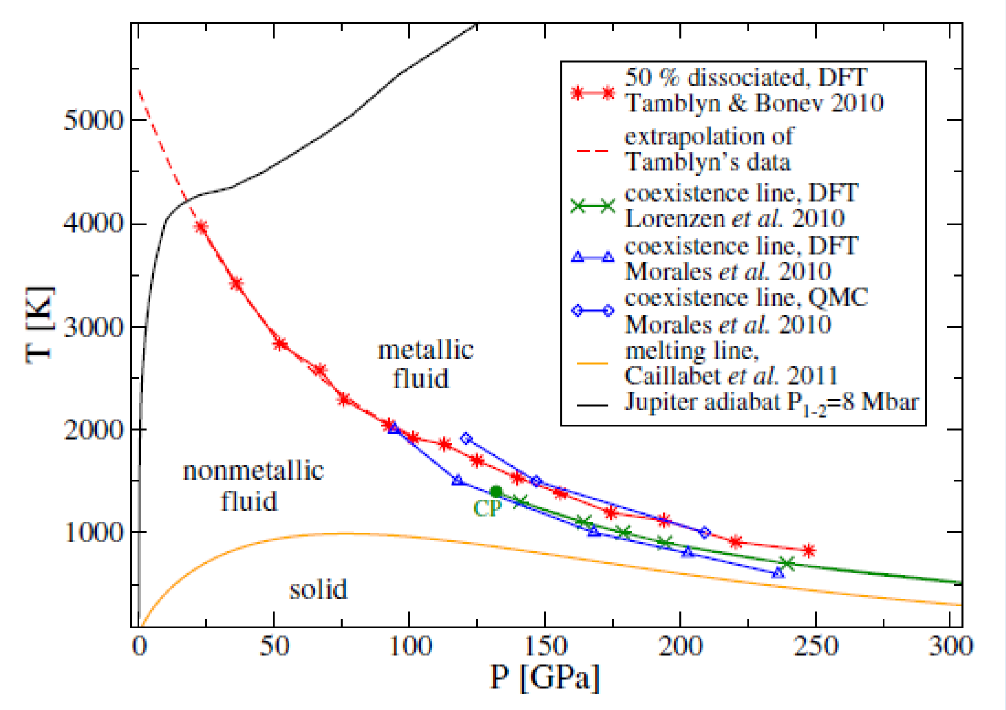

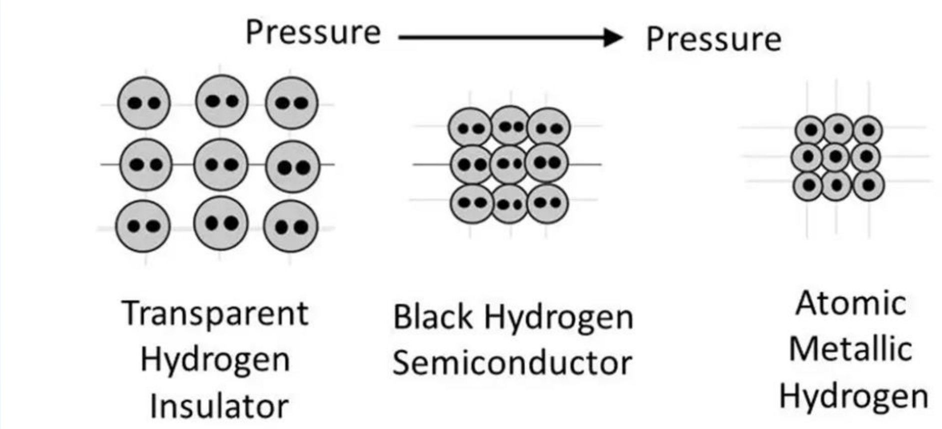

[French et al. 2012]

Conductivity

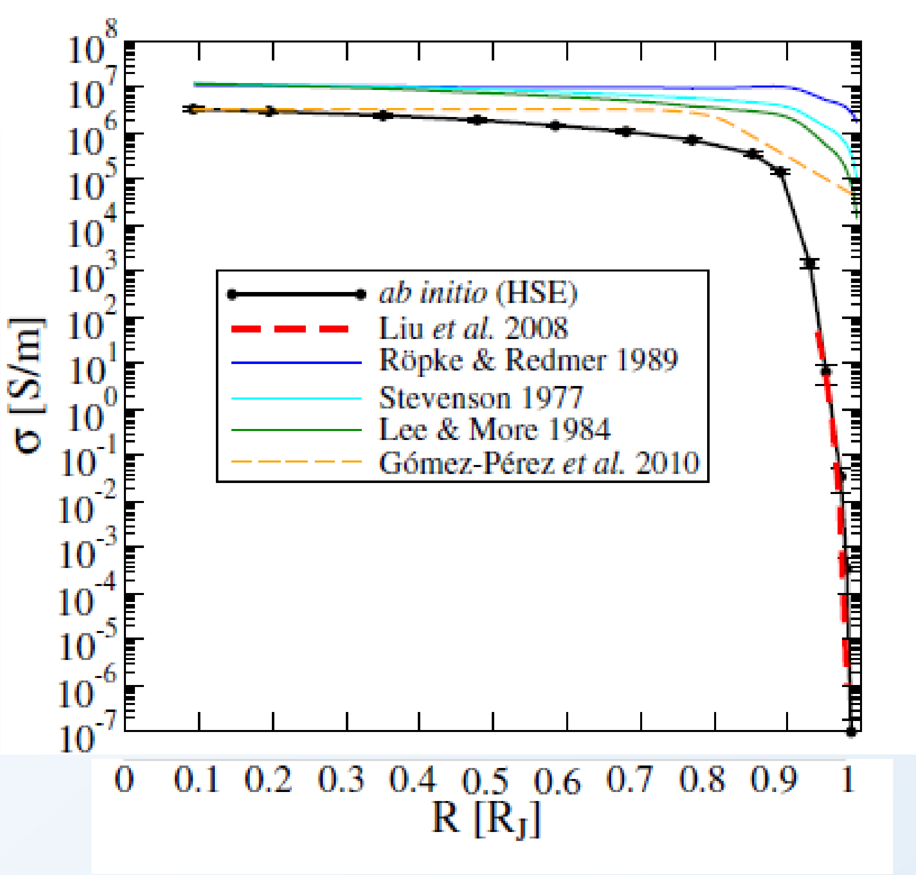

[French et al. 2012]

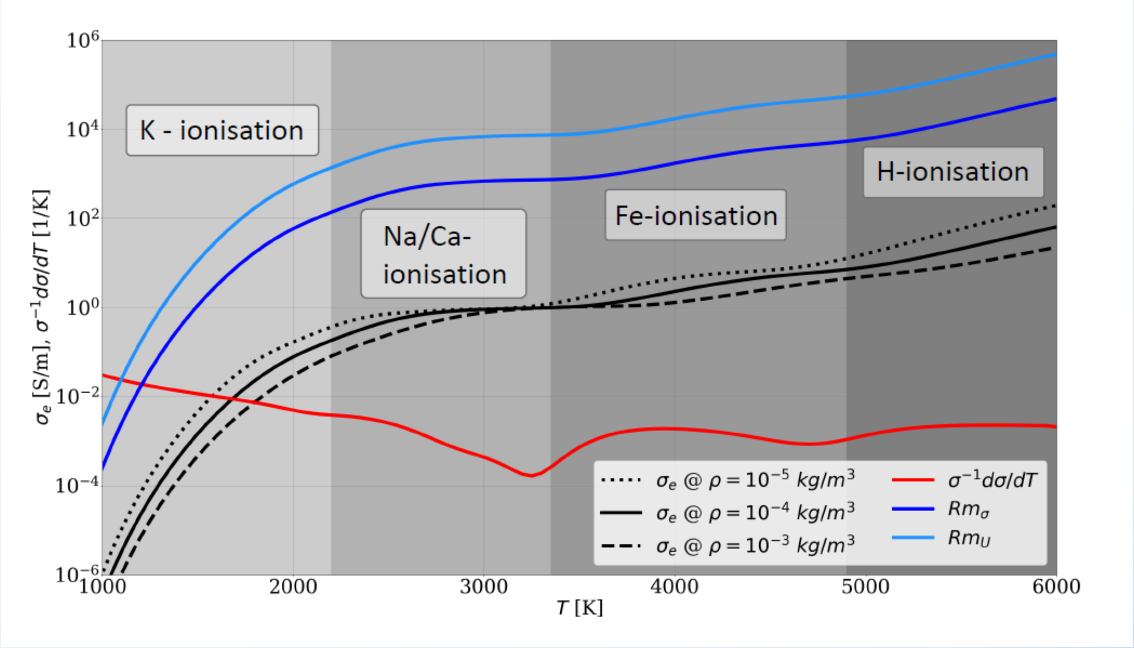

[Dietrich et al. 2022]

In the interior (metallic H) the conductivity is very high. In the atmosphere, we need high temperature to ionize Alkaline metals (possible in Hot Jupiters).

Magnetism in Jupiter: modeling

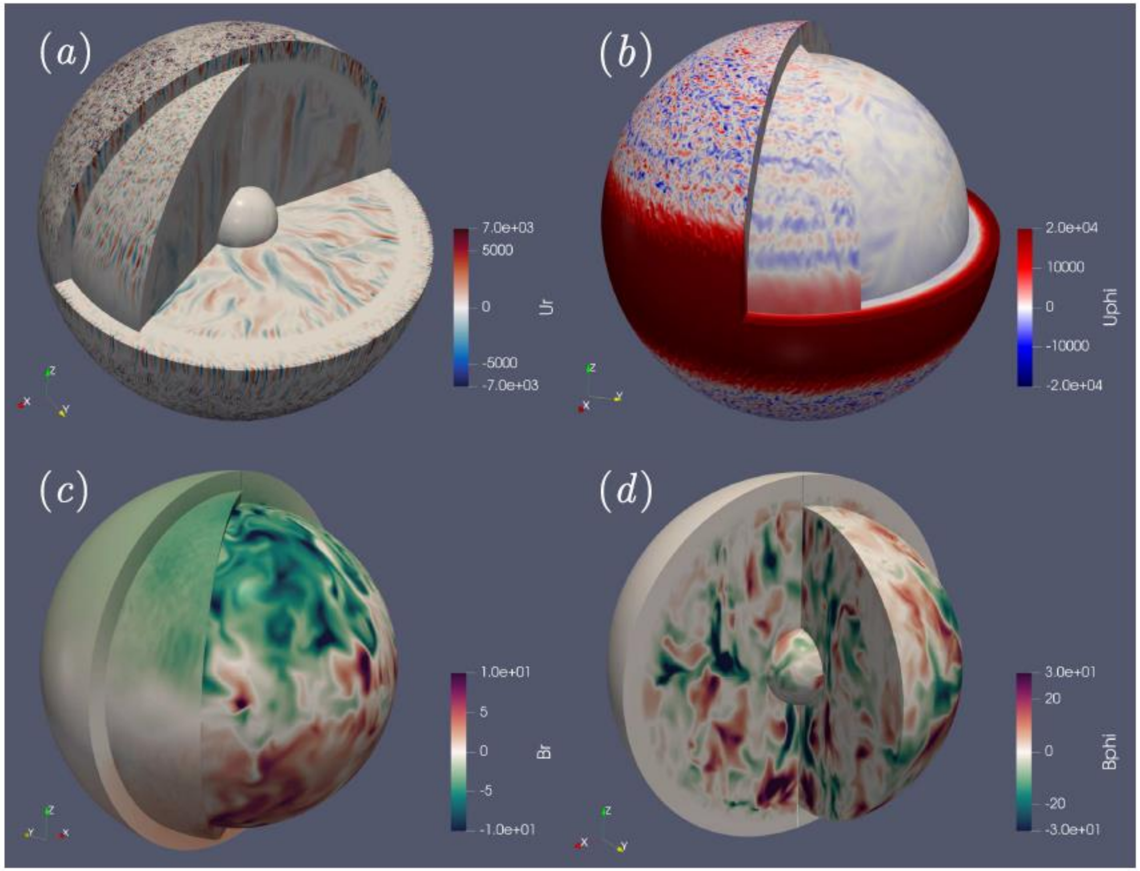

Figure 4: 3-D renderings of the radial velocity u_r (a), of the azimuthal velocity u_ϕ (b), of the radial component of the magnetic field B_r (c) and of the azimuhtal component of the magnetic field B_ϕ (d). The inner sphere in panels (a) and (d) is located very close to the inner boundary at $r = r_i + 0.01$, while in panel (b) and (c) it depicts the lower boundary of the SSL. The intermediate radial cut that spans 30° in longitude in panels (a)-(c) and 90° in panel (d) is located close to the upper boundary of the stably-stratified layer at $r = 0.904\, r_o$. The external radial cut corresponds to $r = 0.992\, r_o$ in panel (a) and to the surface r_o in the other panels.

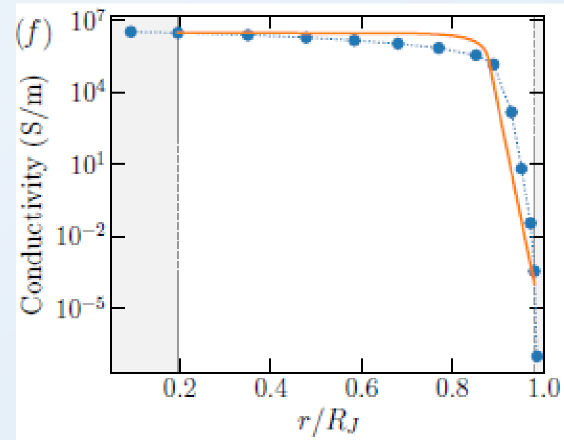

Modelling the details of Jovian magnetic field is very challenging. The latest results (partially) takes into account the internal structure (density, conductivity)

[Gastine et al. 2020]

Magnetism in Jupiter: modeling

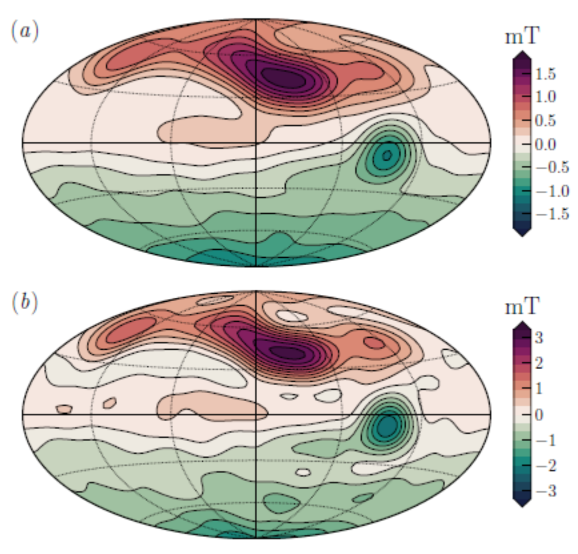

Figure 1: Hammer projections of the radial component of the magnetic field at the surface of Jupiter (upper panel) and at $0.9\,R_J$ (lower panel). These maps have been recontructed using the JRM09 Jovian field model by Connerney et al. (2018).

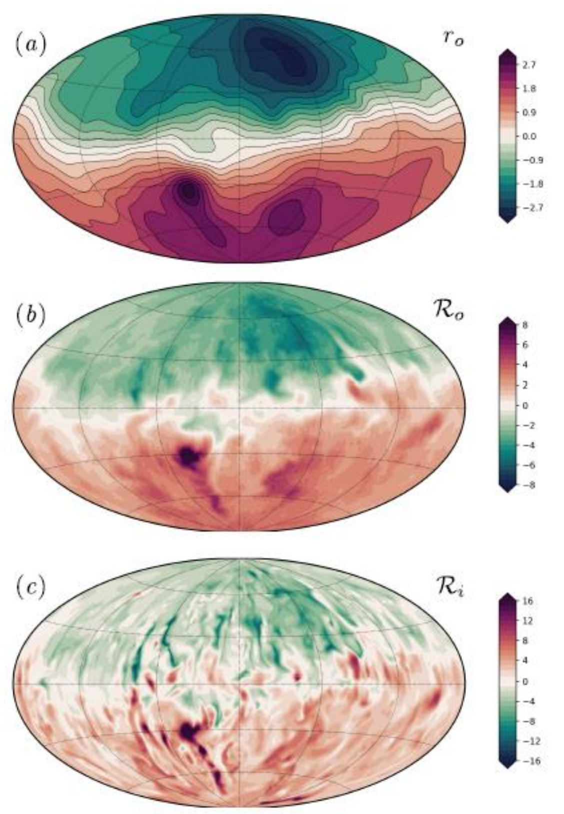

Figure 9: Hammer projection of the radial component of the magnetic field at the surface (*a*), at the upper edge of the SSL $r = \mathcal{R}_o$ (*b*) and at the lower edge of the SSL $r = \mathcal{R}_i$ (*c*).

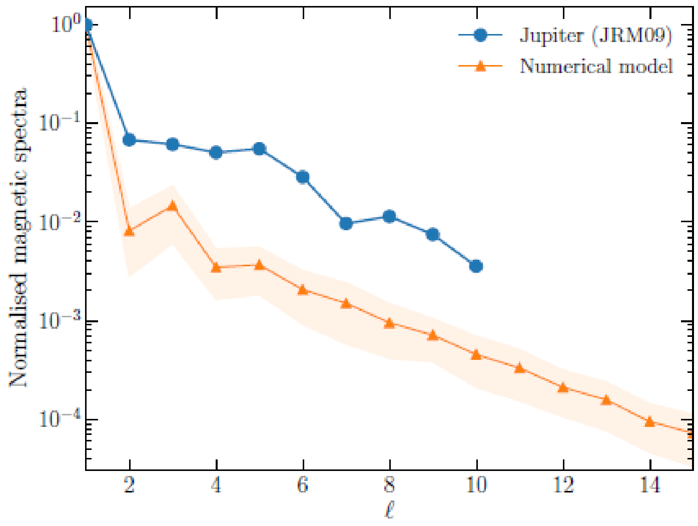

Figure 8: Comparison of normalised time-averaged magnetic spectra at the surface of the numerical model with the Jovian magnetic field model JRM09 by Connerney et al. (2018) for the first 15 harmonic degrees. The shaded regions correspond to one standard deviation across the time-averaged values.

[Gastine et al. 2020]

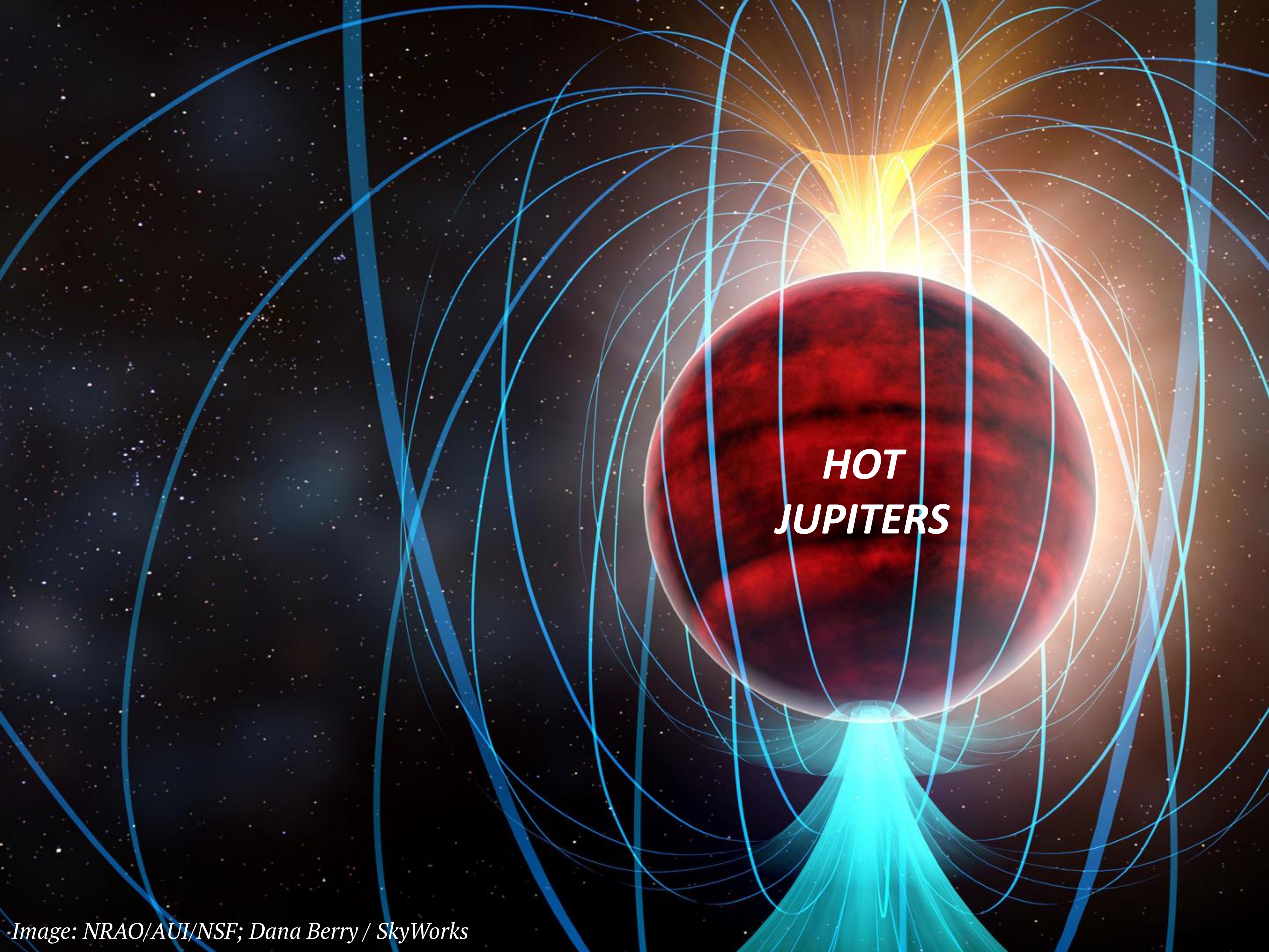
HOT
JUPITERS
Image: NRAO/AUI/NSF; Dana Berry / SkyWorks

Hot Jupiters

Photometry can allow one to reconstruct the temperature map.
The hottest point is often displaced eastward some degrees from the substellar point.

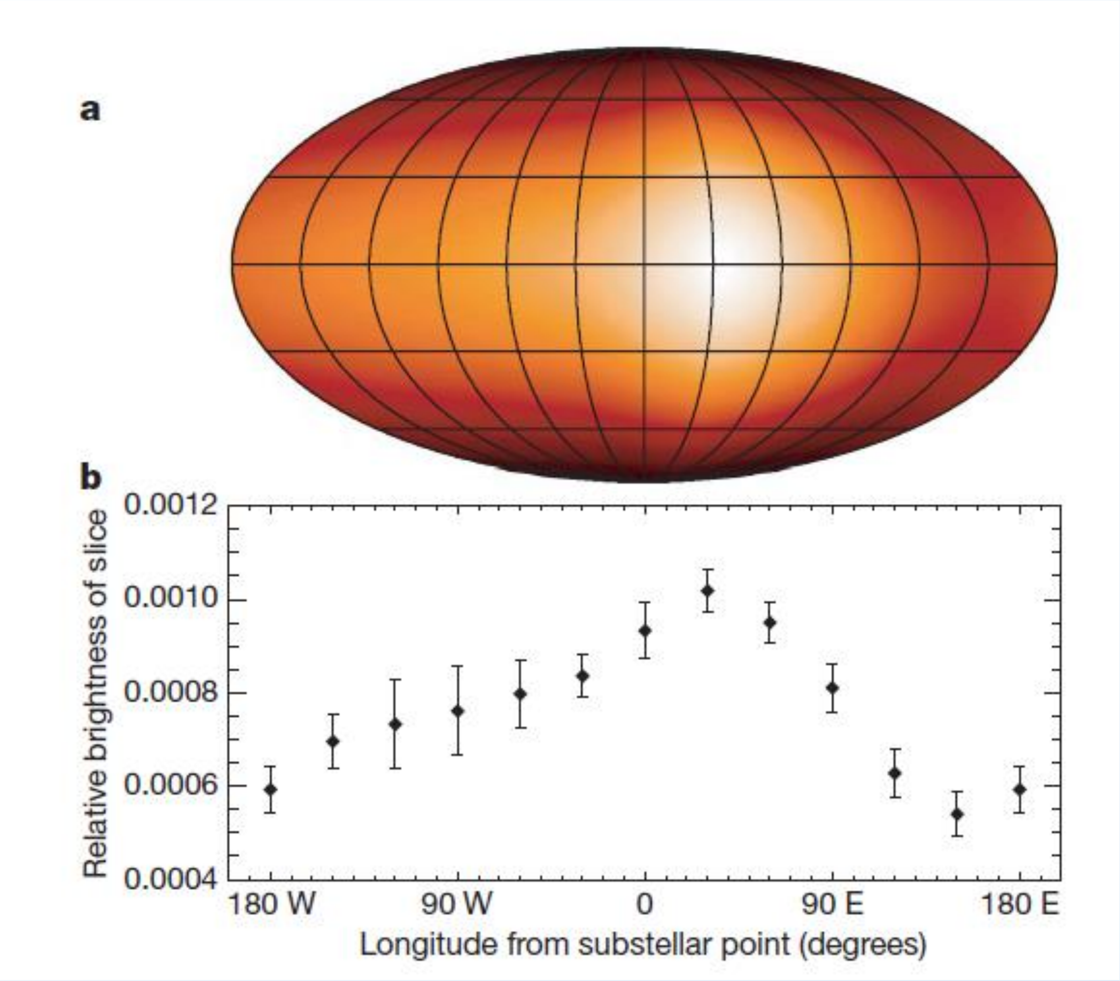

[Knutson et al. 2007]

See Lisa's lecture

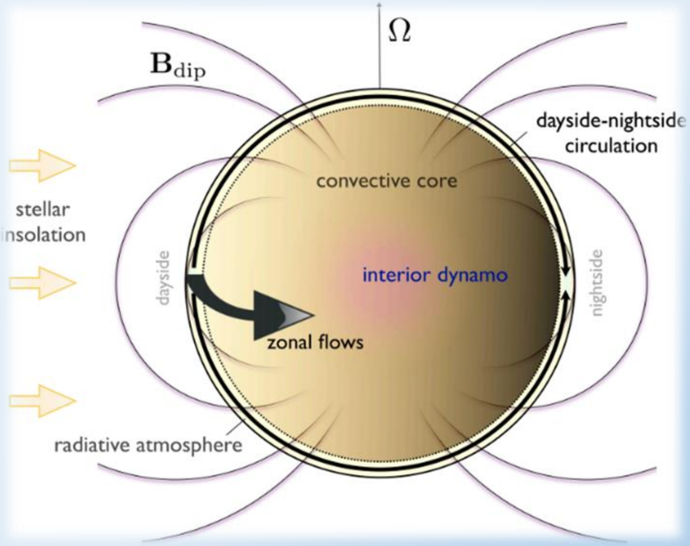

[Batygin et al. 2013]

Global circulation models

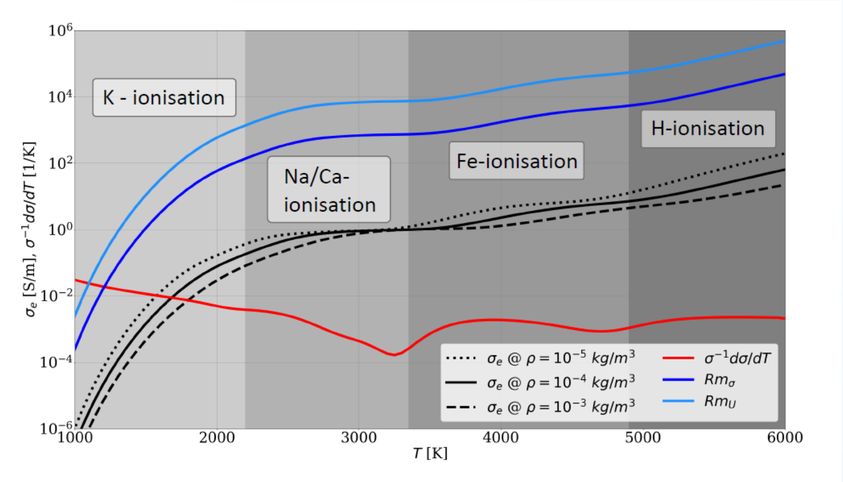

[Dietrich et al. 2022]

Fast, supersonic winds (km/s) induce magnetic field in the atmosphere, by twisting the background field generated from the interior.

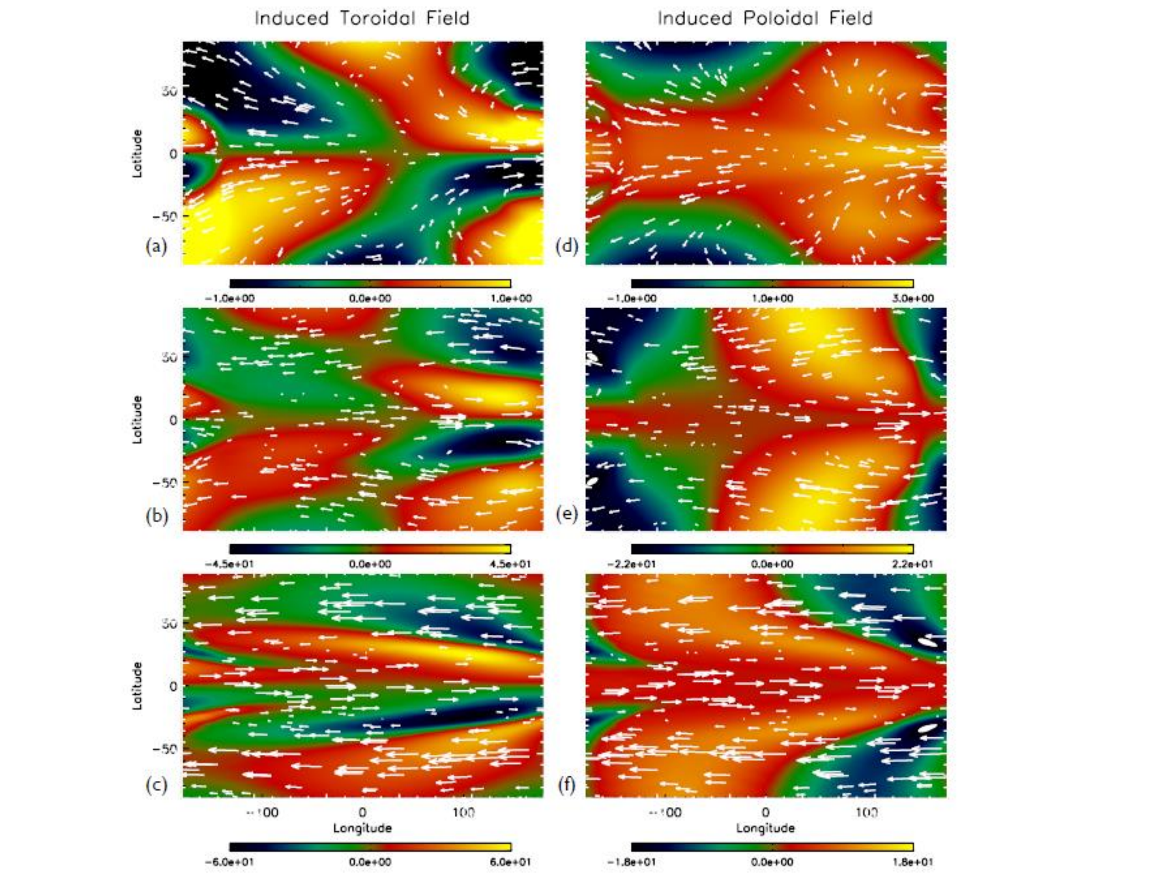

FIG. 3.— Azimuthal and latitudinal components of the magnetic field at 10 Bar (c,f), 1 Bar (b,e) and 10 mBar (a,d). Wind speeds are shown as arrows. Note amplitudes of the latitudinal field are ~4 times the imposed value.

[Rogers et al. 2014]

Global circulation models

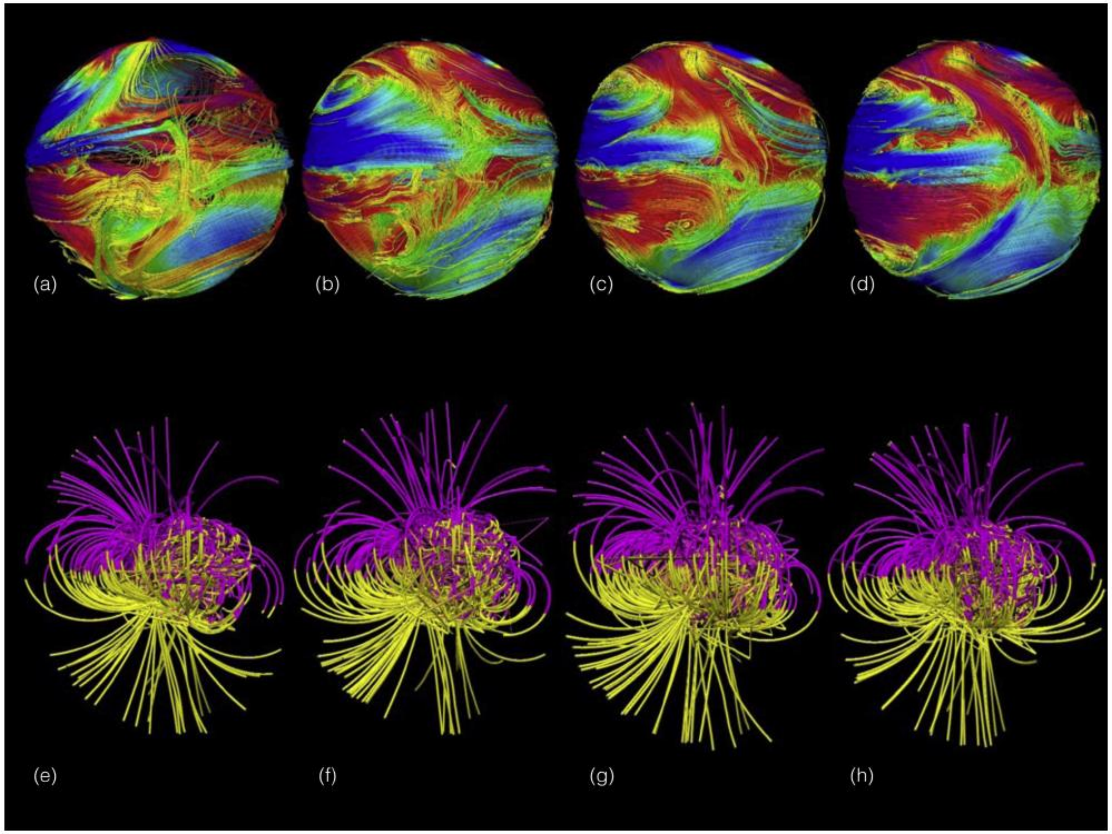

Figure 3. Time snapshots of toroidal (azimuthal) magnetic field (looking onto the terminator) ((a)–(d)) and the radial magnetic field ((e)–(h)).

[Rogers & McElwaine 2017]

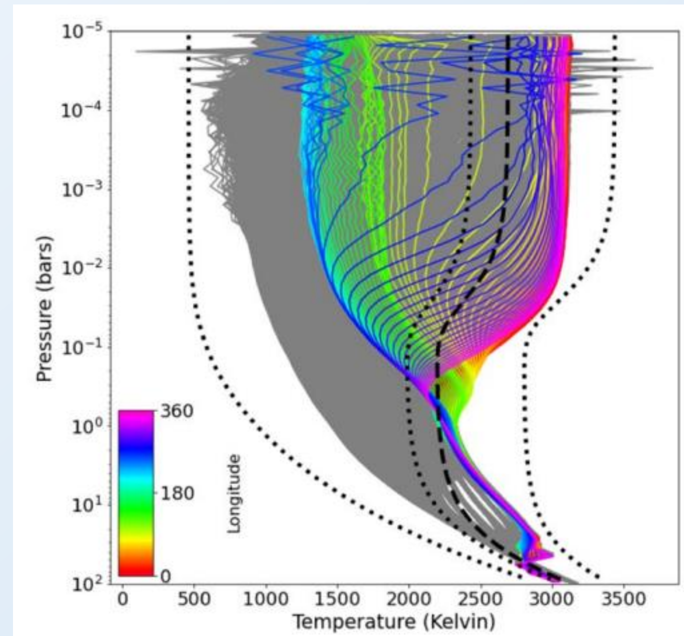

[Beltz et al. 2022]

Global circulation models: the magnetic drag

The induction of magnetic field has a self-regulating, feedback effect on the wind: the Lorentz forces act as a drag (or viscous term), so that the winds cannot be indefinitely fast. This puts a limit on the possible atmospheric induction.

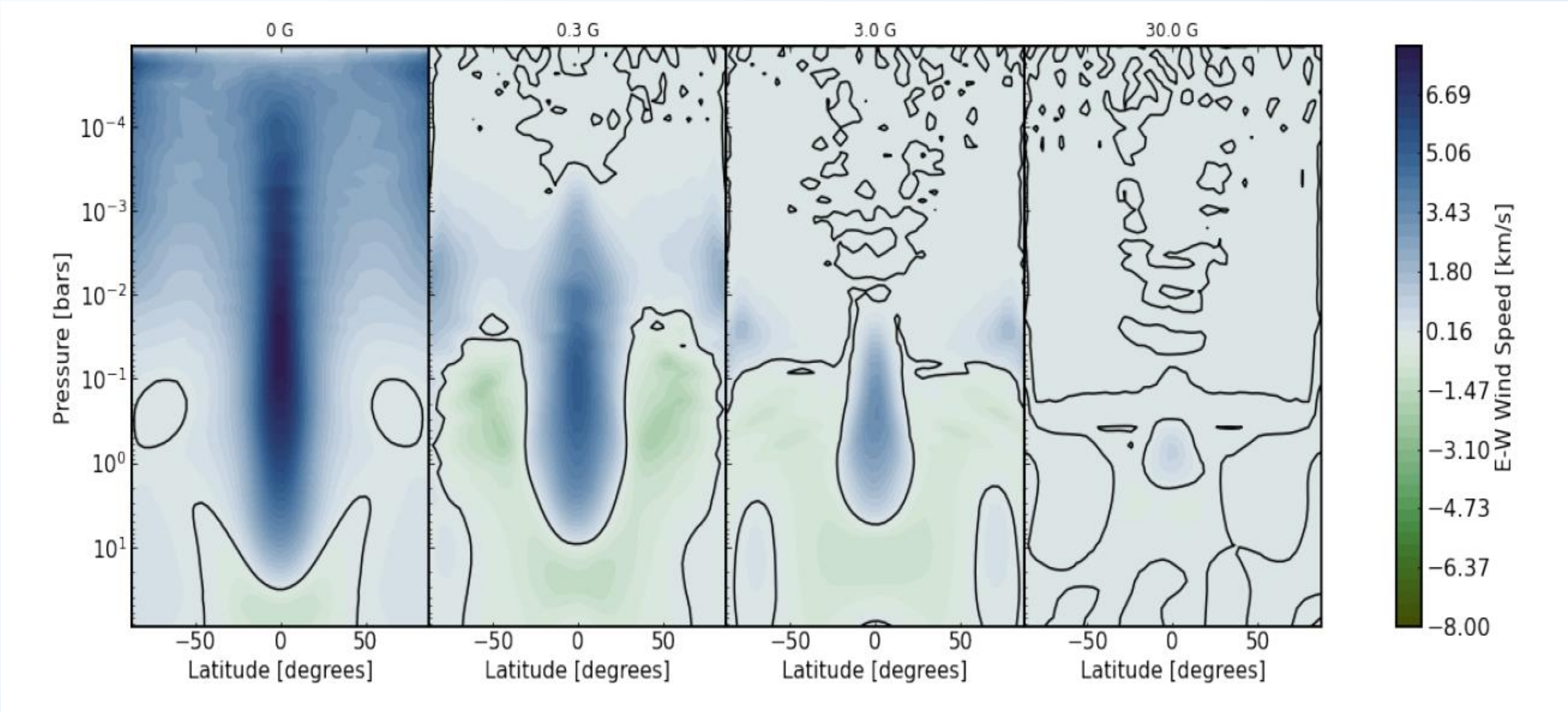

[Beltz et al. 2022]

Global circulation models: the magnetic drag

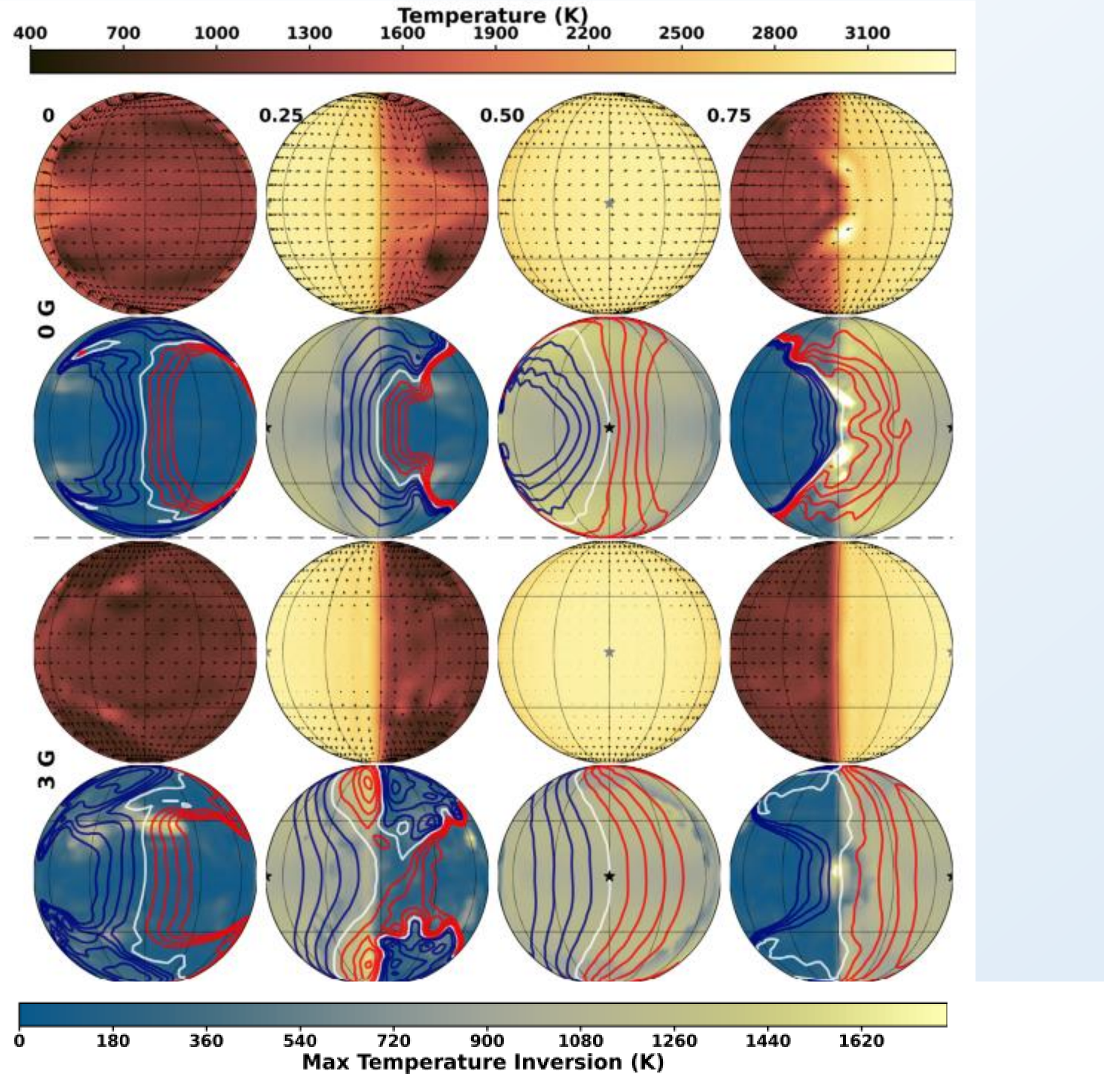

Figure 2. Orthographic projections for the three models presented in this paper (in pairs of rows, from top to bottom: 0 G, 3 G, and uniform) at four orbital phases (from left to right: 0, 0.25, 0.50, and 0.75; transit would be at 0). The first row of each model shows the temperature structure at 10^{-4} bars (within the region probed by spectral line cores), with the wind directions plotted as arrows. The second row for each model shows the maximum vertical temperature inversion at each location. The blue and red contours show constant line-of-sight velocities in increments of ± 2 km s^{-1} at the same pressure level as the temperature plot immediately above it. The differences in temperature structures and wind patterns will influence the high-resolution emission spectra generated from these models.

[Beltz et al. 2022]

Global circulation models

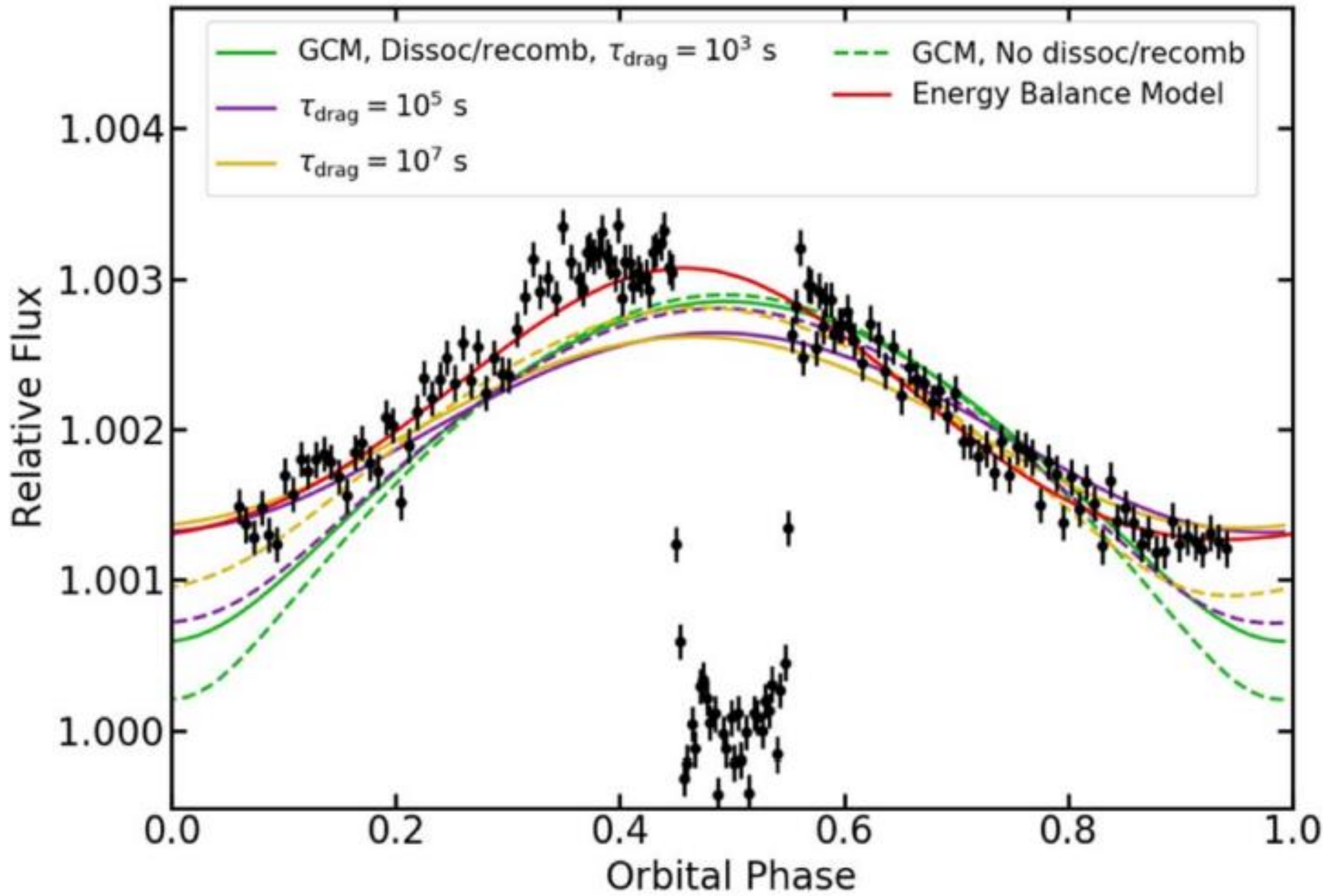

Figure 3. Phase folded phase curve of KELT 9b (black data points). The transit at phases of 0 and 1 is omitted to better show the phase variation. Green, purple, and gold lines show GCMs with drag timescales of 10^3, 10^5, and 10^7 s, respectively (Section 3). Solid and dashed lines indicate GCMs with and without the effects of H_2 dissociation and recombination, respectively. The red line shows the EBM including the effects of H_2 dissociation and recombination (Section 4).

GCMs, however, predict a maximum phase offset of 5°, which disagrees with our observations at $>5\sigma$ confidence. This discrepancy may be due to magnetic effects in the planet's highly ionized atmosphere.

[Mansfield et al. 2020]

Hot Jupiters: inflated radii

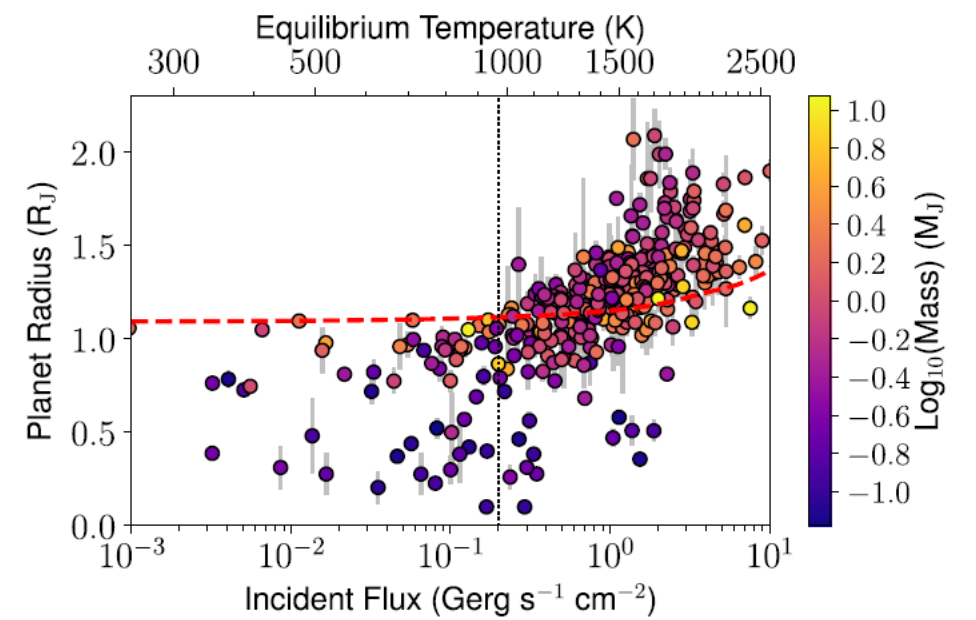

Figure 1. Radii of transiting giant exoplanets plotted against their incident flux (or equilibrium temperature) and colored by mass on the log scale. The dotted red line is the radius of a Jupiter-mass pure H/He model with no inflation

[Thorngren et al. 2018]

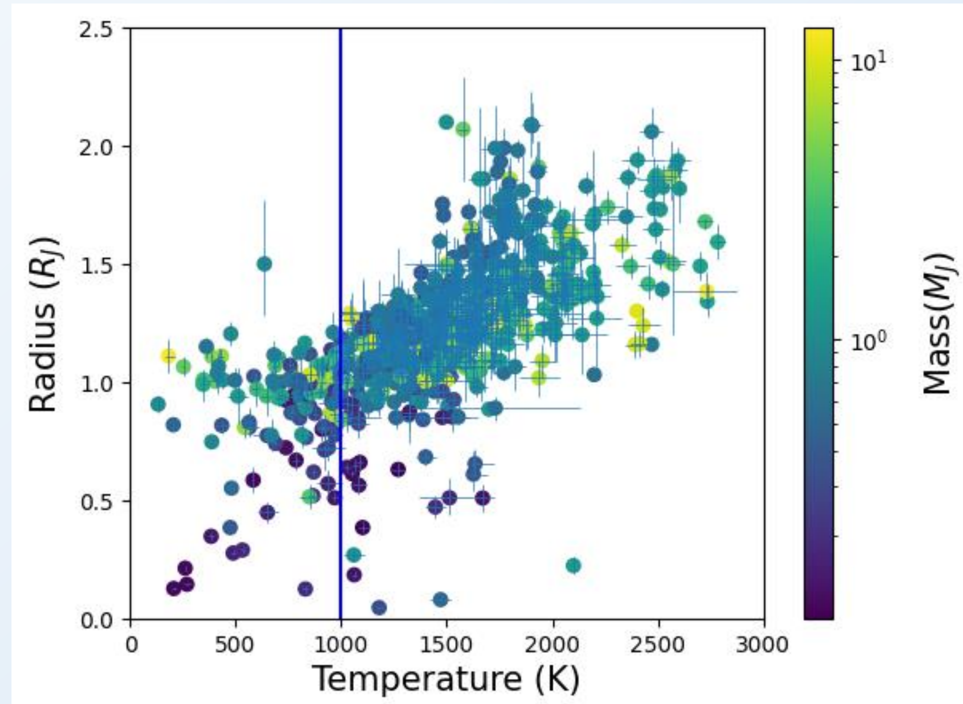

[Clàudia Soriano-Guerrero]

- Giant planets orbiting close to their stars, with equilibrium temperatures > 1000 K.
- Many look "puffy" (inflated radii problem)
- A clear trend with irradiation

Hot Jupiters: cooling models

Main parameters: planetary mass, composition, core mass, atmosphere (boundary condition), irradiation from the star, extra heating sources.
As they cool down, the Radiative-Convective boundary moves inside.

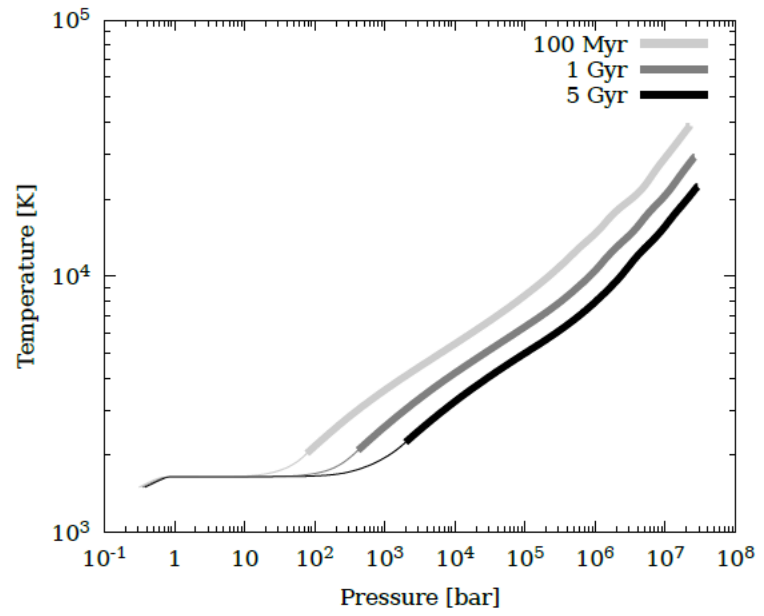

Fig. 2. Temperature as a function of pressure at various moments throughout the evolution of a planet of $1M_J$ with an equilibrium temperature of T_{eq} = 1500 K and no Ohmic heating. The thicker lines correspond to the convective zone (extending all the way to the center). The age for each line is indicated in the key, where it goes from youngest for the top line to the oldest for the bottom line.

The role of the irradiation on the internal structure

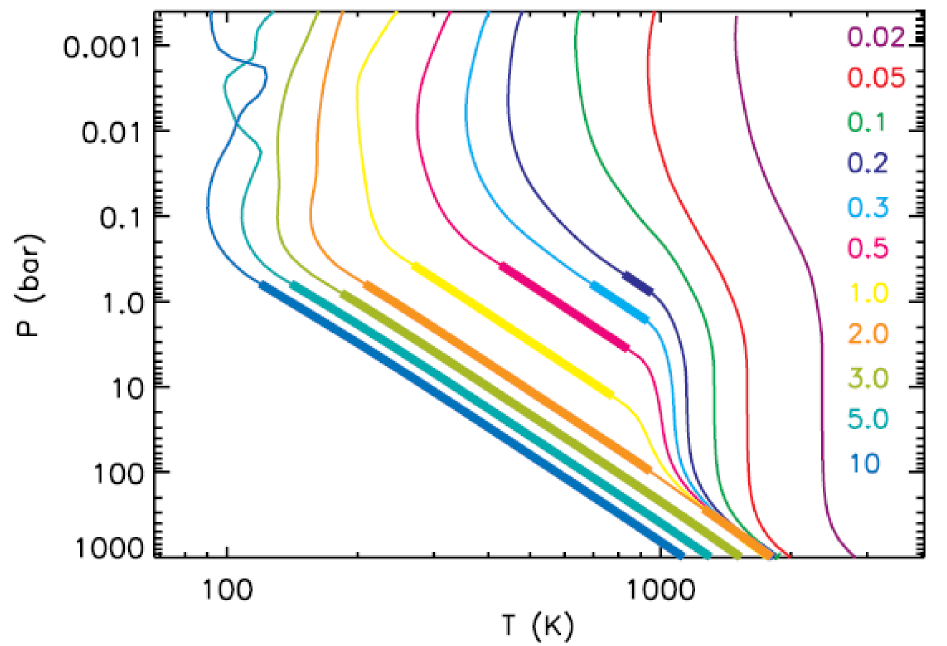

FIG. 3.—Pressure-temperature profiles for ~4.5 Gyr Jupiter-like planets ($g = 25\ \mathrm{m\ s^{-2}}$, $T_{\mathrm{int}} = 100$ K) from 0.02 to 10 AU from the Sun. Distance from the Sun in AU is color coded along the right side of the plot. Thick lines are convective regions, while thin lines are radiative regions. The profiles at 5 and 10 AU show deviations that arise from numerical noise in the chemical equilibrium table near condensation points, but this has a negligible effect on planetary evolution.

[Fortney et al. 2007]

Hot Jupiter inflation radii: slowed down cooling?

Irradiation alone: not enough.

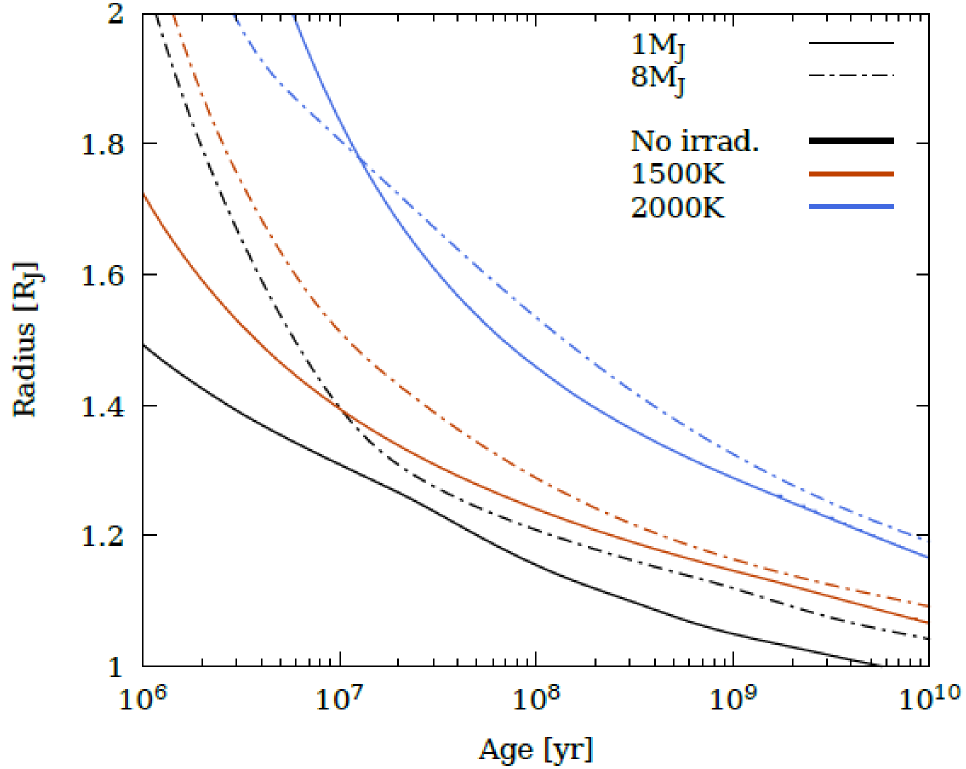

Fig. 3. Evolution of the radii of planets with masses $1M_J$ (solid lines) and $8M_J$ (dash-dotted lines), up to an age of 10 Gyr when no Ohmic heating is present. Three sets of curves are shown: black lines are for no irradiation; red lines are for T_{eq} = 1500 K; and blue lines are for T_{eq} = 2000 K. Here we show the cases for relatively high temperatures, as the inflation for T_{eq} < 1000 K remains relatively moderate (close to the black lines). Note that the maximum inflation for the models shown here is approximately 20%.

Hot Jupiter inflation radii: slowed down cooling?

1. Enhanced opacities (Burrows et al. 2007): might work for some planets.

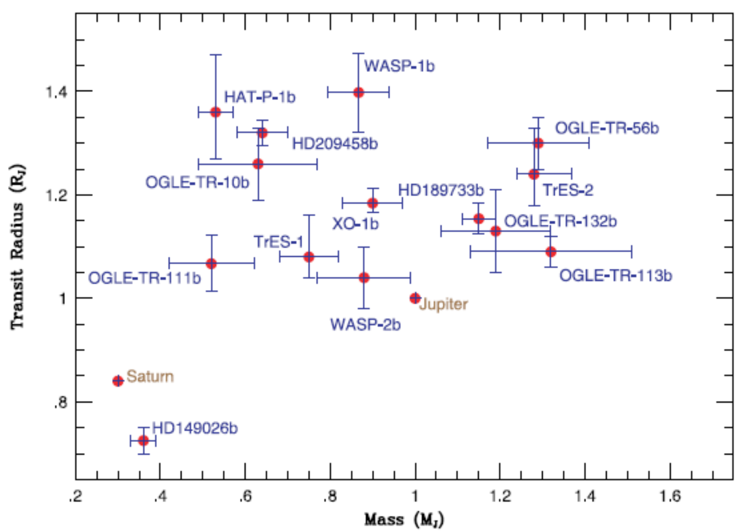

FIG. 1.— Transit radii, R_p (in R_J), of all of the irradiated EGPs listed in Table 1 vs. planet mass, M_p (in M_J), along with published 1 σ error bars for each quantity. For comparison, points for Jupiter and Saturn themselves are also shown.

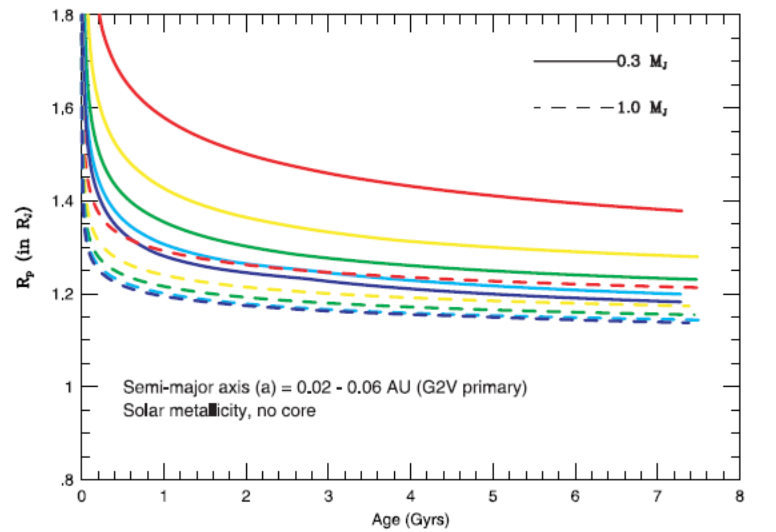

FIG. 3.— R_p (in R_J) vs. age (in Gyr) for model planets with masses of 1 M_J (*dashed lines*) and 0.3 M_J (*solid lines*) for different distances [0.02 (*red lines*), 0.03 (*yellow lines*), 0.04 (*green lines*), 0.05 (*aqua lines*), and 0.06 AU (*blue lines*)] from a G2 V primary. The models have no cores and assume solar metal-

2. Reduced heat transfer due to double-diffusive convection (Chabrier & Baraffe 2007)

Hot Jupiter inflation radii: need for additional heat

Komacek et al. 2017, Thorngren et al. 2018: an additional heat of a few % of the irradiation level is enough.

There must be a temperature-dependence to explain data.

$$\frac{dL}{dm} = \frac{d(L_{\rm rad} + L_{\rm conv})}{dm} = \epsilon_{\rm grav} + \epsilon_{\rm extra},$$

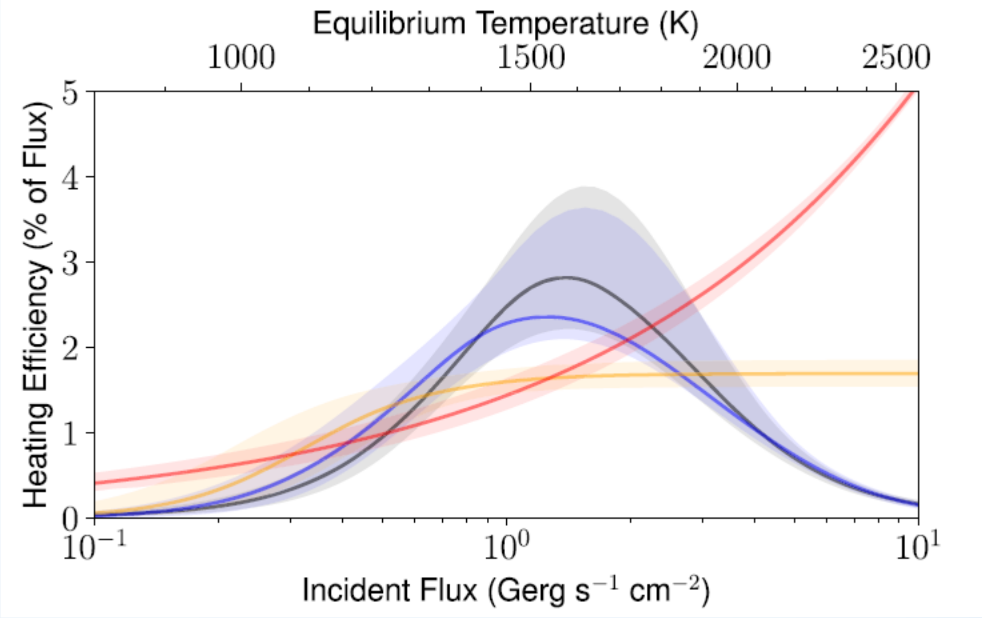

[Thonrgren et al. 2018]

Hot Jupiter inflation radii: need for additional heat

The heat needs to be deposited in the convective region to be effective.
The heat also affects the Radiative-Conductive boundary [Komacek & Youdin 2017]

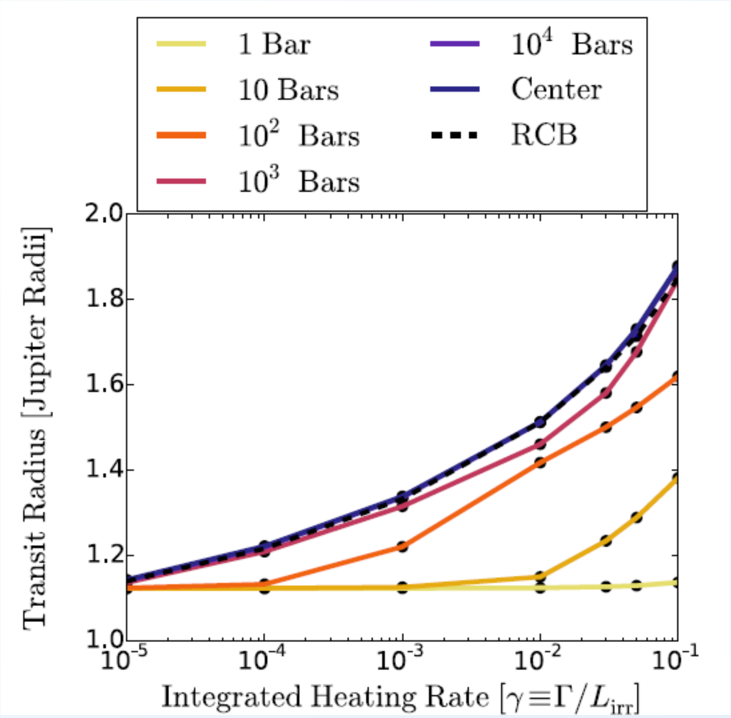

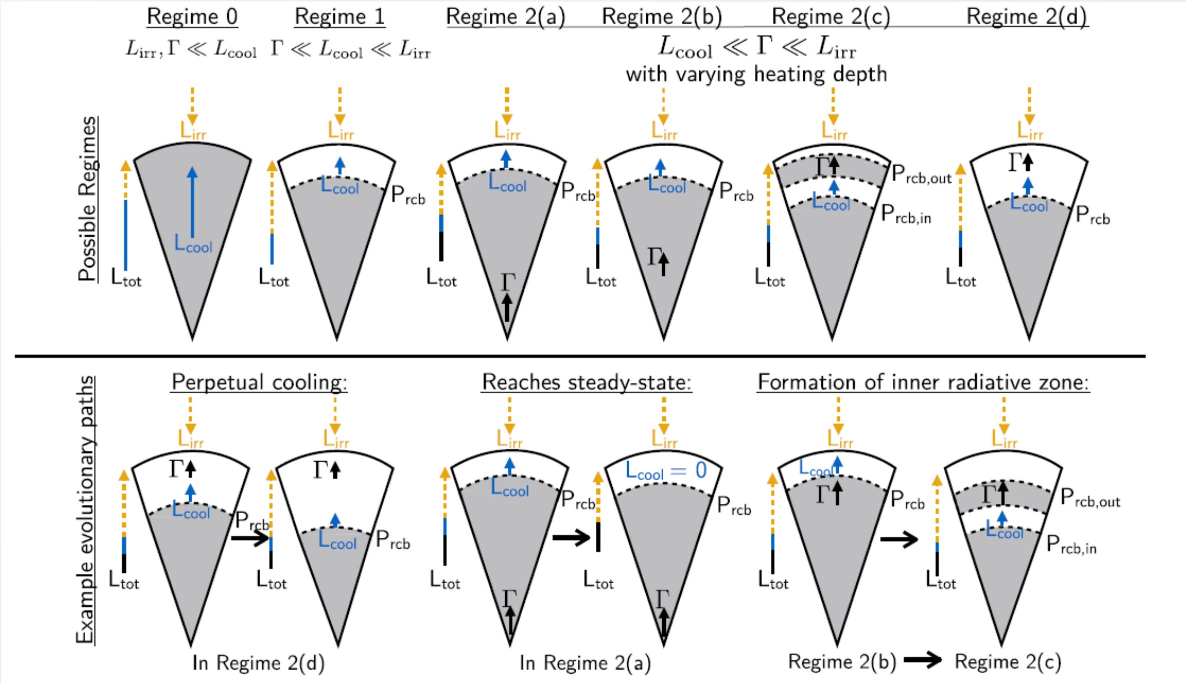

Hot Jupiter inflation radii: which heating mechanisms?

Tidal effects due to eccentricity (Bodenheimer et al. 2001): difficult to sustain eccentricity for so many planets.
Turbulent dragged inside (Youdin & Mitchell 2010)
Ohmic dissipation (Batygin et al. 2010, Perna et al. 2010)

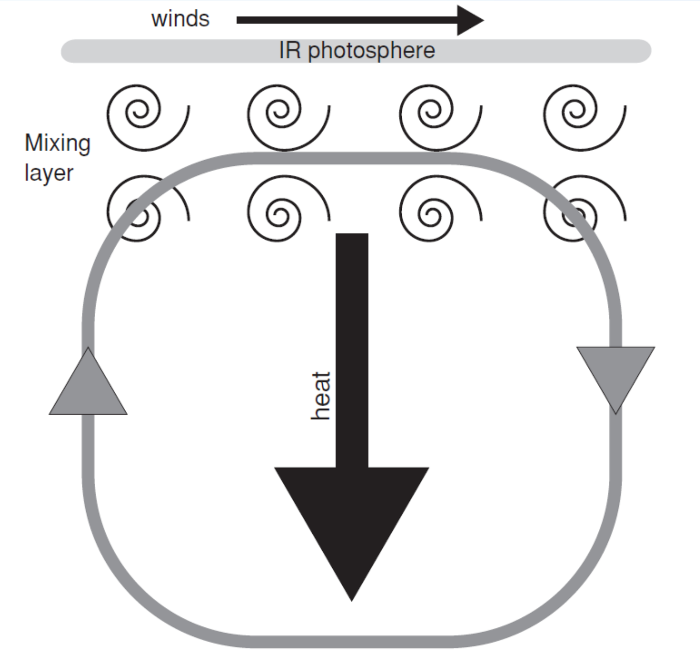

Figure 1. Schematic of the mechanical greenhouse effect to inflate hot Jupiters. A downward flux of heat (large black arrow) is driven by turbulence in the convectively stable "mixing layer" and deposited in the deep interior.

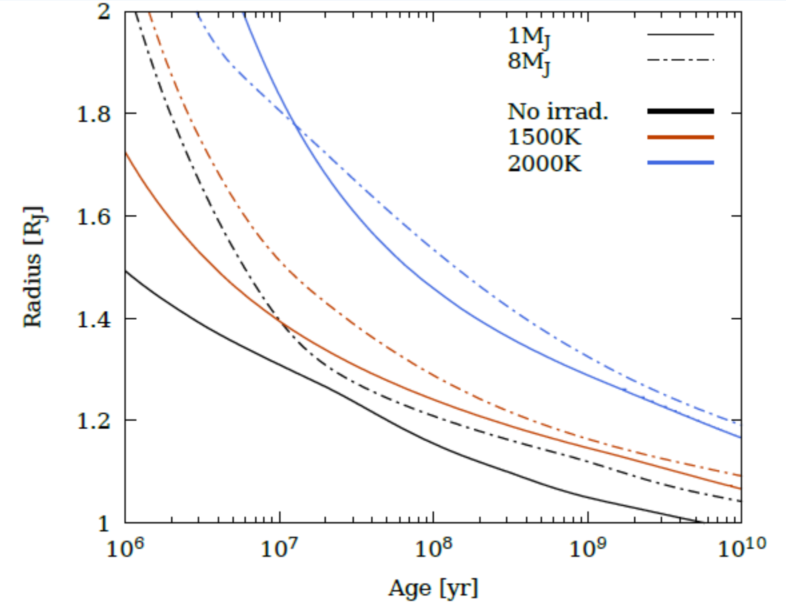

Fig. 3. Evolution of the radii of planets with masses $1M_J$ (solid lines) and $8M_J$ (dash-dotted lines), up to an age of 10 Gyr when no Ohmic heating is present. Three sets of curves are shown: black lines are for no irradiation; red lines are for T_{eq} = 1500 K; and blue lines are for T_{eq} = 2000 K. Here we show the cases for relatively high temperatures, as the inflation for T_{eq} < 1000 K remains relatively moderate (close to the black lines). Note that the maximum inflation for the models shown here is approximately 20%.

Ohmic dissipation in Hot Jupiters: winding

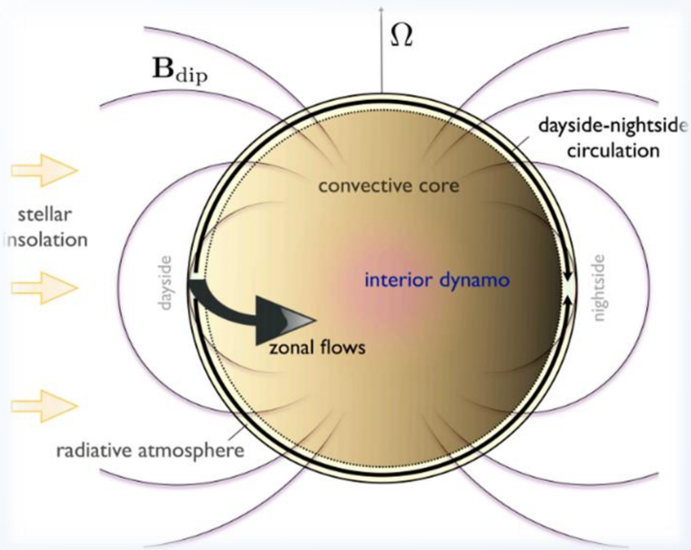

[Batygin et al. 2013]

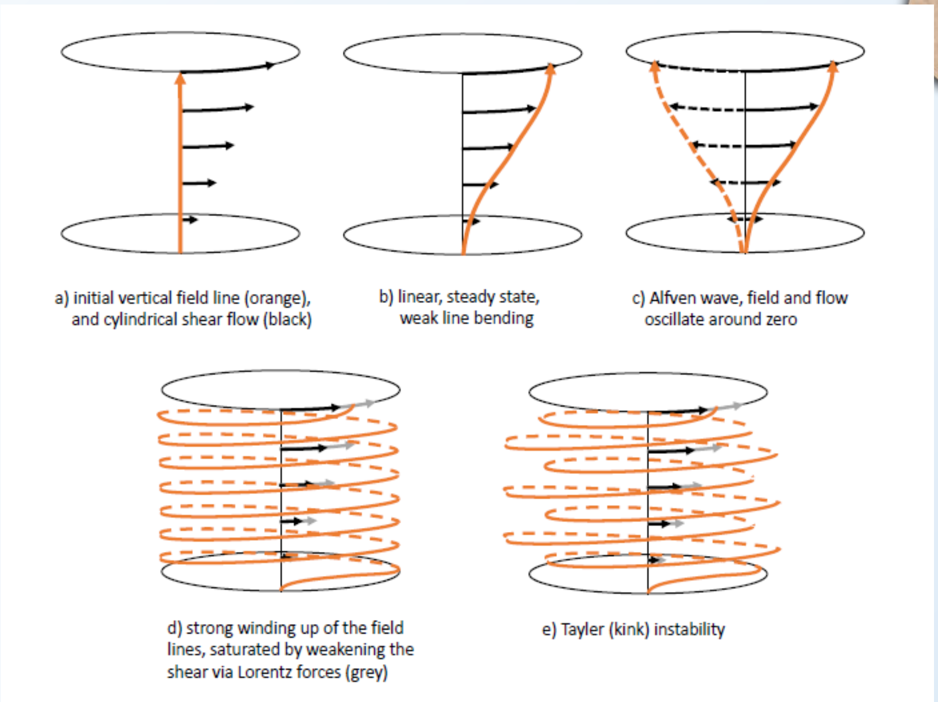

[Dietrich et al. 2022]

The strong supersonic thermal jets, since the material is ionized, induce currents, i.e., atmospheric magnetic fields.
This induction involve also the deeper layers, if they are not completely insulating.

Ohmic dissipation in Hot Jupiters

Finite conductivity indirectly induces field also in the interior.

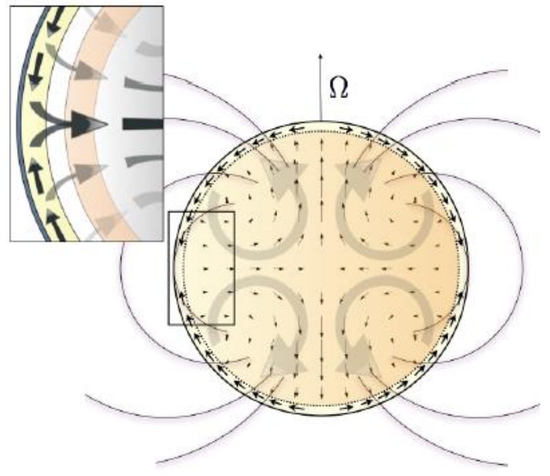

FIG. 3.— Side view cross-section of induced current due to zonal wind flow. The interior vector field, plotted with small arrows, is a quantitative result of the model. The large semi-transparent arrows are illustrations. The yellow shell in the inset represent the region to which we confine the zonal flow (10-0.03 Bars). The orange region denotes the region of interior heating.

$$\vec{J}_{ind} = \sigma \left(\vec{v} \times \vec{B}_{dip} - \vec{\nabla}\Phi \right).$$

$$\mathbb{P} = \int\int\int \frac{\vec{J}^2}{\sigma(r)} dV.$$

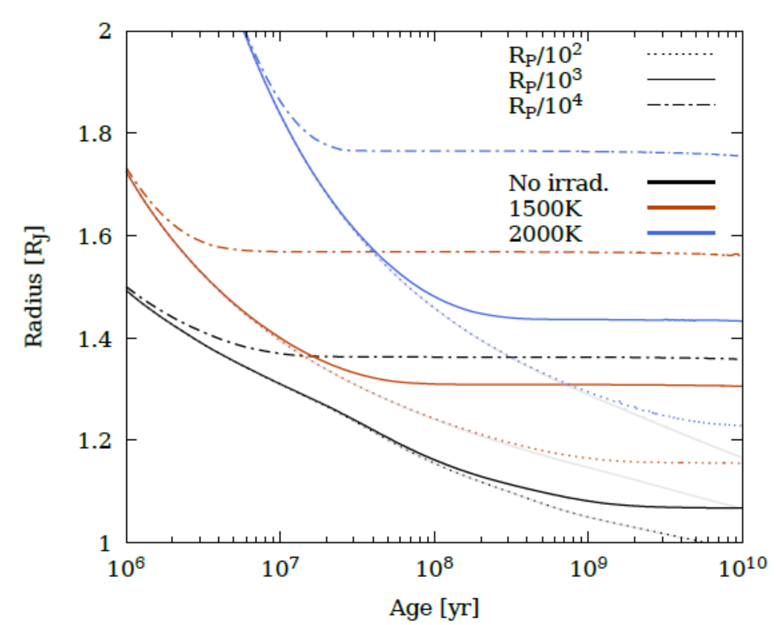

By introducing a Ohmic heating as an energy source in the cooling models, we quantitatively keep the planets more inflated.

[Batygin et al. 2010, Perna et al. 2010, Akgün et al. 2024]

Atmospheric turbulence in Hot Jupiters

Turbulence might be expected and produce additional heat.

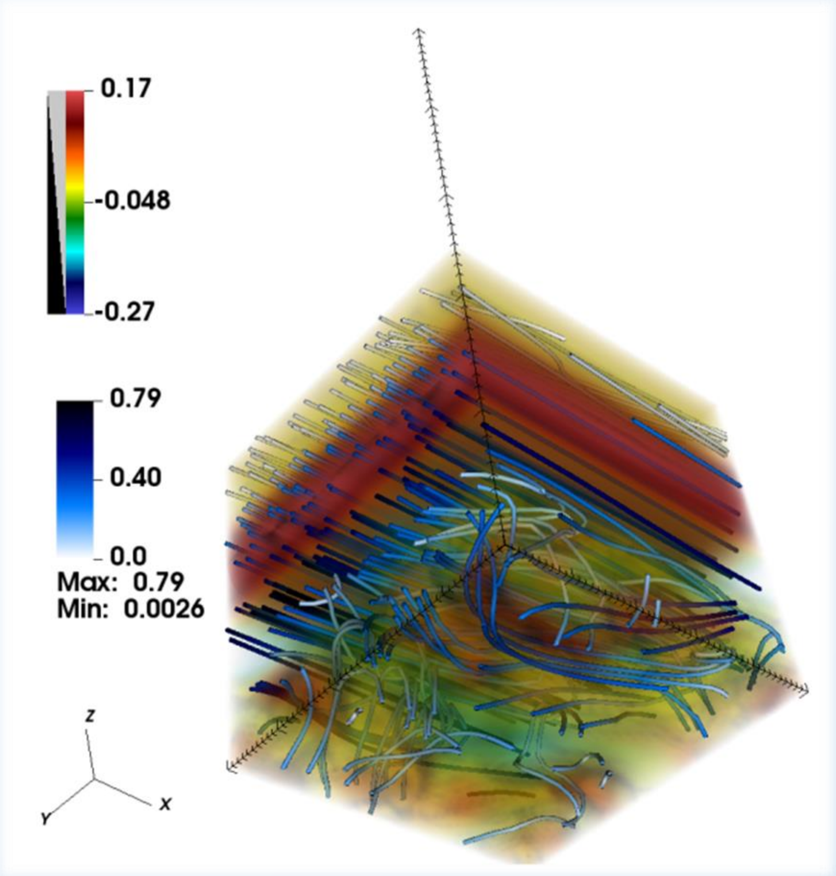

[Soriano-Guerrero et al. 2023]

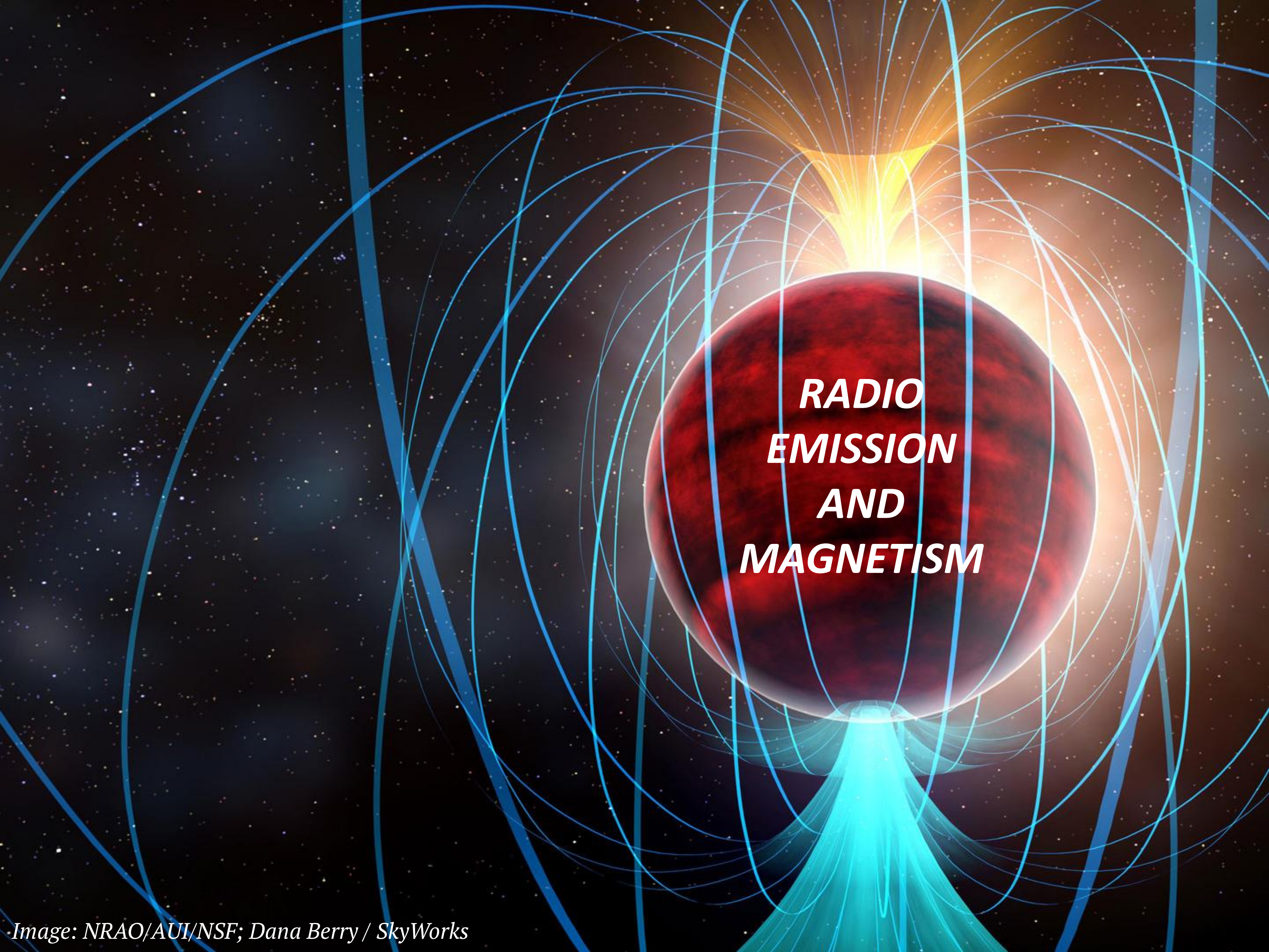

Image: NRAO/AUI/NSF; Dana Berry / SkyWorks

Radio waves

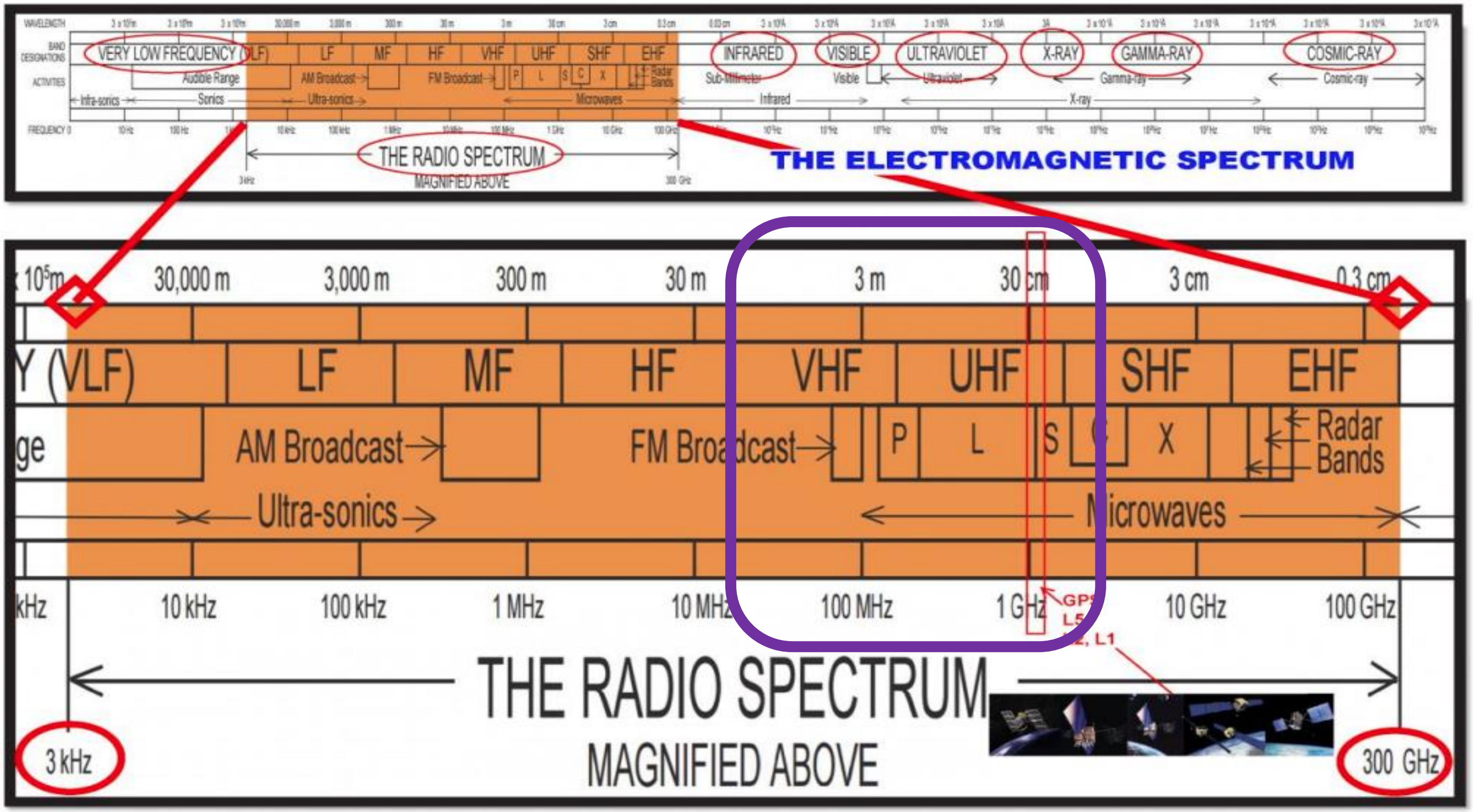

Below 10 MHz, the ionosphere is opaque

Relevant radio emission mechanisms

In astrophysics, radio emission can come from two kinds of processes:

- Thermal, when involving thermal motion of the emitting p articles.
- Non-thermal, when particles are accelerated, and their energy follow a non-thermal distribution. In radio, they usually involve magnetic fields.

Thermal processes are then related to blackbody emission (usually irrelevant) or bremsstrahlung, which is related to the electric interaction between charged particles. A particularly relevant one is the electron-electron interaction in ionized media, called also “free-free” emission.

Thermal emission is a dominant source of radiation at high frequencies (mm) and is particularly important in extended sources like disks or jets.

See Dulk et al. 1985 “Radio emission in stars” for a more rigorous description!

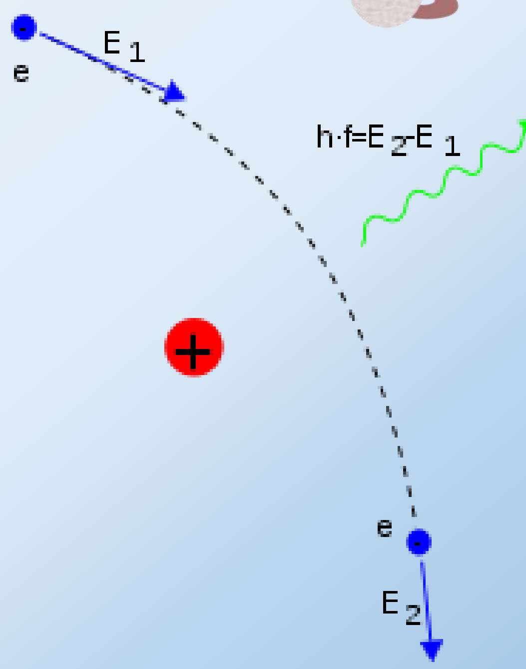

Polarization

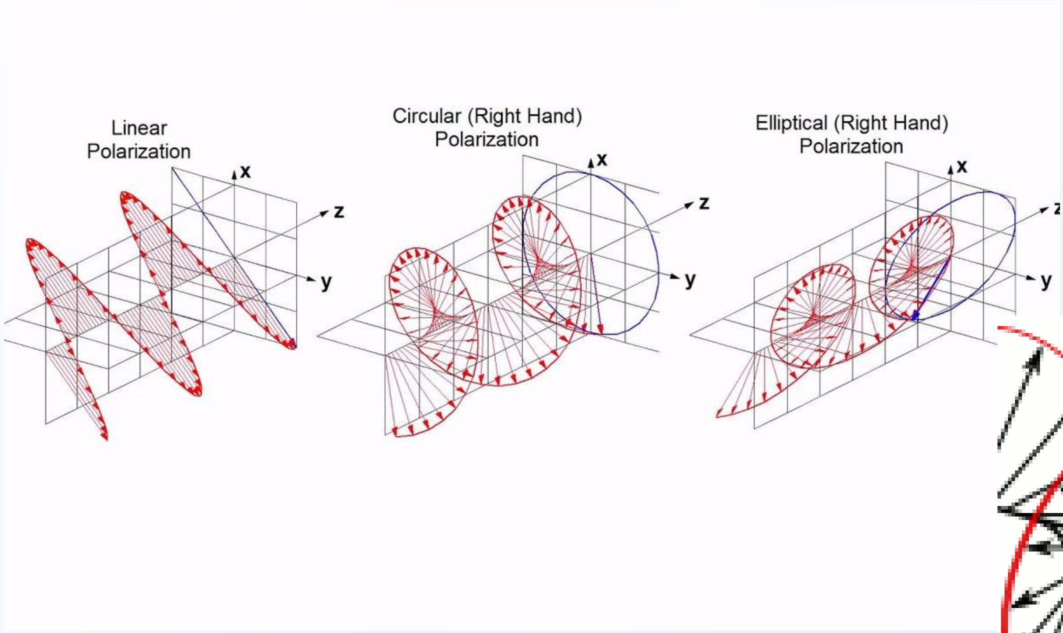

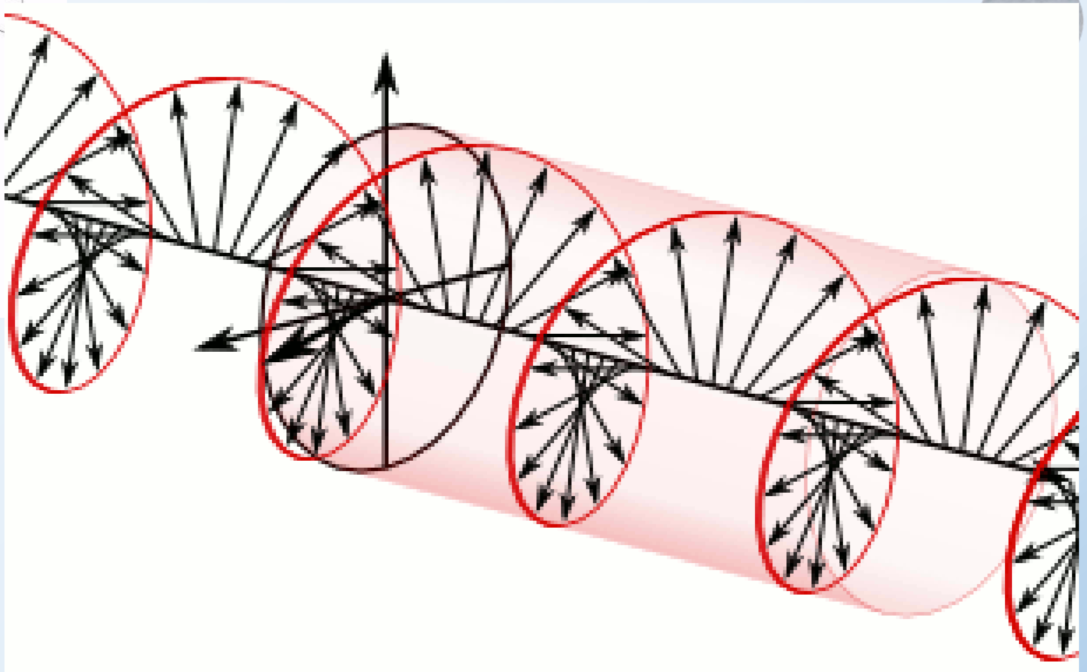

Circular polarization is a characteristic signature of magnetic fields, and usually is observed in coherent emission. It brings information on the direction of the local magnetic field in the emitting region

Gyro-resonance/Cyclotron, Gyro-synchrotron, Synchrotron

Particles (usually electrons) embedded in a magnetic field spiral around it and produce radiation.

The properties of this radiation (spectrum, polarization) depend essentially on the magnetic field intensity and direction and on the energy of the charged particles.

Typically, these mechanism have a negative spectral index, which is the result of the contributions of the entire electron population. They are **incoherent**

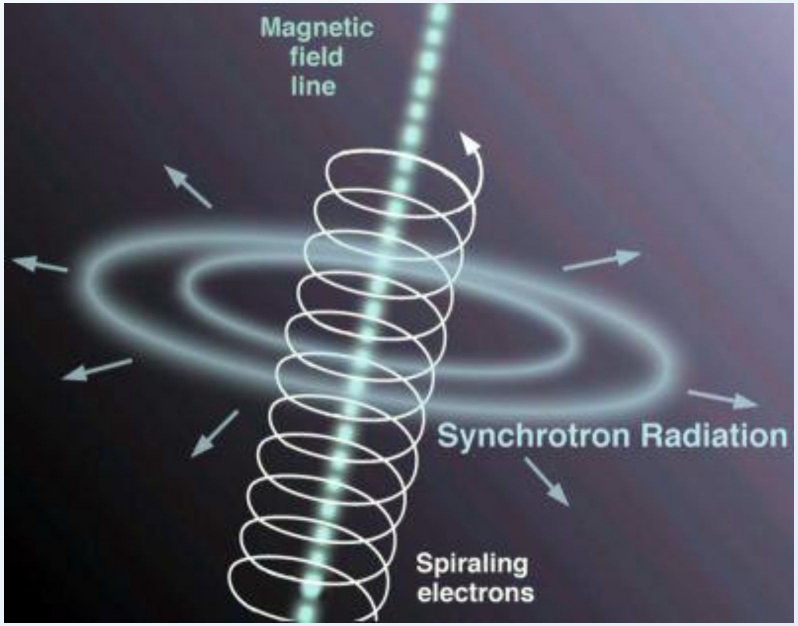

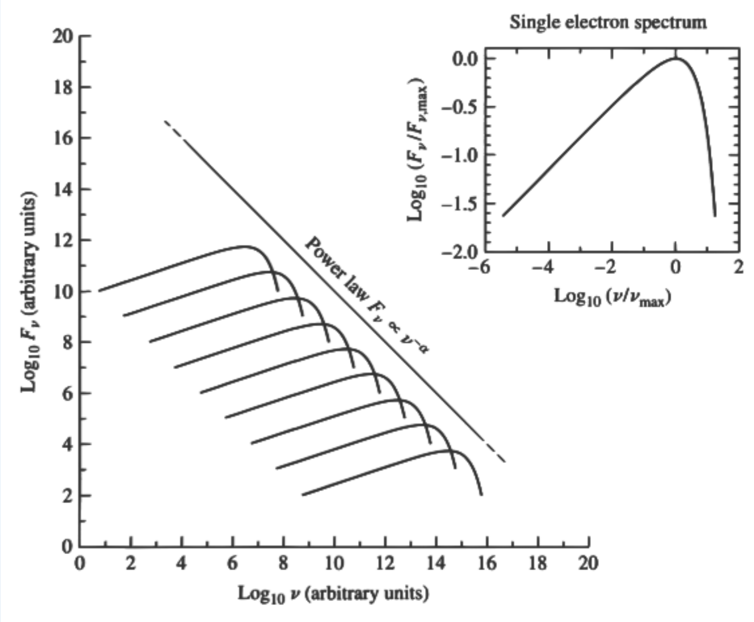

What's this Salamander-like emission seen in radio?

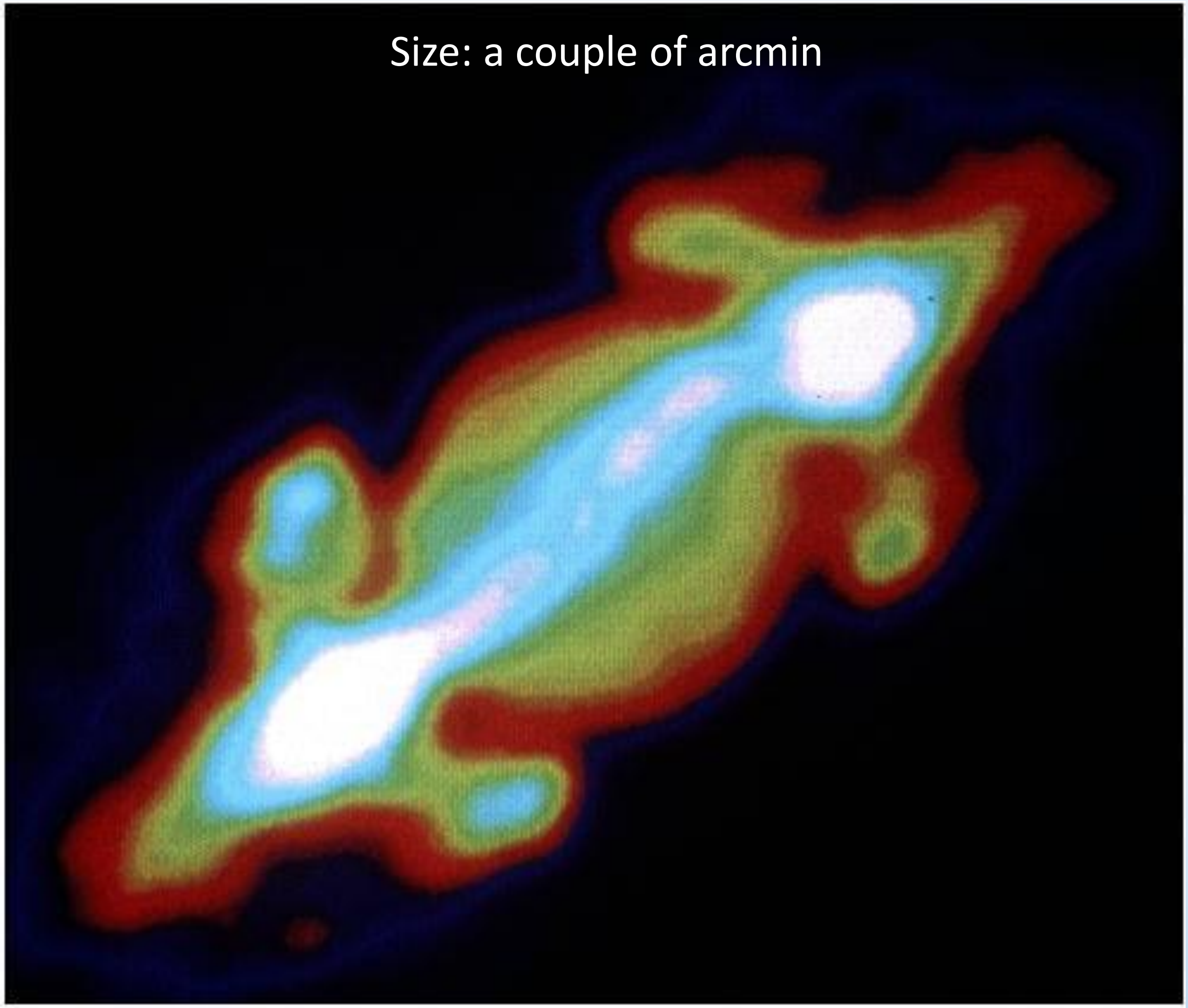

Coherent mechanisms: Plasma emission

Plasma emission is often seen in Solar bursts and sometimes associated to Solar Coronal Mass Ejections.

It happens at the plasma frequency, ν_{ep}. In general, one expects plasma emission to be favoured at lower frequencies compared to synchrotron emission (since the latter is absorbed at $\nu < \nu_{ep}$)

$$\omega_{pe} = \sqrt{\frac{n_e e^2}{m^* \varepsilon_0}}, [\mathrm{rad/s}]$$

It can have high circular polarization fraction and is usually a transient emission.

It'a coherent process (involving excitation of Langmuir waves)

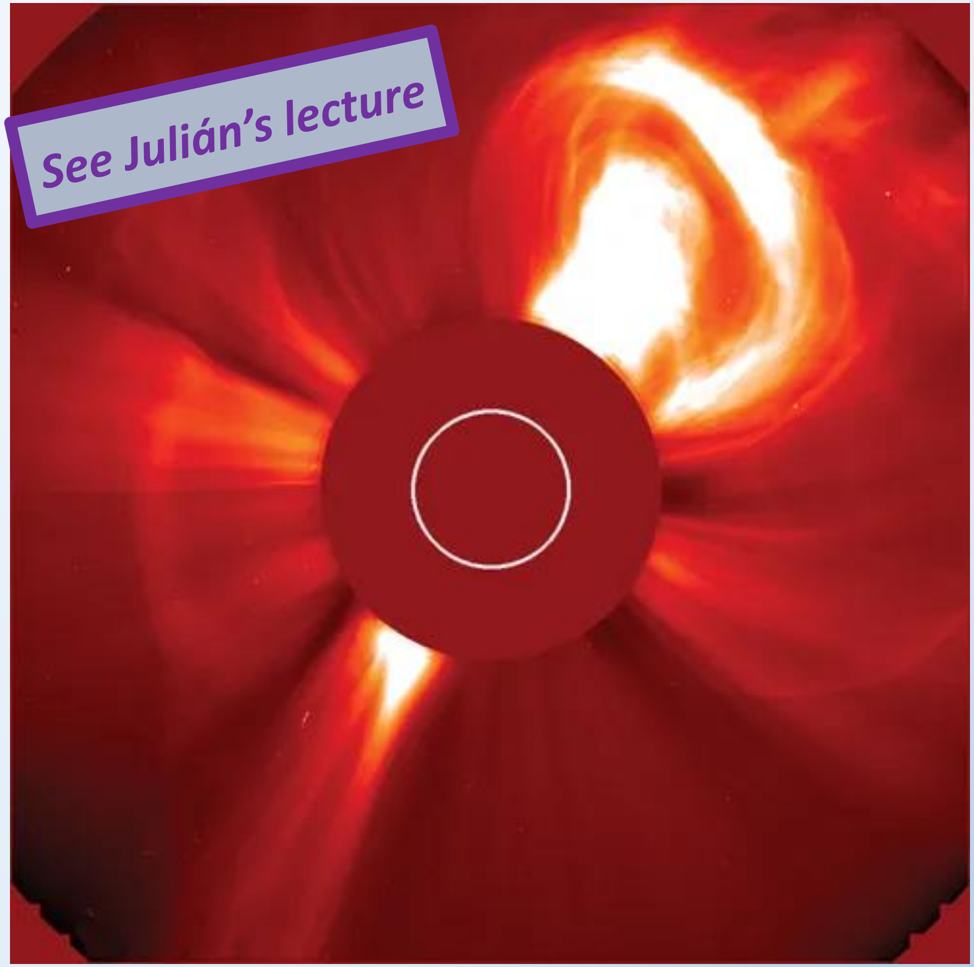

Coherent mechanisms: electron cyclotron maser

See Jan-Matthias' lecture

Magnetospheric coherent emission driven by the electron cyclotron maser* (ECM). Ingredients needed: large plasma supply, due to stellar wind or interaction with a satellite.

**Maser: microwave amplification by stimulated emission of radiation. It's only an analogy to a laser and refers to an enhanced emission at the same frequency.*

ECM, at a given location, emits at a very narrow band around the Larmor frequency, with a 100% circular polarization, **ν = 2.8****B[G]*** **MHz**

Since the magnetic field intensity (and direction) change, the observed ECM is usually broadband, with a cut-off at the maximum magnetic field intensity in the emitting region. The polarization fraction can then also be reduced (simultaneous contribution from regions with different magnetic field direction).

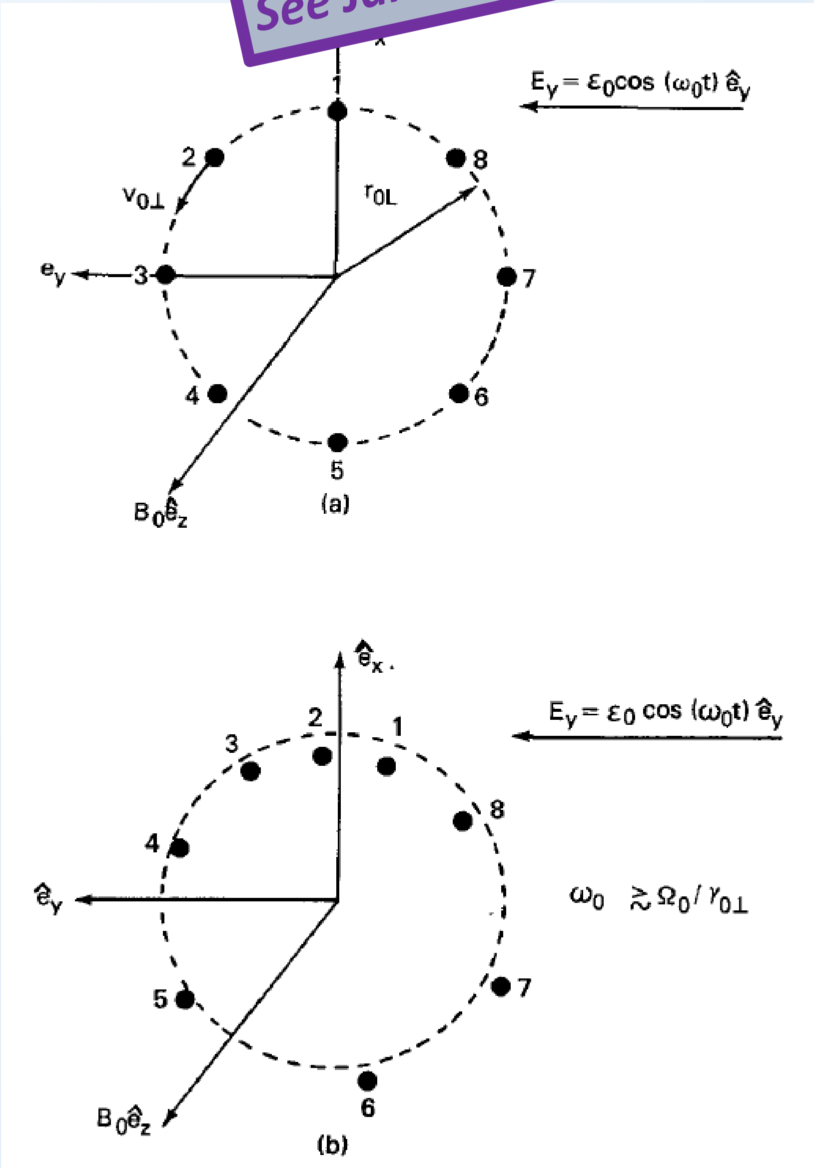

VLA

Karl Jansky Very Large Array (VLA), Socorro, New Mexico (USA)
Interferometer with 28 antennas, 25 meters diameter
Baseline up to 36 km
Resolution: 0.2 arcseconds to 0.04 arcseconds
1-50 GHz (plus a 74 MHz receiver)

GMRT

(Upgraded) **Giant Metrewave Radio Telescope**
Khodad, Pune (India)
30 steerable parabolic telescopes.
Baseline up to 25 km
150 MHz - few GHz, res. 2” at 1.4 GHz

MWA

Murchison Widefield Array (Australia)
Thousands of cross dipole antennas. Serves also as a pathfinder for SKA.
70-300 MHz

Merkaat

Merkaat national park (Northern Cape), South Africa
64 dishes of 13.5 m diameter
precursor of Square Kilometer Array
550 MHz-3.5 GHz

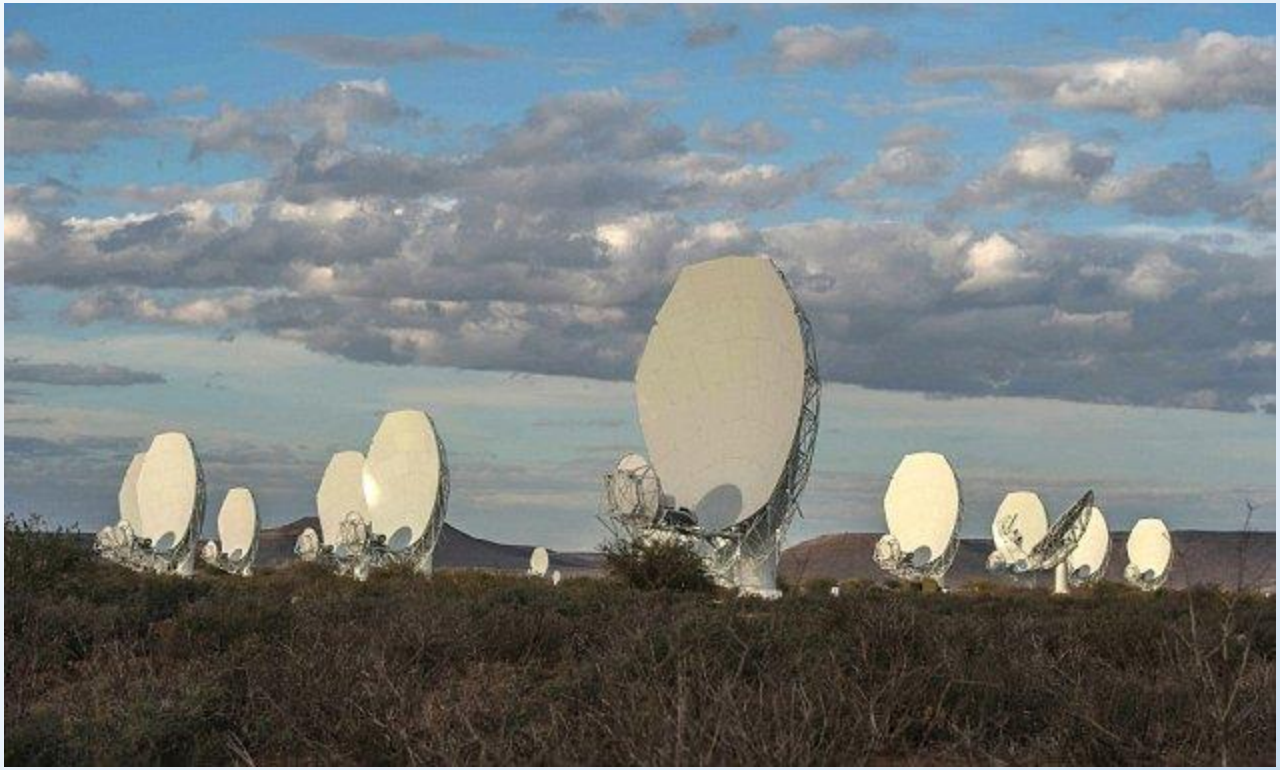

UTR-2 (mostly destroyed)

UTR-2 (close to Shevchenkove, Ukraine)
Largest low-frequency radio telescope of the world, decameter wavelengths
2040 dipole elements
8-33 MHz, 10 mJy sensitivity

LOFAR: the state of the art

LOFAR (Low-Frequency Array), core in the Netherlands
+ stations in Germany and other EU countries
LBA (Low Band Antenna) is the most sensitive facility at frequencies 10-80 MHz
sensitivity < 1 mJy beam^{-1} , resolution < 15″

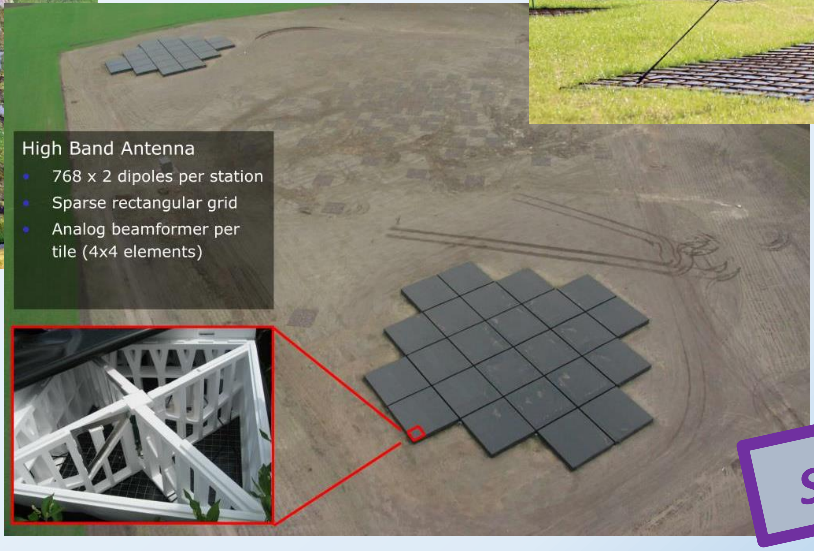

See Ekaterina's lecture

Instruments: upcoming

Low-Band Square Kilometer Array (SKA-low), Australia
131,072 antennas, >60 km baseline
70 MHz - 350 MHz
Improvement in sensitivity 8x LOFAR:
range of 10 microJy (for 1 hour), enough to detect Jupiter's bursts at 10 pc

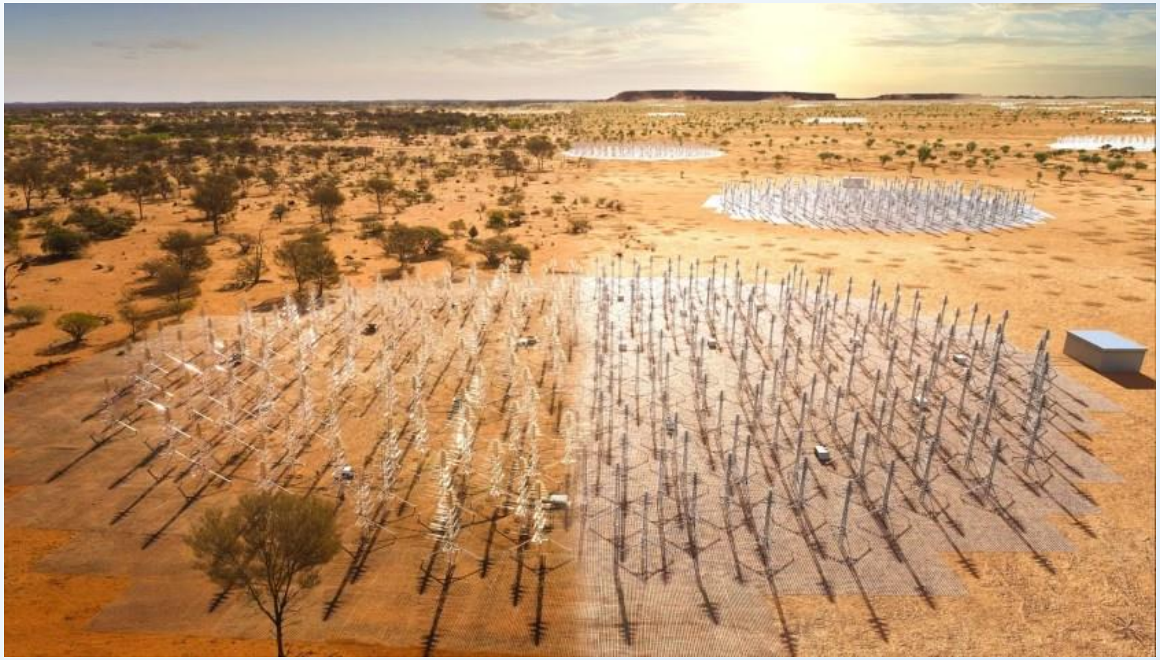

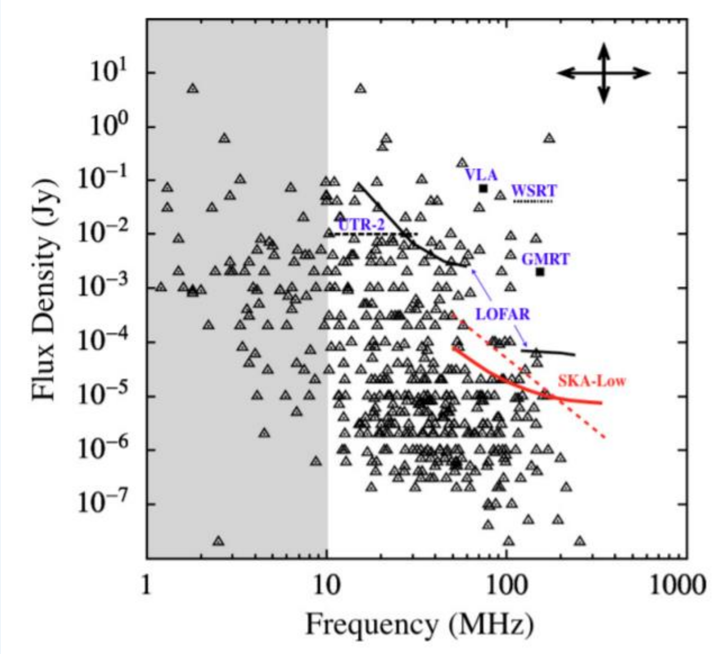

Jupiter in radio

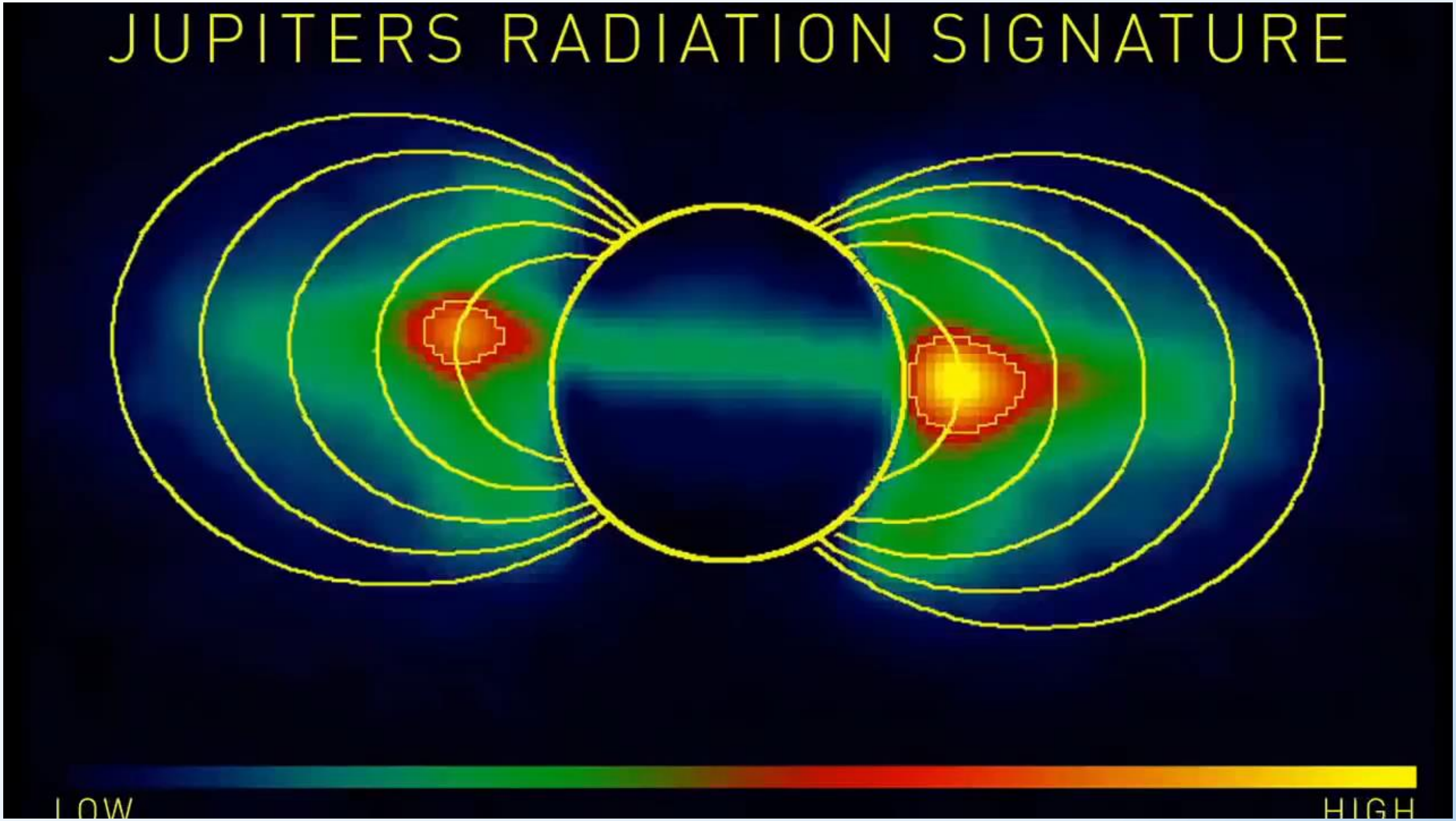

[NASA Juno YouTube channel]

Different radiation detected by space missions

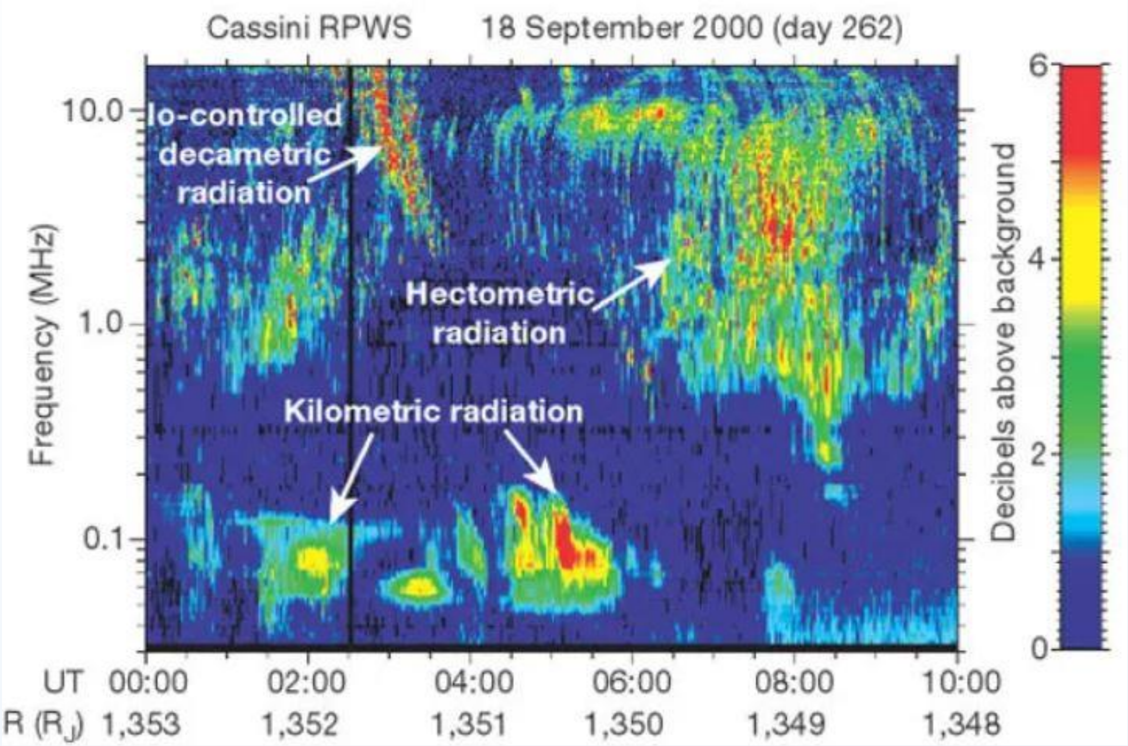

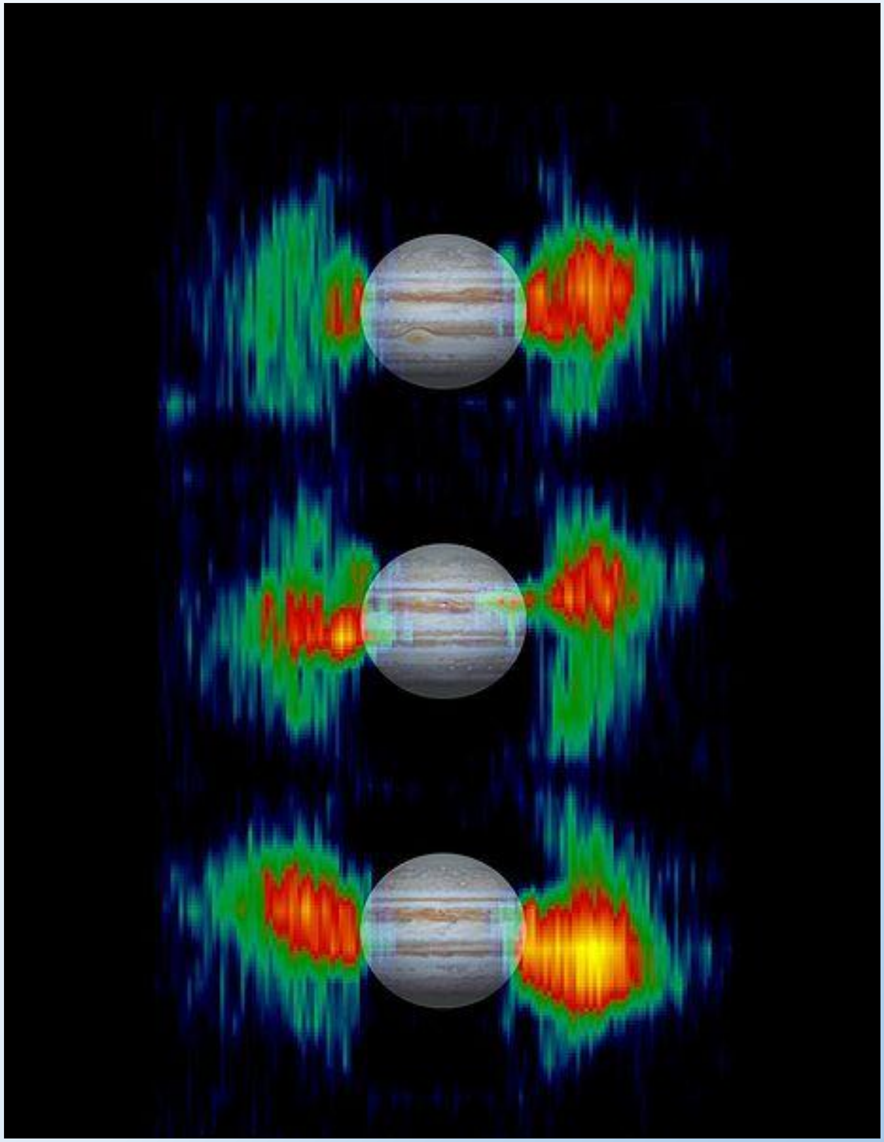

[Gurnett+ 2002]

Decametric radiation: in part induced by Io satellite, in part connected to aurorae.
Hectometric radiation: connected to UV aurorae
Kilometric radiation: mostly bursts (seconds to minutes) – plasma waves?
High temporal variability

Jupiter's radio emission

Io represent an important source of plasma for the Jovian magnetosphere, and it leaves a clear imprint in the associated radio emission.

See Jan-Matthias' lecture

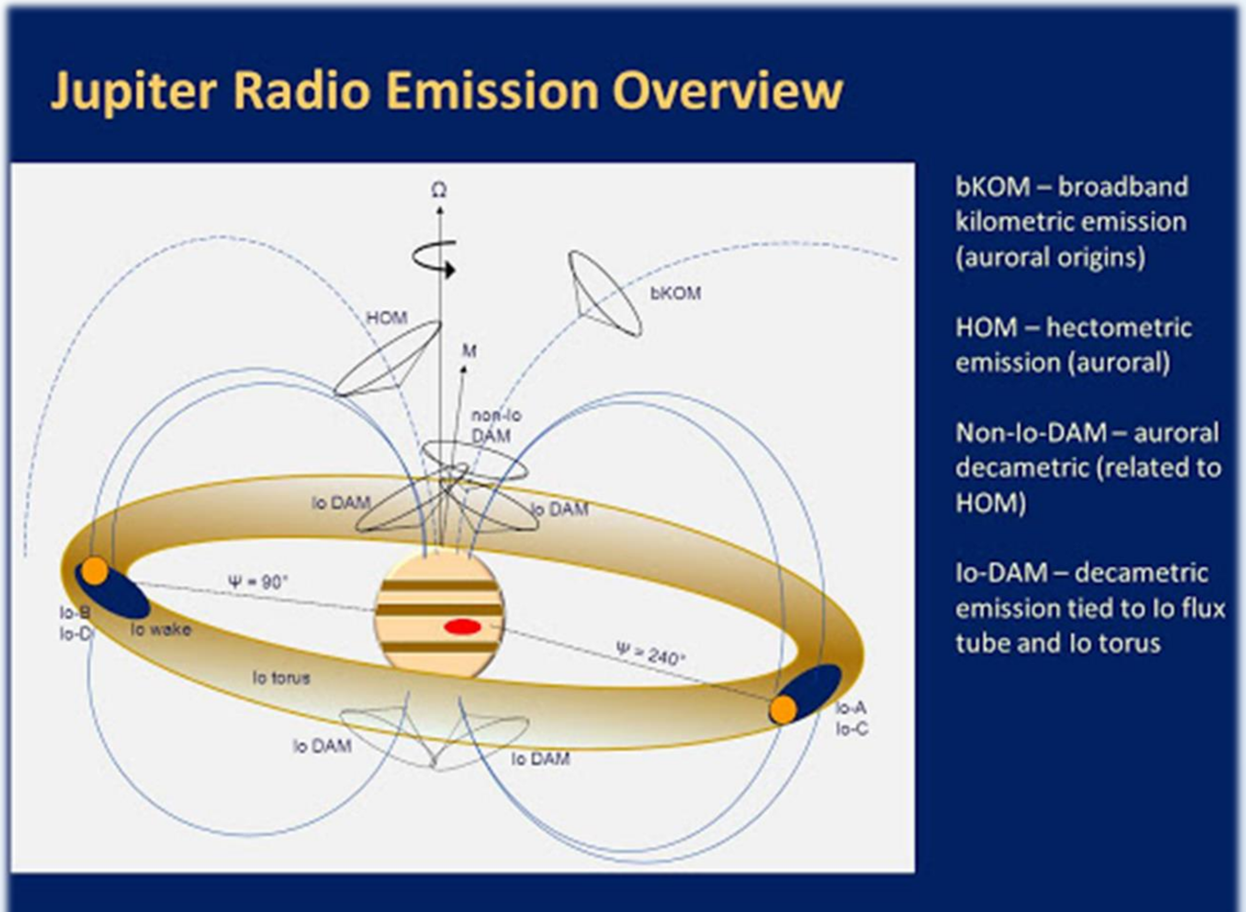

Jupiter in UV: aurorae

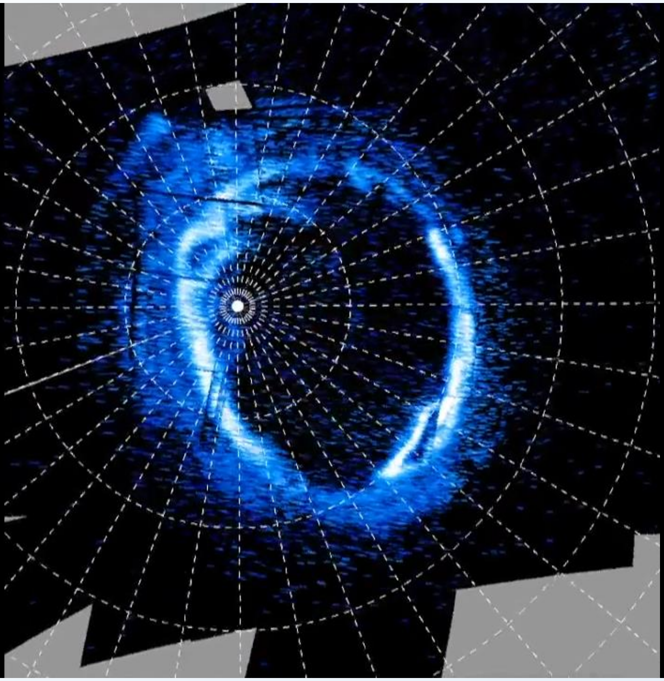

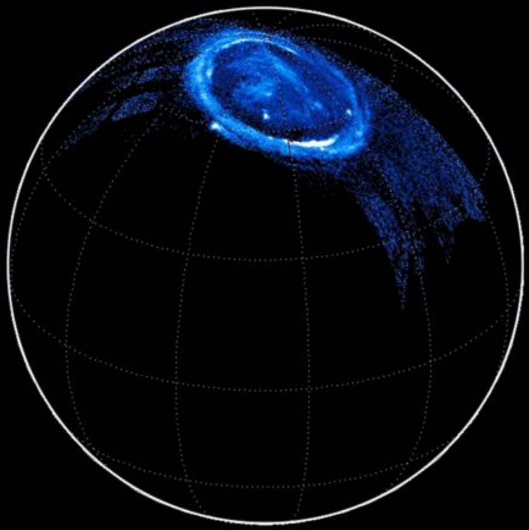

[NASA Juno UV Spectrograph]

Intense acceleration of particles due (also) to strong electric potentials along the magnetic field: 400.000 V, tens of times higher than on Earth.

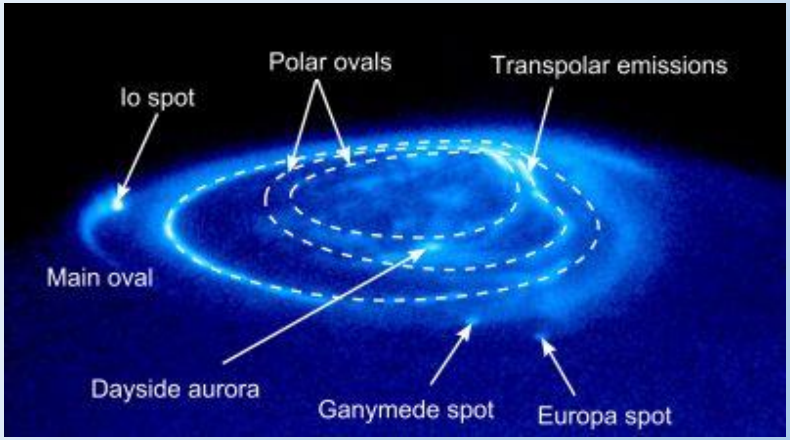

Jupiter in X-rays: aurorae

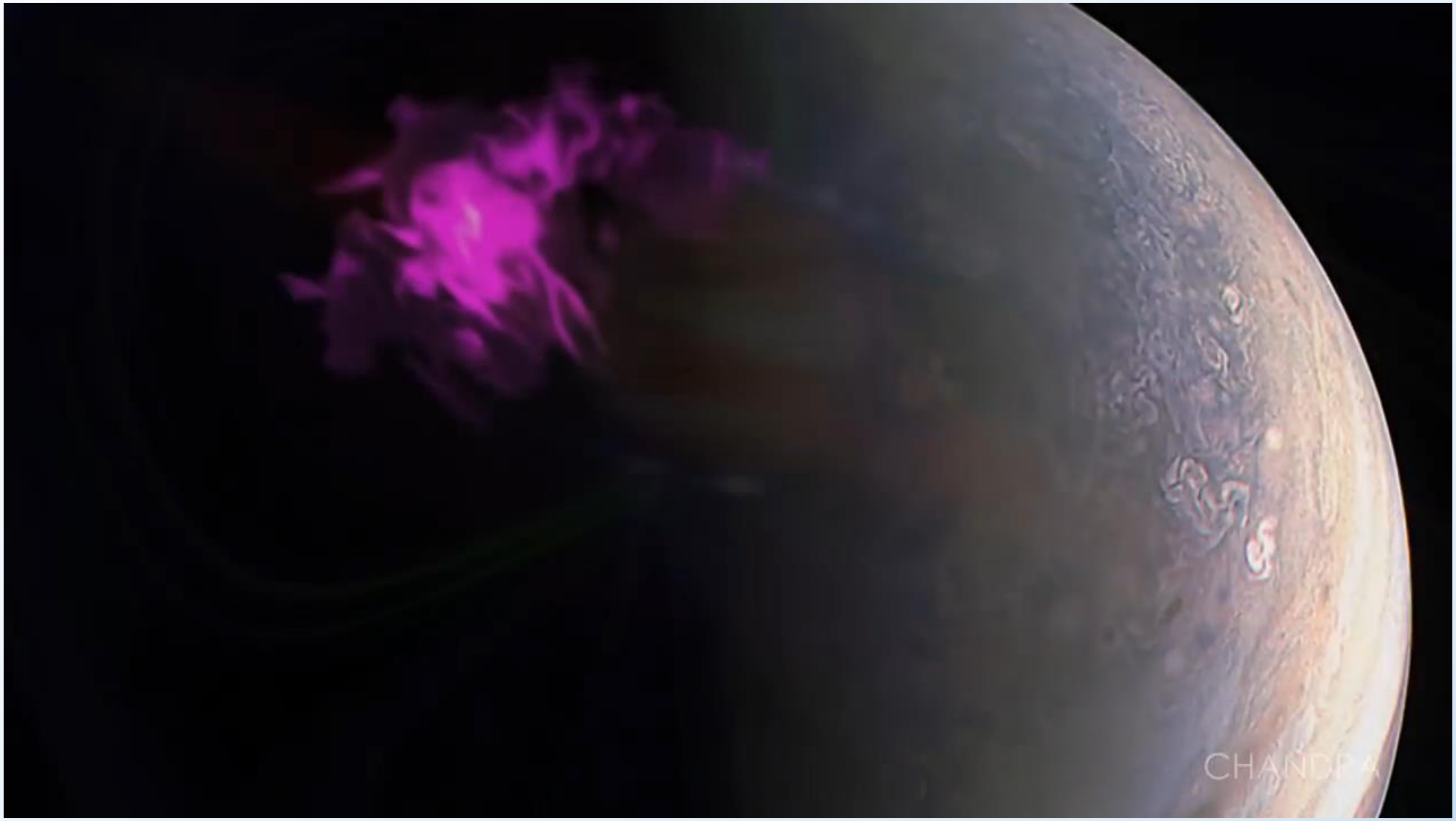

Chandra ACIS detect aurorae from Oxygen ions, implying potentials of 10 million Volts. The mechanism to accelerate particles is not like Earth or Saturn (triggered by solar activity): fast rotation, strong magnetic field, Io volcanism represent a huge plasma supply.

Saturn

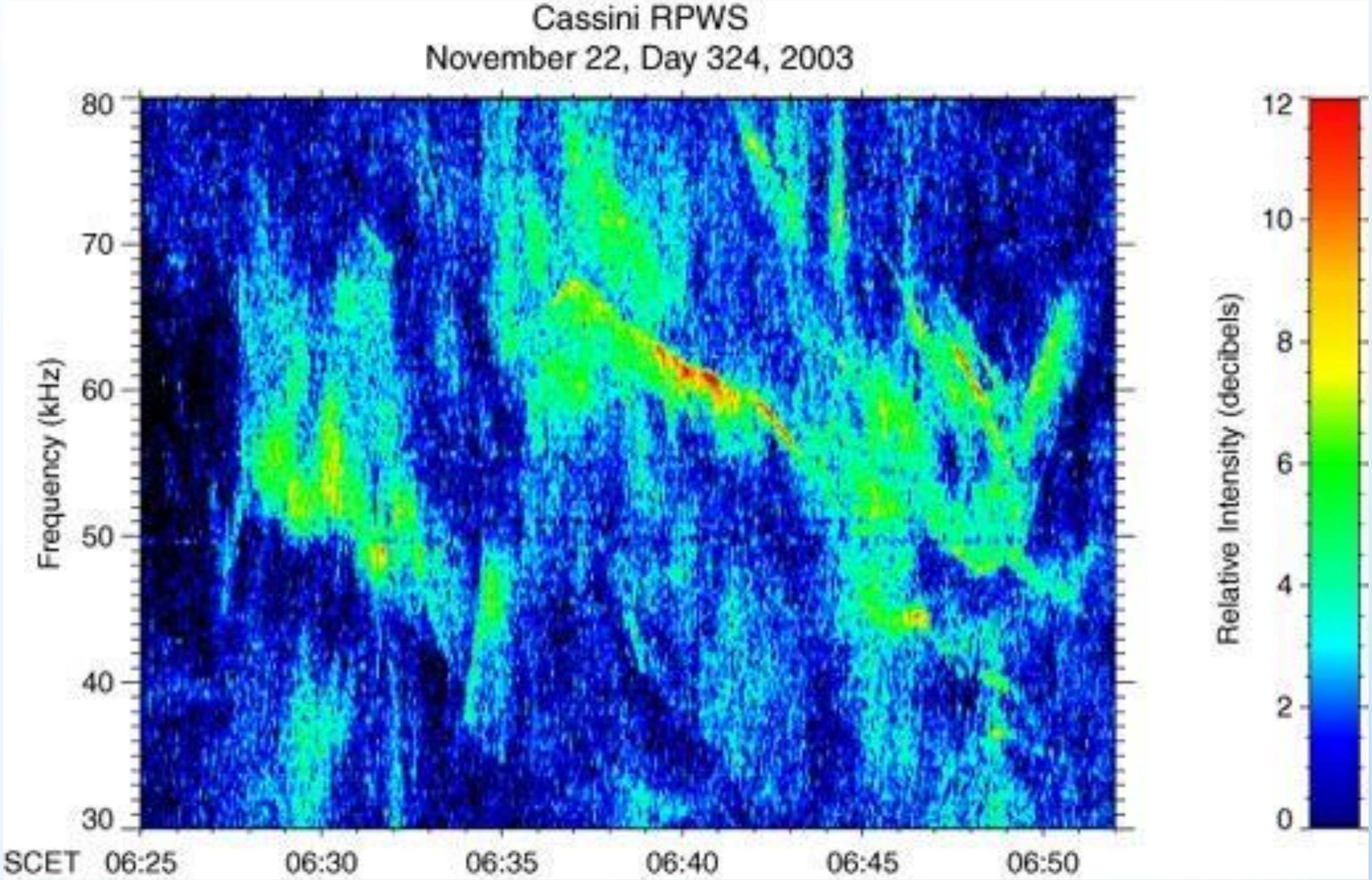

Cassini radio emission (undetectable from Earth due to low frequency)

Earth from space

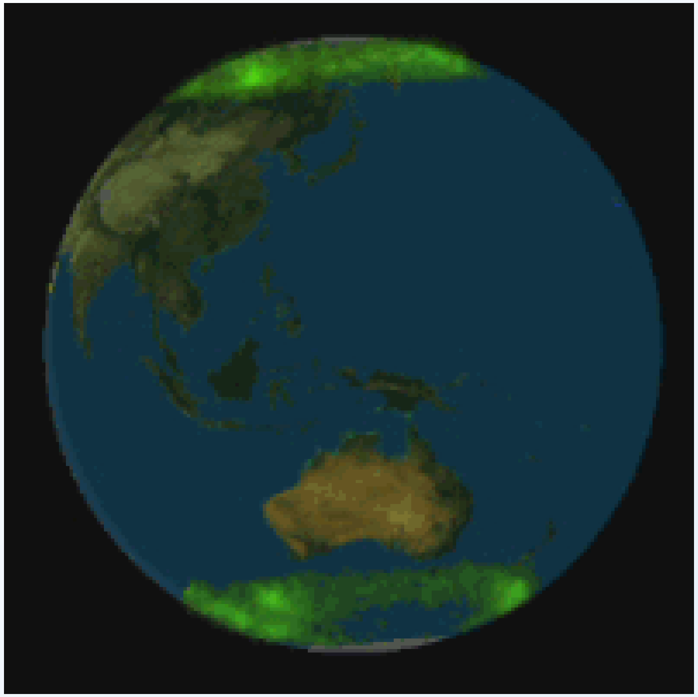

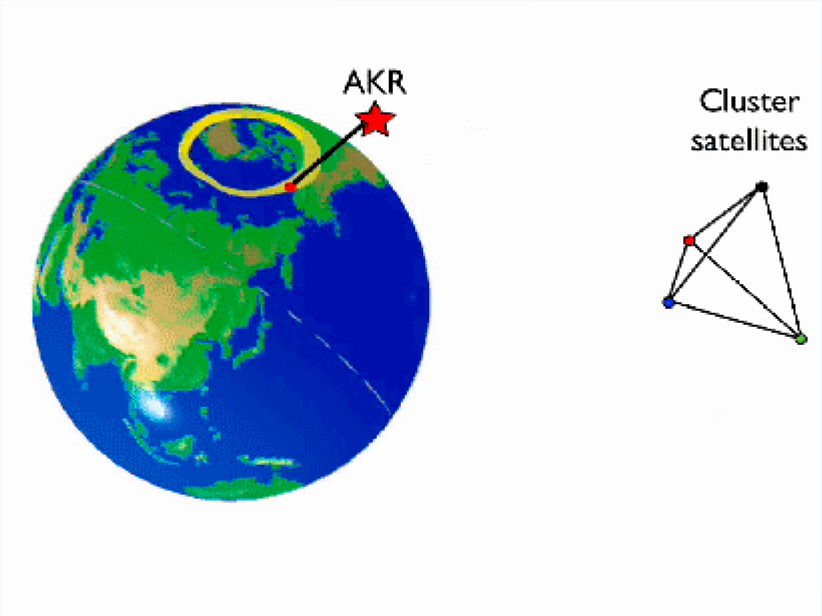

[ESA Cluster satellites, Mutel+ 2003]

Beamed Kilometric radiation from the Earth seen from Space
Related to the accelerated electrons that also generate aurorae

Planetary radio emission: ECM

- Coherent radio emission comes from **Electron Cyclotron Maser**
- **Very high Circular Polarization**
- Maximum frequency: ν **= 2.8*$B[G]$ MHz** (Jupiter: 40 MHz)
- Earth's ionosphere opaque below 10 MHz: emission detectable from ground-based telescopes only if at least Jupiter-like magnetic field.

See Jan-Matthias' lecture

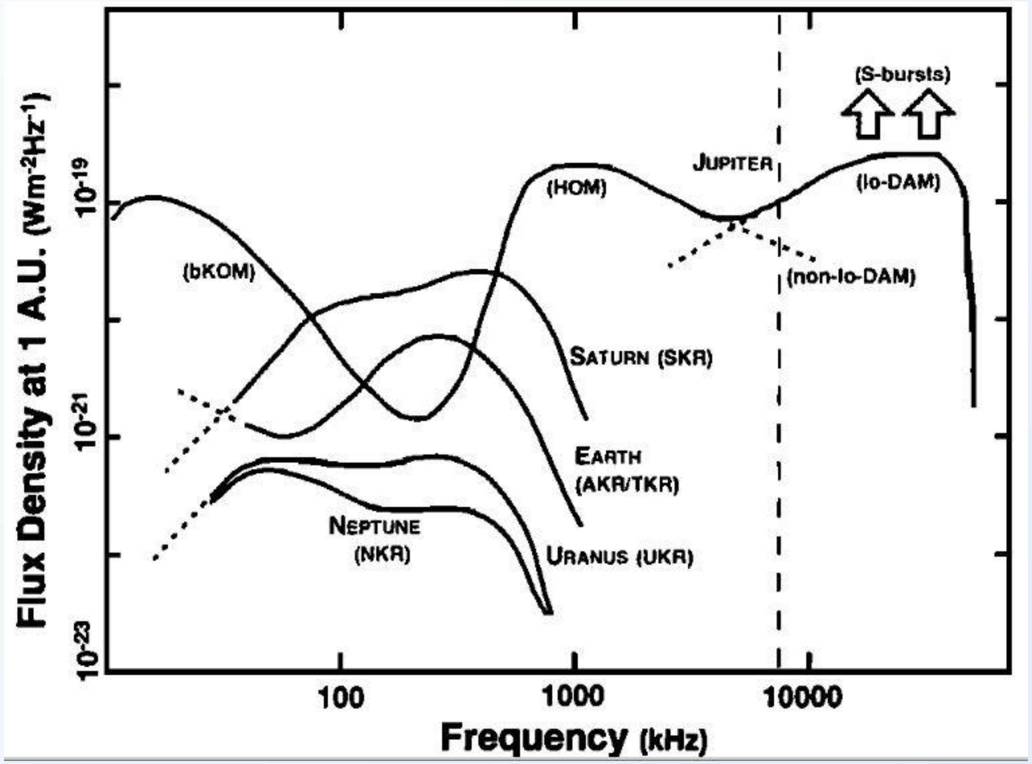

[Zarka 1998]

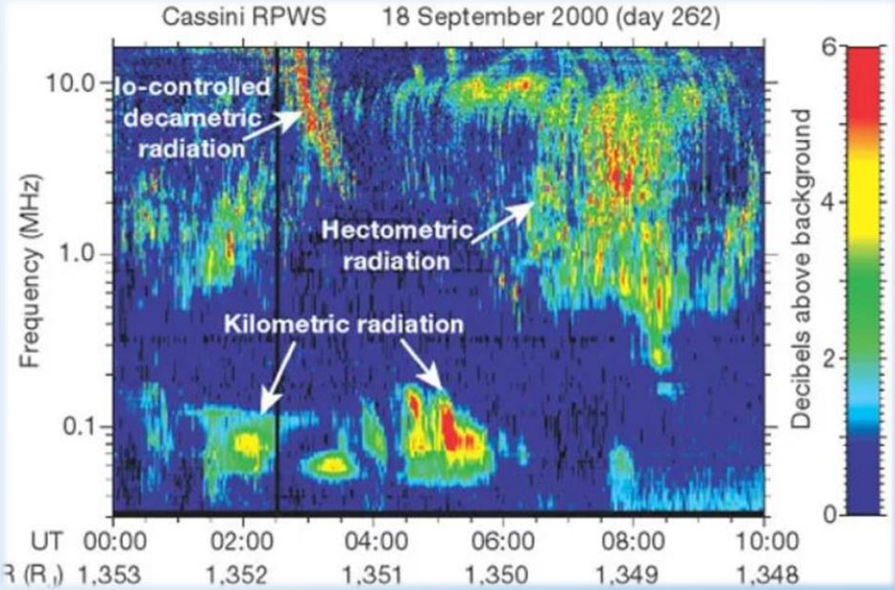

Radio emission: summary of upper limits

Almost all campaigns for radio emission from planets have targeted hot Jupiters, since they are natural candidates to host larger magnetic fields.

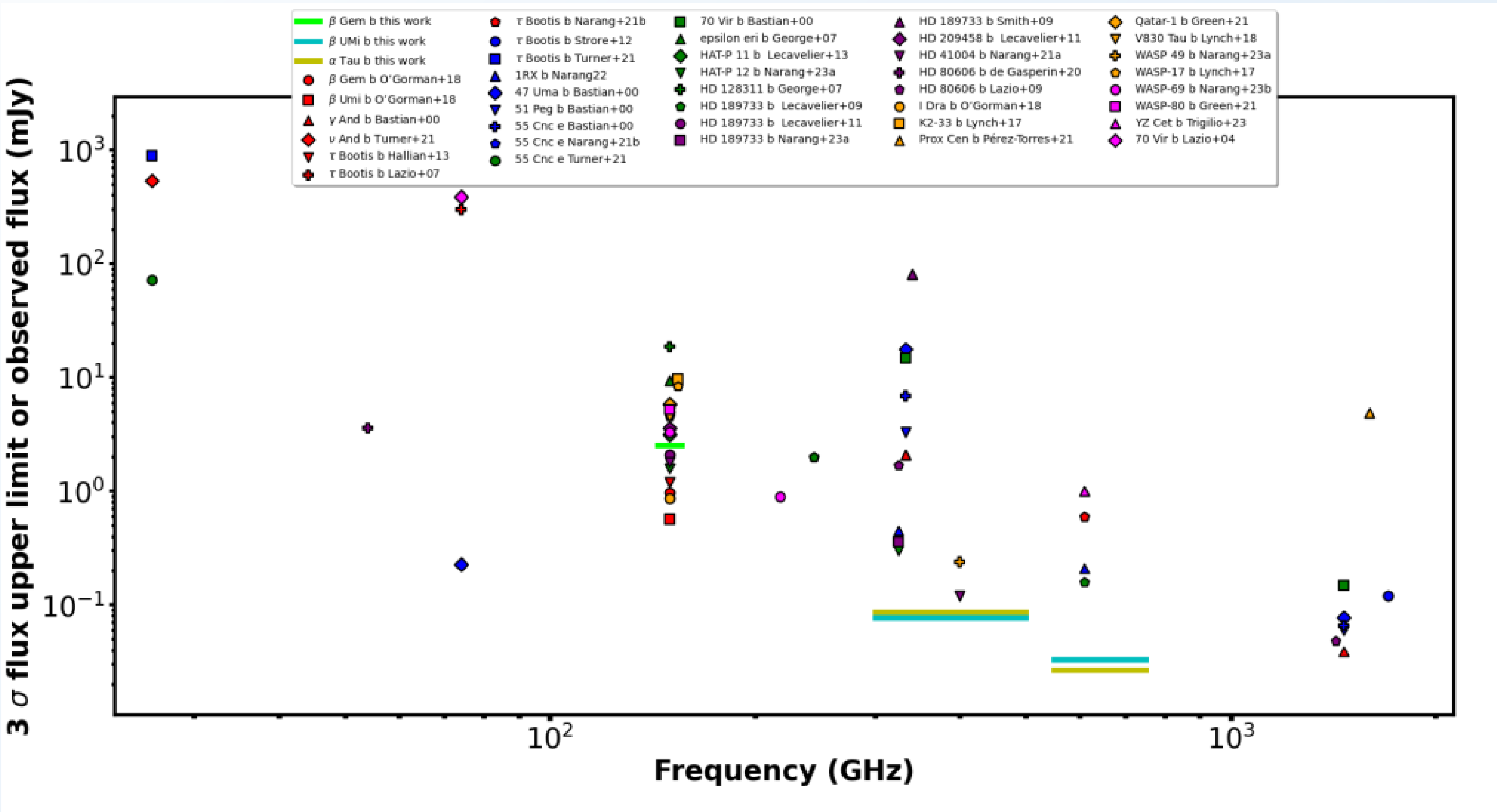

[Narang et al. 2024]

Claimed detections of exoplanetary magnetism

Coherent radio bursts from τ Bootis system, with LOFAR (tens of MHz). Follow-up campaign on-going.

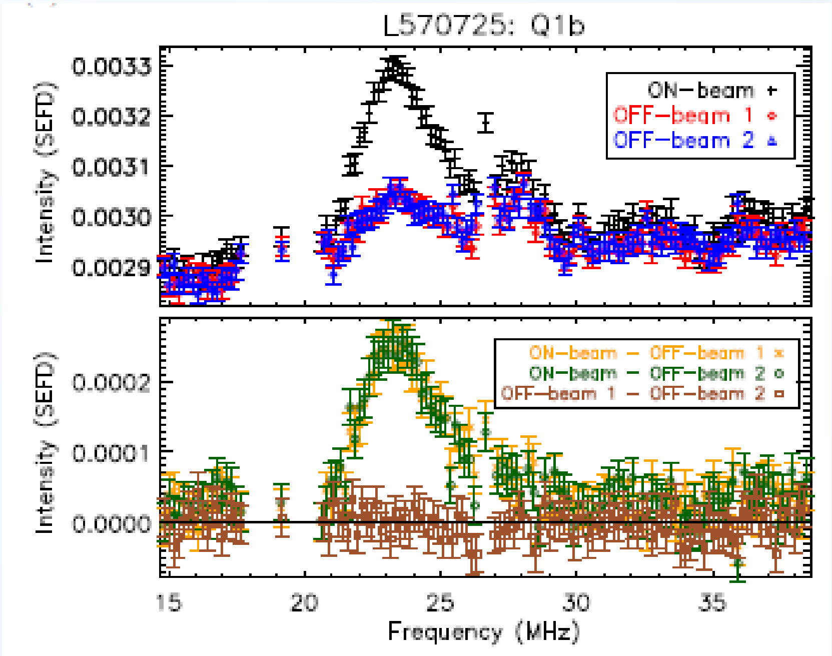

[Turner+ 2021]

Other indirect measurements, for instance via modelling the global circulation model or chromospheric emission and star-planet interaction models.


Published: 15 May 2017

Constraints on the magnetic field strength of HAT-P-7 b and other hot giant exoplanets

T. M. Rogers

Nature Astronomy 1, Article number: 0131 (2017)

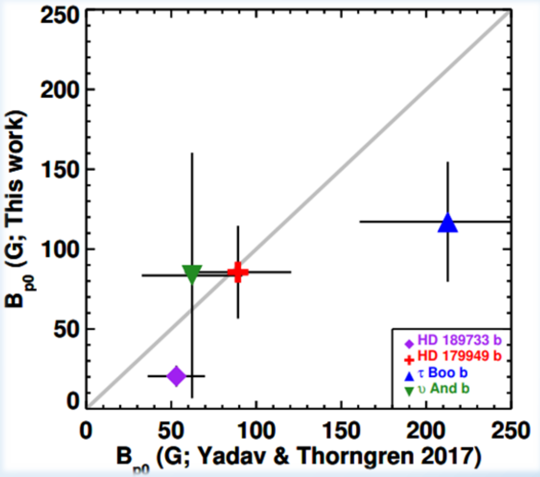

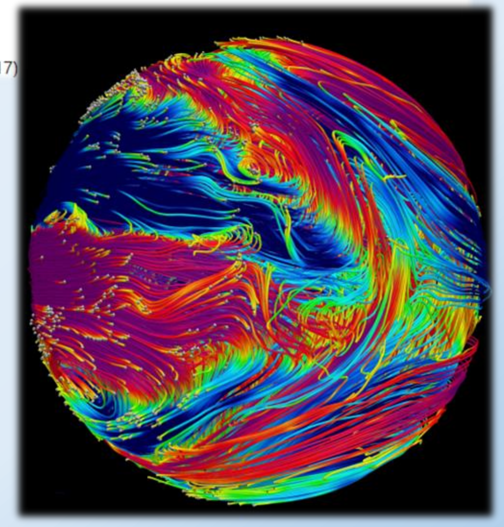

[Cauley+ 2019]

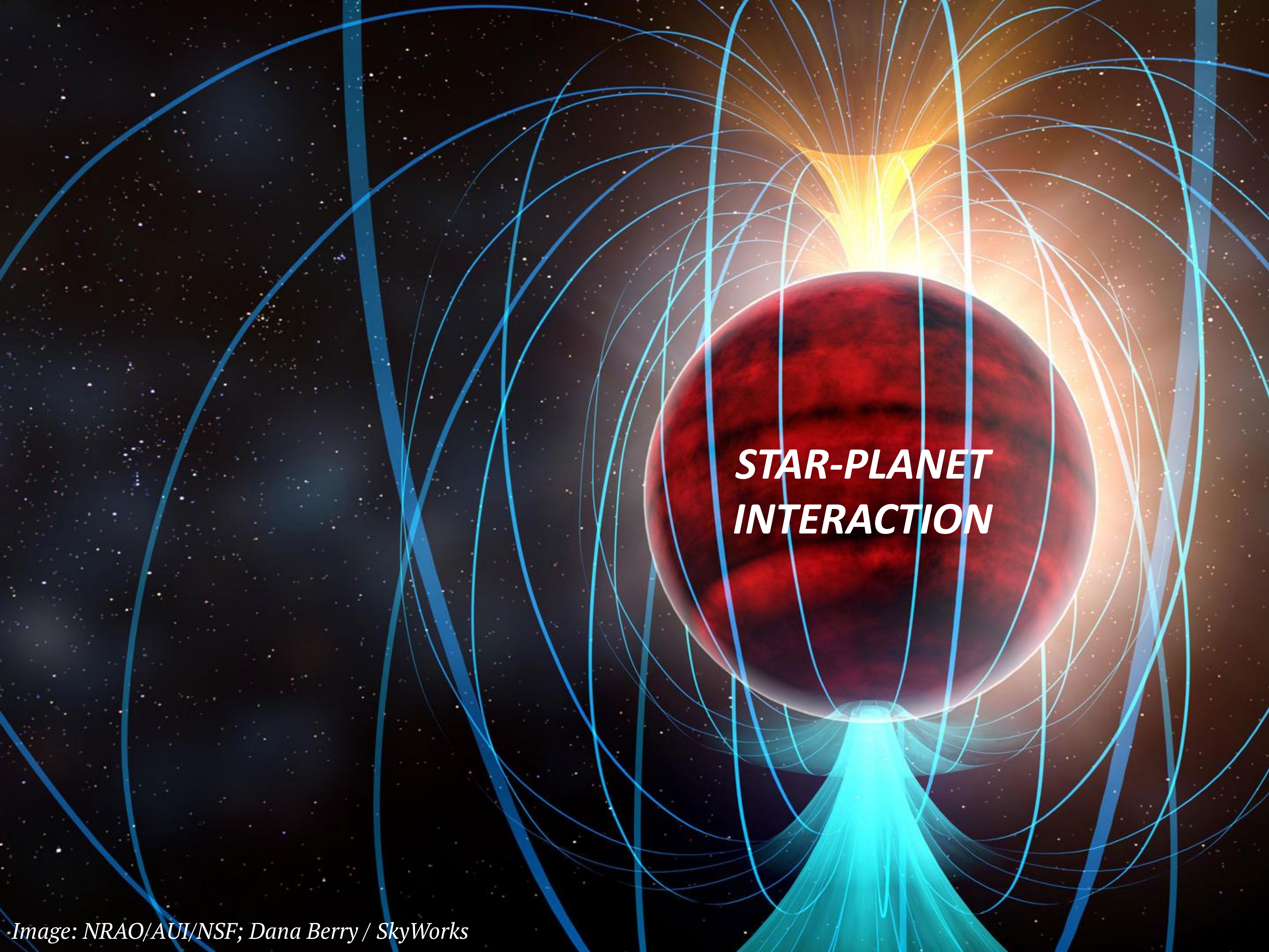

Image: NRAO/AUI/NSF; Dana Berry / SkyWorks

Radio emission and star-planet interaction

Star-planet interactions can induce aurorae on stars, again ECM as a mechanism, in Io-Jupiter fashion.
It's a proxy to stellar magnetic field, so that, if we have a stellar kG field, can be seen at a few GHz (**ν = 2.8*$B[G]$ MHz**). There's no need of a magnetic planet.
The basic requirement is short distance and sub-Alfvenic values of the relative planet-wind velocity (meaning, strong stellar fields).

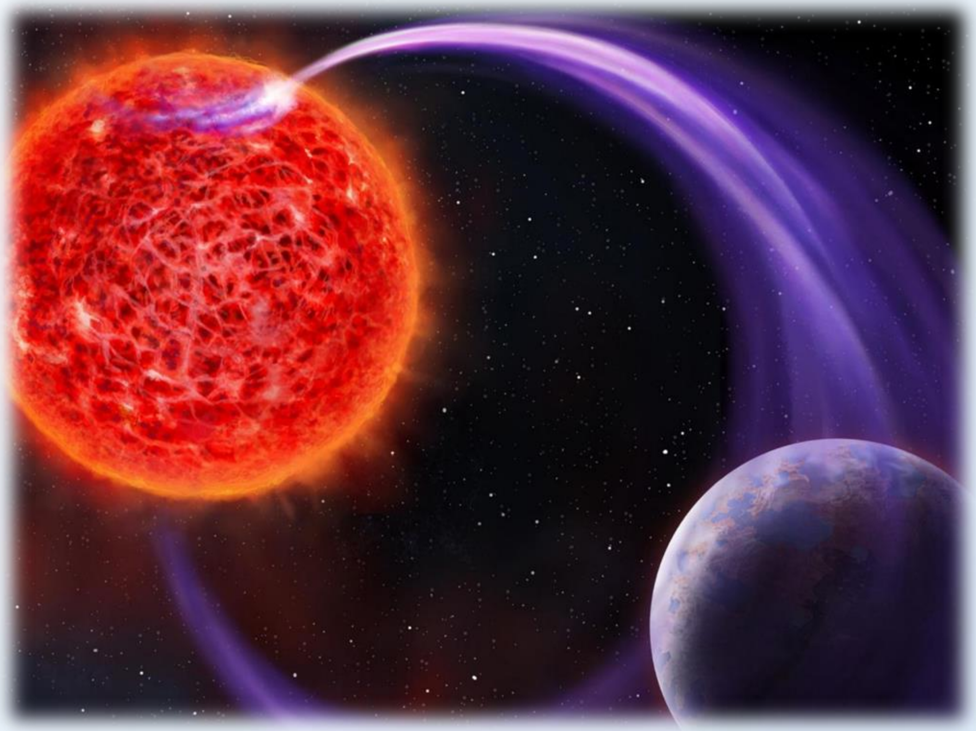

See Ekaterina's lecture

Radio emission from SPI? Proxima Cen b and GJ 1151

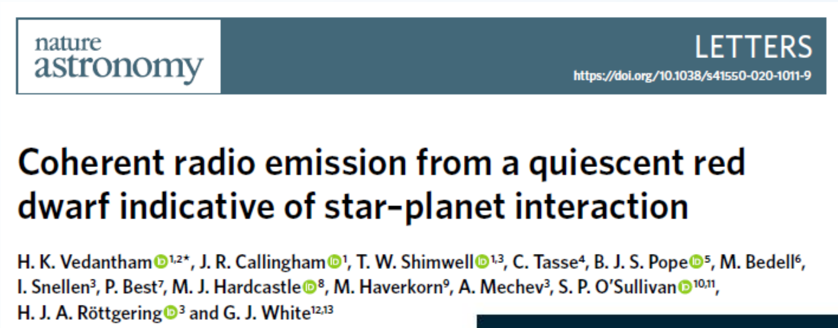
nature astronomy — LETTERS
https://doi.org/10.1038/s41550-020-1011-9

Coherent radio emission from a quiescent red dwarf indicative of star–planet interaction

H. K. Vedantham[1,2*], J. R. Callingham[1], T. W. Shimwell[1,3], C. Tasse[4], B. J. S. Pope[5], M. Bedell[6], I. Snellen[3], P. Best[7], M. J. Hardcastle[8], M. Haverkorn[9], A. Mechev[3], S. P. O'Sullivan[10,11], H. J. A. Röttgering[3] and G. J. White[12,13]

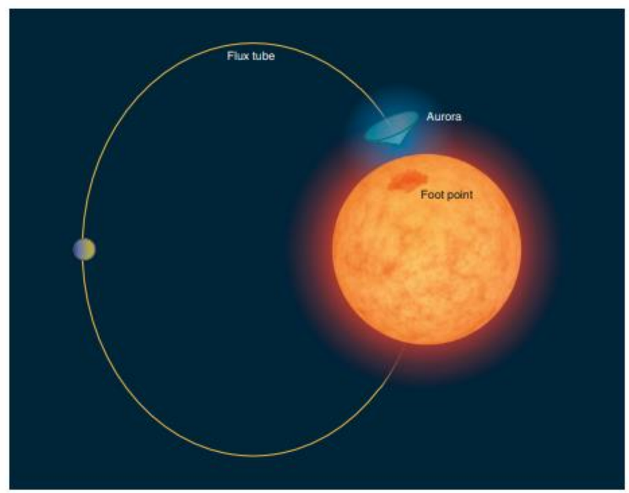

Fig. 1 | The putative exoplanet generates a stellar aurora. The planet candidate around GJ 1151 is expected to be linked to its host star through a magnetic flux tube, causing a stellar aurora at its foot.

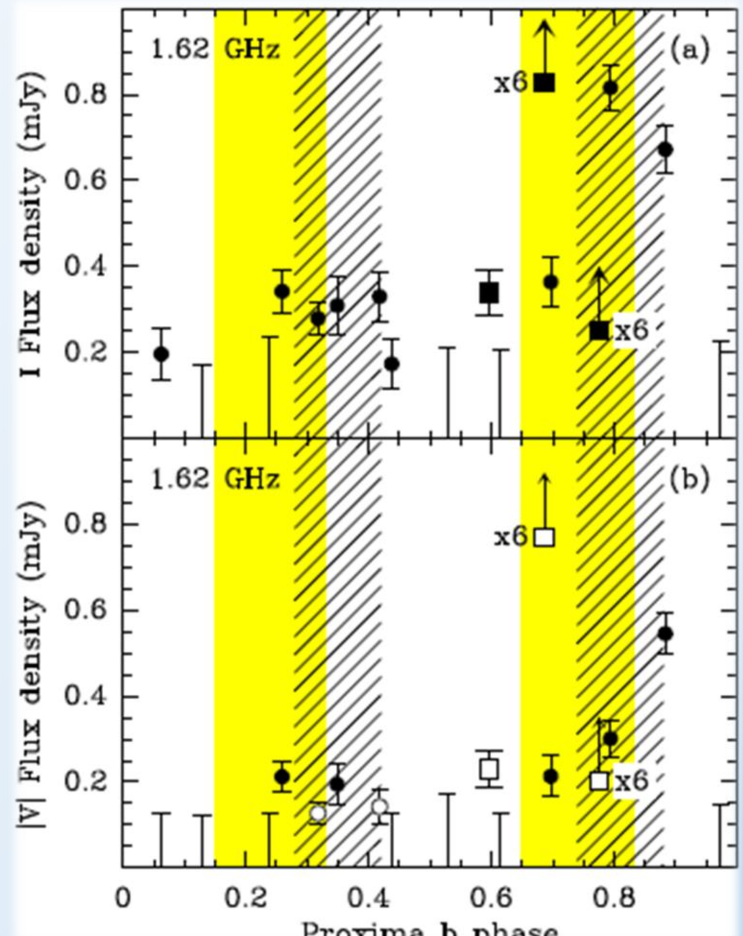

Radio emission in Proxima Centauri [Perez-Torres et al. 2021]

An initial claim of RV detection of a 2-days-orbit planet in GJ1151 [Mahadevan+ 2021] then refuted by follow-up observations with CARMENES [Perger et al. 2021].

Radio emission from star-planet interaction

Recent cross-matching of Gaia nearby stars with low-frequency surveys (LOFAR) reveal very few (only two dozen out fo tens of thousands!) radio-loud stars. Sub-mJy fluxes, coherent ($T_b > 10^{12}$ K), hours-long emission, highly circular polarized (>60% most of them), different from typical main sequence star radio emission (unpolarized or polarized but shorter).

In almost half of the cases, no correlation with X-ray (Güdel-Benz relation), stellar activity indicators, or Rossby number (rotation): planet-induced ECM favoured?

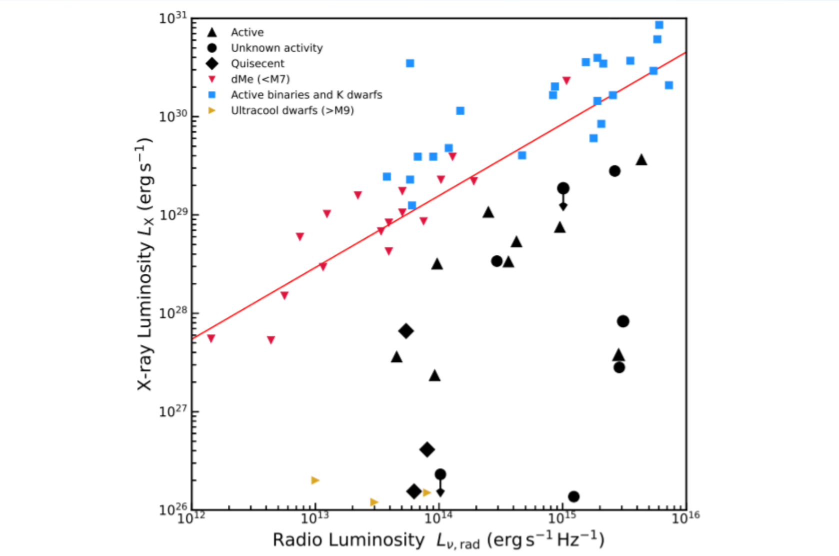

Supplementary Information Figure 2. Soft (0.2-2.0 keV) X-ray luminosity L_X against radio luminosity $L_{\nu,rad}$. The literature data for the chromospherically-active stars used to derive the original Güdel-Benz relation are plotted as coloured triangles or squares[84,85], with the best fit to the literature data indicated by the red line ($L_X \propto L_{\nu,rad}^{0.73}$).

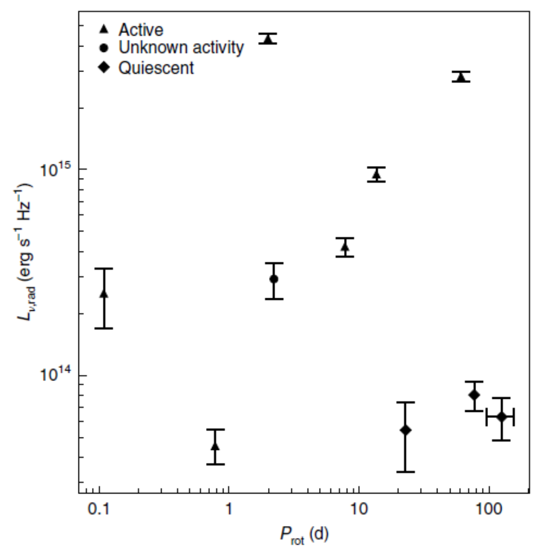

Radio emission from about 20 M-dwarfs with LOFAR [Callingham+ 2021, Vedantham+2021, Yiu et al. 2024]

Radio emission from star-planet interaction

GHz radio emission from red dwarfs can be induced or enhanced by planets. Not many stars are known to be radio-loud, and usually they have high X-ray and activity indicators, or they are young stellar objects (still embedded by a disk), or binary systems. Possible mechanisms:

1. *Purely stellar emission, that should correlate with magnetic activity indicators*
2. *ECM due to either co-rotation breakdown for fast rotators (less than a few days)*
3. *ECM triggered by the presence of a planet around the star*

A more solid confirmation would need:

- Planet detection by i.e. RV (difficult when the star is very active or the planet is small).
- Long-term follow-up, with a clear periodicity of the signal, different from the stellar spin and magnetic cycle.

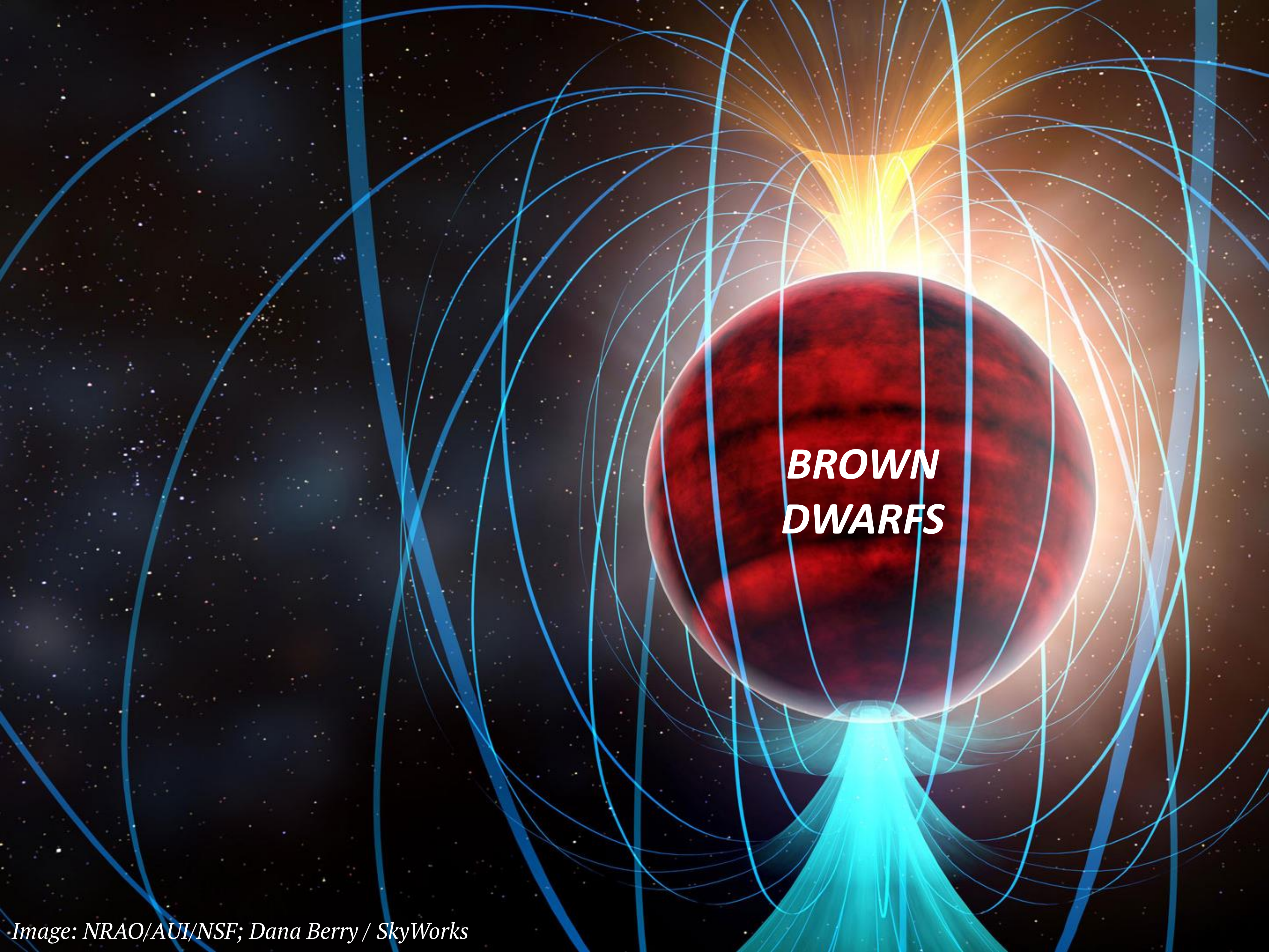
BROWN
DWARFS
Image: NRAO/AUI/NSF; Dana Berry / SkyWorks

Almost stars

- Bridge between planets and stars (13-80 M_j), fully convective.
- Deuterium fusion ($M>13\ M_j$) for a limited period of time, then they cool down: M(>5.5)-L-T-Y sequence.
- Ultra Cold BD are as cold as 300 K.
- Thousands known today.
- Zeeman-Doppler Imaging and Zeeman broadening not feasible for late-type dwarfs: **coherent radio (ECMI) emission proxy to B, like in planets.**

[GD165B, 1st discovered (L-type) BD in IR, around a WD in 1988]

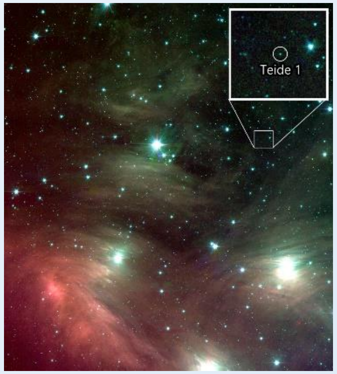

[Teide 1, 1st discovered M-type BD, 1995]

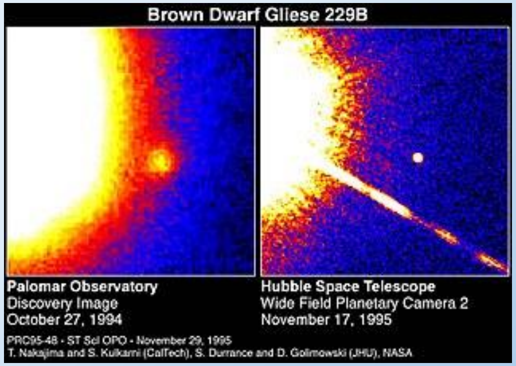

[1st T-type BD, 1995, around a Red Dwarf]

Radio emission from BDs

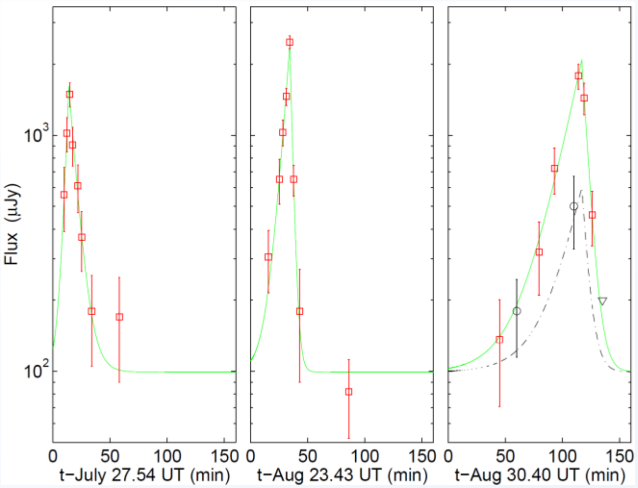

[Berger+ 2001, first BD radio detection (incoherent)]

- Searches of coherent radio emission from Brown Dwarfs have been almost unsuccessful until recently.
- For BDs showing hints for auroral activities in IR and Hα activity indicators, there are VLA detection, indicating **kG magnetic fields.**
- Key point: fast rotation (few hours)

AURORAL RADIO EMISSION FROM LATE L AND T DWARFS: A NEW CONSTRAINT ON DYNAMO THEORY IN THE SUBSTELLAR REGIME

MELODIE M. KAO[1], GREGG HALLINAN[1], J. SEBASTIAN PINEDA[1], IVANNA ESCALA[2], ADAM BURGASSER[2], STEPHEN BOURKE[1], AND DAVID STEVENSON[3]

[Kao+ 2016,2018,2019]

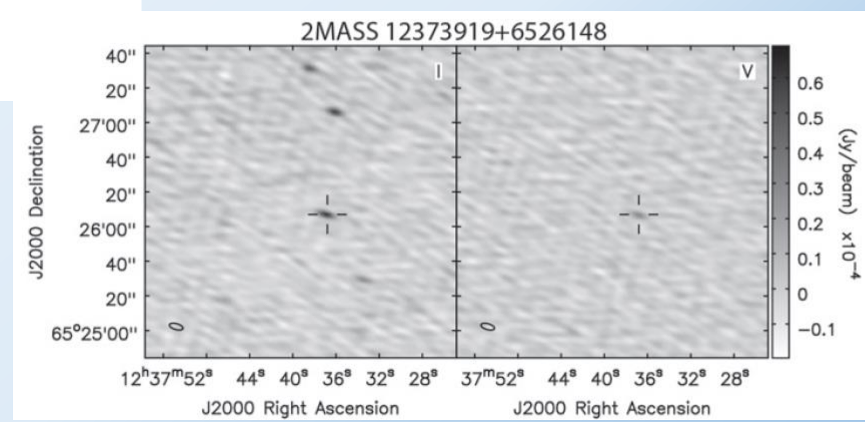

Brown Dwarfs

The Strongest Magnetic Fields on the Coolest Brown Dwarfs

Melodie M. Kao[1,2], Gregg Hallinan[2], J. Sebastian Pineda[3], David Stevenson[4], and Adam Burgasser[5]
[1] California Institute of Technology, Department of Astronomy, 1200 E California Boulevard, MC 249-17, Pasadena, CA 91125, USA
[2] Arizona State University, School of Earth and Space Exploration, 550 E Tyler Mall, PSF 686, Tempe, AZ 85287, USA; mkao@asu.edu
[3] University of Colorado Boulder, Laboratory for Atmospheric and Space Physics, 3665 Discovery Drive, Boulder CO 80303, USA
[4] California Institute of Technology, Division of Geological & Planetary Sciences,1200 E California Boulevard, MC 150-21, Pasadena, CA 91125, USA
[5] University of California San Diego, Center for Astrophysics and Space Sciences, 9500 Gilman Drive, MC 0424, La Jolla, CA 92093, USA
Received 2017 August 2; revised 2018 May 2; accepted 2018 May 3; published 2018 July 31

Abstract

We have used NSF's Karl G. Jansky Very Large Array to observe a sample of five known radio-emitting late-L and T dwarfs ranging in age from ~0.2 to 3.4 Gyr. We observed each target for seven hours, extending to higher frequencies than previously attempted and establishing proportionally higher limits on maximum surface magnetic field strengths. Detections of circularly polarized pulses at 8–12 GHz yield measurements of 3.2–4.1 kG localized magnetic fields on four of our targets, including the archetypal cloud variable and likely planetary-mass object T2.5 dwarf SIMP J01365663+0933473. We additionally detect a pulse at 15–16.5 GHz for the T6.5 dwarf 2MASS 10475385

Magnetism in BDs

The detected coherent radio quiescent (tens μJy) and flaring (O(0.1) mJy) emission at 4-18 GHz, compatible with kG magnetic fields, larger than those predicted by theory. Is BD magnetism a continuum with planets?

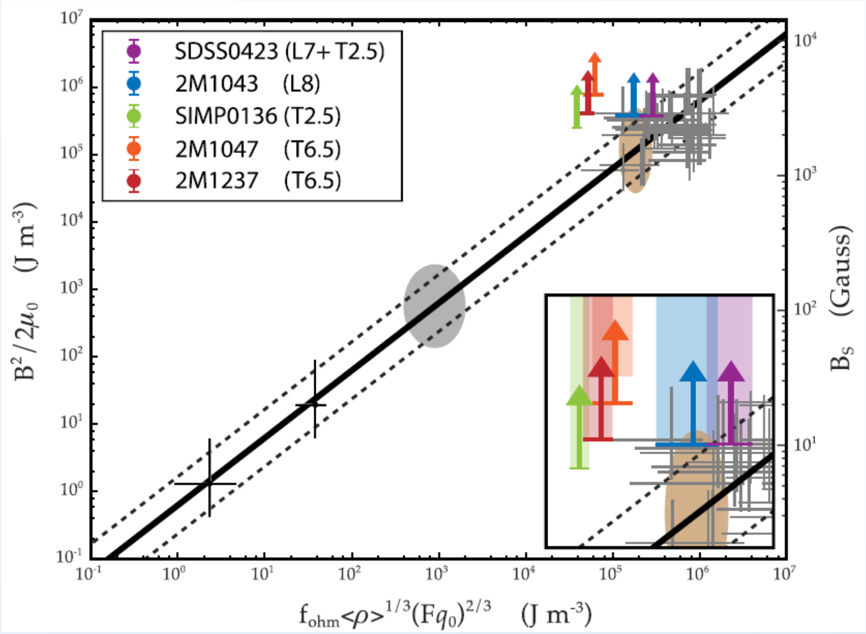

[Kao+ 2019]

LSR 1835+3259: first resolved extrasolar magnetosphere

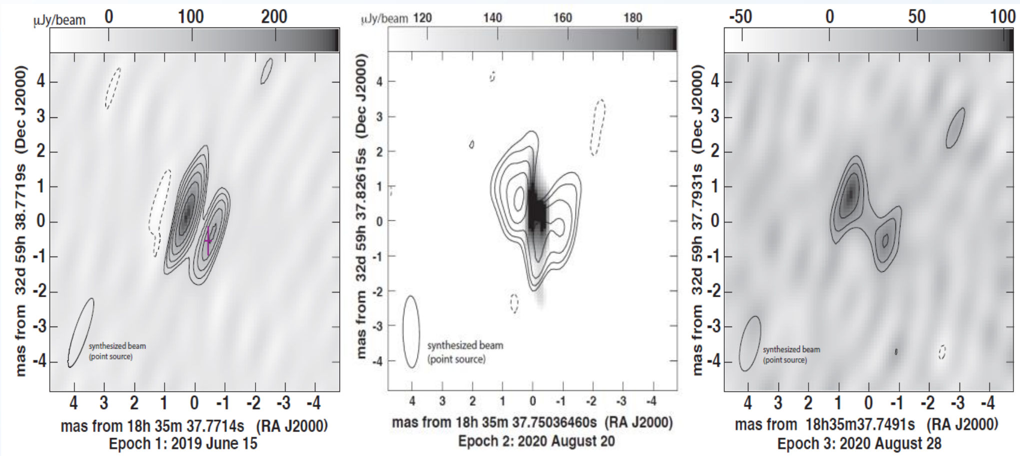

[Kao+ 2023]

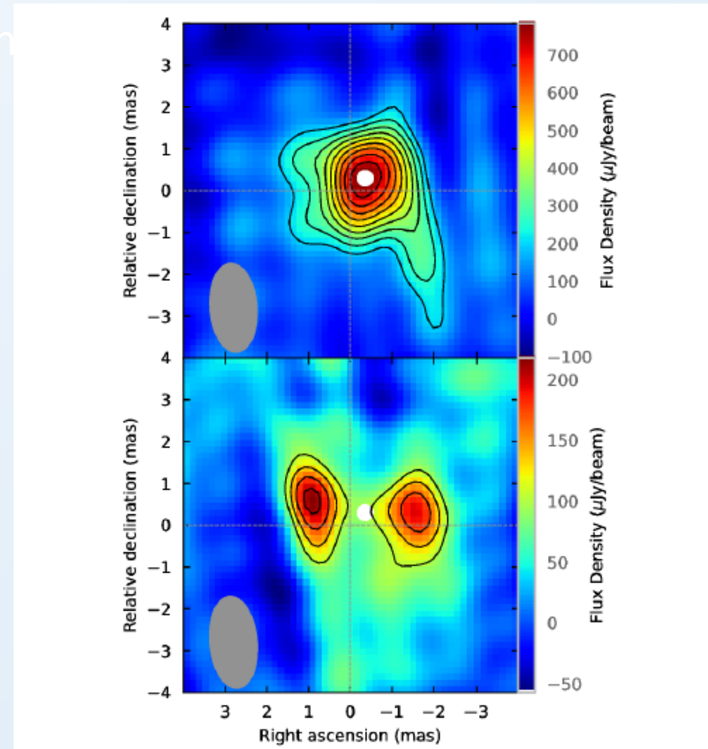

Fig. 3. Reconstructed images of LSR J1835+3259 during the first radio burst. Reconstructed images of LSR J1835+3259 during a 30-minute window centered around burst B1 ($0.29 < \phi < 0.47$). Top and bottom panel show the LCP and RCP images, respectively. The white circle represents the expected position of the photosphere assuming an ECMI mechanism for the origin of the bursting emission and a dipolar magnetic field (see Methods). The beam size is 1.06 x 2.14 mas at 5.36°.

[Climent+ 2023]

Aurorae (periodic bursts) + persistent side lobes tracking the magnetosphere

LSR 1835+3259: first resolved extrasolar magnetosphere

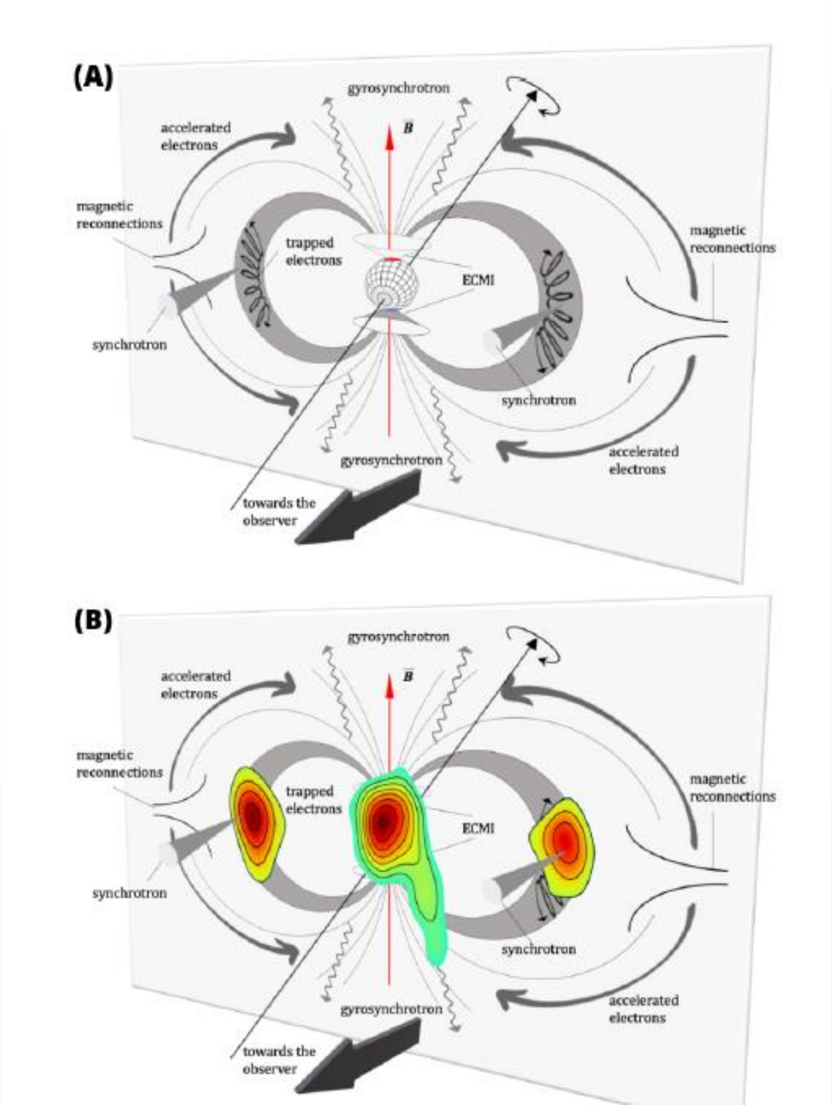

Estimate of electron energy: 15 MeV, similar to Jupiter [Kao+ 2023].

The bursts corresponds to the phases where the magnetic-rotation plane is orthogonal to the line-of-sight.

Upper limit of about 55 Jupiter mass on companion at few mas separation, still possible but no signs in observations. It would help providing the needed plasma.


THANKS!
Daniele Viganò